PHYSICAL BASED ANALYSIS AND MODEL REDUCTION OF ENGINEERING SYSTEMS

by

Âli Yurdun Orbak

B.S., Mechanical Engineering, Istanbul Technical University, 1992

M.S., Mechanical Engineering, Massachusetts Institute of Technology, 1995

M.E., Mechanical Engineering, Massachusetts Institute of Technology, 1998

Submitted to the Institute for Graduate Studies in
Science and Engineering in partial fulfillment of
the requirements for the degree of
Doctor of Philosophy

Graduate Program in Mechanical Engineering

Boğaziçi University

2003

This thesis is dedicated to,
Nurten Orbak, M. Günhan Orbak, İlkün Orbak,
and Aslı Erdiller...

ACKNOWLEDGEMENTS

I would like to thank my advisors *Professor Osman S. Türkay* and *Associate Professor Eşref Eşkinat* for their guidance and support throughout my Ph.D. degree. I am looking forward to our collaboration on many challenging projects in the following years.

Thanks to my friends at Boğaziçi University, İstanbul and Bursa who were always around and ready to help when I needed them. Among these, I especially thank *Nazım Mahmutyazıcıoğlu*, *Levent Öztürk*, and *Serhat Onay*, who, I believe, are among the rarest friends one can have.

I would like to thank *Aslı Erdiller*. She is 'the' special person in my life and her spiritual help cannot be left unnoticed.

And finally I would like to thank my parents and my brother, for their love, never ending moral support and encouragement. Thanks for helping me go through my studies in the United States and then in Turkey; these years would not have been the same without your love.

ABSTRACT

PHYSICAL BASED ANALYSIS AND MODEL REDUCTION OF ENGINEERING SYSTEMS

There is a need for obtaining low order approximations of high order models of physical systems as low order models result in several advantages including the reduction of computational complexity and improved understanding of the original system structure. Different methods have been suggested in literature for obtaining suitable low order approximations, but these approaches do not reflect the relation between the mathematical model and the physical components of a system.

In this thesis, some new approaches are provided for model reduction in the physical domain. The approaches that are presented use the idea of decomposition of physical systems which is useful for the identification of dominant components or subsystems. The procedures are applied to the physical systems that are represented by bond graphs as they lead to better understanding of the system structure. One of the proposed methodologies exploits the idea of decomposition of physical systems. The proposed decomposition and model reduction procedures are directly implemented on the model providing a better perception of the physical model reduction and a better design point of view. As a second methodology, the determination of subsystems and/or components that influence a given eigenvalue of the overall system has been explored. A set of theorems and definitions are proposed that lead to an efficient procedure for this aim. After the calculation of eigenvectors, "effect" matrices are produced that indicate the relative importance of physical parameters in a selected eigenvalue. Using these matrices, an efficient physical model reduction procedure is constructed. The advantages of the presented approaches over existing methodologies are emphasized through several examples.

ÖZET

MÜHENDİSLİK SİSTEMLERİNİN FİZİKSEL TEMELLİ ANALİZİ VE MODEL İNDİRGEMESİ

Fiziksel sistemlerin yüksek dereceli modellerinin düşük dereceli yaklaşıklıklarını elde etmek için artan ihtiyaç vardır. Düşük dereceli modellerin kullanımı, hesaplama karmaşıklığını azaltmayı ve orijinal sistem yapısının anlaşılmasını artırmayı da içeren birçok avantaj ile sonuçlanmaktadır. Literatürde, düşük mertebeden modellerin elde edilebilmesi için değişik yöntemler sunulmaktadır, ancak bu yöntemler matematiksel model ile sistemin fiziksel bileşenleri arasındaki ilişkiyi verememektedirler.

Bu tezde, fiziksel alanda model indirgenmesi için bazı yeni yaklaşımlar sunulmaktadır. Sunulan yaklaşımlar, baskın bileşenlerin veya alt sistemlerin belirlenmesine yarayan fiziksel sistemlerin ayrıştırılması fikrini kullanmaktadırlar. Yöntemler sistem yapısını daha iyi anlamaya yarayan bağ çizgesi ile ifade edilmiş olan fiziksel sistemlere uygulanmıştır. Sunulan yöntemlerden biri, baskın alt sistemlerin belirlenmesine uygun olan fiziksel sistemlerin ayrıştırılması fikrini kullanmaktadır. Açıklanan indirgeme yöntemleri model üzerine doğrudan uygulanmakta ve böylece fiziksel model indirgemesi ve tasarım için daha iyi bir anlayış sağlamaktadır. İkinci bir yöntem olarak, bütün sistemden seçilen bir özdeğere etki eden alt sistem ve/veya bileşenlerin belirlenmesi konusu araştırılmıştır. Bu amaç için etkili bir yöntemi oluşturan bir seri teorem ve tanım sunulmuştur. Öz vektörlerin hesaplanmasından sonra, seçilmiş bir özdeğere etki eden fiziksel parametrelerin göreceli olarak önemini veren "etki" matrisleri üretilmektedir. Bu matrisler kullanılarak etkili bir fiziksel model indirgeme yöntemi kurulmuştur. Sunulan yöntemlerin mevcut yöntemlere göre avantajları çeşitli örnekler kullanılarak araştırılmıştır.

TABLE OF CONTENTS

LIST OF FIGURES

LIST OF TABLES

LIST OF SYMBOLS/ABBREVIATIONS

$\mathbf{A, B, C, D}$	system matrices
b	damper coefficient $(N\ sec/m)$
$\mathcal{C}$	field of complex numbers
C	bond graph capacitance element
$\mathbf{E}_{IC}$	effect matrix for energy storage elements
$\mathbf{E}_{R}$	effect matrix for energy dissipation elements
F	force input (N)
F_{k_i}	force in spring i (N)
$\mathbf{G}$	transfer function matrix
G	transfer function
G_{IC}	$I - C$ loop gain
G_{IR}	sum of loop gains of $I - R$ pairs
G_{RC}	sum of loop gains of $R - C$ pairs
$\mathbf{H}$	participation matrix
I	bond graph inertial element
$\mathbf{J}$	connectivity matrix
k	spring coefficient (N/m)
m	mass (kg)
M, U	right eigenvector matrix
$\mathcal{P}$	power associated with a bond (W)
$\mathbf{P}$	controllability gramian
P	generalized participation factor
p	participation factor
$\mathbf{Q}$	observability gramian
$\mathbf{R}$	partial fraction expansion residue matrix
$\mathcal{R}$	field of real numbers
R	bond graph resistance element
t	multiplication factor for energy storage elements
$\mathbf{u}$	input vector

$\mathbf{V}$	Vandermonde matrix
$\mathbf{v}$	right eigenvector
$\mathbf{w}$	left eigenvector
$\mathbf{W}$, $\mathbf{V}$	left eigenvector matrix
$\mathbf{W}_c$	controllability matrix
$\mathbf{W}_o$	observability matrix
$\mathbf{W}_{co}$	cross gramian matrix
$\mathbf{x}$	state vector
$\mathbf{y}$	output vector
z	multiplication factor for energy dissipation elements
λ	eigenvalue
$\mathbf{\Omega}$	inverse of the Vandermonde matrix
ω	frequency (rad/sec)
σ	Hankel singular value
ζ_{i-j}	local damping ratio of local loop between mass i and mass j
ARMA	Autoregressive Moving Average
DAE	Differential Algebraic Equation
HSV	Hankel Singular Value
LTI	Linear Time Invariant
MIMO	Multi-Input Multi-Output
PFE	Partial Fraction Expansion
RMS	Root Mean Square
SISO	Single-Input Single-Output

1. INTRODUCTION

1.1. Motivation

The rising importance of multi energy domain dynamic systems has motivated intensive research activities on modeling methodologies. A multi energy domain dynamic system may include mechanical, electrical, fluidic and / or thermal components / subsystems. A multi energy domain system usually contains many of these components. With the growing system complexity, the simulation, analysis and synthesis procedures depend increasingly on accurate and compact models, which in turn calls for systematic modeling procedures. As a result of decades of significant research effort, detailed models for complex systems can now be built efficiently with various computer software packages such as Matlab and Simulink[1] , Easy5 and 20Sim [1, 2, 3, 4, 5].

While complex models can be very accurate, they may also be difficult to handle. Not all of the components of a system make significant contribution to the system dynamic behavior. Therefore, a vital step in modeling is to reduce the model to a more manageable size. Low order models possess some advantages including the reduction of computational difficulty and understanding of the physics of the original system in a simpler way.

It is often desired to approximate the high order model by a reduced low order model in such a way that the relevant dynamics are preserved. Mathematically, this is usually done by the minimization of a suitable norm. A reduced order model should be used instead of the full order one in the control design, and still meet the performance objectives for the controlled physical system. If this is true, then the reduced order model, which is computationally less demanding and possibly numerically more reliable, can be used in controller design and later in the analysis.

The model reduction and the control problem are not independent of each other [6,

[1] MATLAB and SIMULINK are registered trademarks of The MathWorks, Inc.

7]. Although this being the case, in the literature two different concepts exist: model reduction and controller reduction. These are based on different strategies, but they point to the same result, which is to obtain a low order controller. The difference in these two approaches can be summarized as follows:

- *Model reduction* is based mainly on open loop considerations. First, the high order model is reduced. Then, this reduced order model is used in the design of low order controller.
- *Controller reduction* is related mainly to the closed loop aspects, such as preserving the closed loop stability and performance.

In addition to these two approaches, there is also control oriented model reduction [8, 9], but since the aim of this thesis is to provide means for physical model reduction and not directly control related reduction problems, this topic will not be explored.

As a result, the main reasons for using reduced order models can be summarized as follows:

- Using low order models simplifies the understanding of the full system. This is because they focus on the most dominant modes of the system.
- The design of the controller is numerically more efficient.
- Computational complexity is reduced and numerical drawbacks can be avoided to a certain extent.
- From the controller point of view, as the control laws become simpler, the hardware requirements are also reduced.

This thesis concentrates on physical model reduction of causal linear time invariant (LTI) lumped parameter systems. Specifically, the study focuses on understanding of the relation between system dynamics and system parameters and/or structure.

From the theoretical perspective, this thesis gives a fundamental framework for

a systematic model reduction in the physical domain. Past researches on physical domain model reduction methods are reconsidered. Advantages and restrictions of some of the past work are reviewed and new concepts and solutions are proposed. From the practical point of view, the approaches in this thesis can be applied to both single-input single-output (SISO) and multi-input multi-output (MIMO) systems.

1.2. Background

The topic of model reduction has been studied for many years now, and many methods have been suggested for obtaining suitable low order approximations. Most of the techniques in the literature take into account a criterion for the 'goodness' of the reduced model. For example, the balancing approach [10] uses coordinate transformations to convert the system to a special balanced form from which a reduced model can be obtained. The techniques based on balancing aim at reducing the order of the transfer matrix between the input and output by targeting at the worst-case scenarios. Therefore the error bound of the reduced model is guaranteed. However, transfer matrices and their realizations do not contain the information about the internal structure of the system. Therefore, in general, these procedures may not be directly applied to the modelling and reduction of systems in the physical domain.

There exist several time and frequency domain methods that generally provide good approximations. Some of the well-known time domain methods are the approximate moment matching method [11] that utilizes the elimination of some time moments with the employment of a singular-value decomposition approximation, and the least squares model reduction method [12] that uses the power of curve fitting by calculating a low order autoregressive moving average (ARMA) predictor equation. A number of the principle frequency domain methods are the followings: the component cost analysis for model reduction [13] that uses a quadratic cost measure for eliminating the modes, Padé approximations [14] and continued fraction methods [15] that employ the continued fraction expansion and inversion processes with a generalized matrix Routh algorithm to expand a matrix transfer function into the matrix continued fraction of matrix Cauer forms. Additionally, balance and truncate type of approaches [16] that

exploit the balancing idea are present in which the drawbacks of [10] are eliminated via projections defined in terms of arbitrary bases for the left and right eigenspaces associated with the large eigenvalues of the product of the observability and controllability gramians.

In addition to the purely 'numerical' procedures above, a useful type of reduced model is obtained by removing some physical components from the original model. This approach is known as model reduction in physical domain. In these methods either the components associated with small power flow are eliminated as they have small contribution to the dynamic behavior of a system [17, 18] or singular perturbation method is used to reduce the dimension of the system by considering only one part, namely the slow or fast part, depending on the frequency domain of interest [19, 20].

The power method uses various time averages of the power flow associated with a component to measure the corresponding power level [18] or energy level [17]. The model reduction approaches in [18] and [17] are conceptually similar to each other. These are established on power/energy criteria and consist of the following three major steps, (i) Calculating the system's time response under certain input with numerical simulation, (ii) Measuring the power flow in and out of a component, and (iii) Removing the components associated with low power flow level. Specifically, Rosenberg and Zhou [18] used bond graph for measuring the power response to determine a simplified model for controller design, parameter optimization and to gain insight into the model behavior. The power responses are obtained by applying a step input for a given time interval and calculating the power on all bonds of the bond graph. Then, a root mean square (RMS) average of each power is calculated. Finally, the bonds with low average values are eliminated from the bond graph model. Louca et al. [17] preferred to employ energy as a metric instead of power because energy being the time integral of power it is more advantageous for use throughout the simulation time in case there are time varying elements in the system. The authors claimed that the RMS power metric might also provide false information due to heavy weighing of peak responses. Hence they defined an energy based 'element activity index' which is calculated as the ratio of the energy flowing through an element to the total system energy. Then the bonds that are

deemed unnecessary are eliminated from the bond graph model by removing the low activity elements according to a chosen appropriate threshold value. The attractive advantage of the method is that by utilizing the sinusoidal excitation input the most appropriate reduced model can be obtained as a function of a predefined frequency range of interest. Although the authors claimed that the method could be applied for model reduction of non-linear systems, they acknowledged the need of further study for the application of the method to non-linear models. The methods [17, 18] are not strictly proven mathematically but they have of course clear physical interpretations for model reduction. They eliminate elements that are considered unnecessary according to power or energy level information without indicating which subsystems to retain or remove in a systemic perspective view as it is done in the methods explained in this thesis.

Another physical based model reduction technique developed in [19] makes use of the singular perturbation method. The fast and slow dynamics of bond graph models are estimated by the determination of causal loop gains and by utilizing reciprocal systems. In this method, when the dynamic subsystems are well separated, the resulting reduced model is very near to the one deduced from the singular perturbation method.

In this thesis, some new approaches for physical domain model reduction are developed and assessed. One of the approaches that is presented uses the idea of decomposition of physical systems which is useful for the identification of dominant components or subsystems. The presented approaches are applied on the systems' bond graph representation. In addition to the proposed procedures, a relationship is indicated between the numerical and physical approaches. This adds a new understanding of the numerical methods, and can be used to produce physical reduced order models with using numerical procedures.

The contribution of this thesis can be summarized as follows:

- Theoretical explanation of physical domain model reduction based on eigenvalue distribution is provided. Based on this explanation, a comparison between this

method and commonly used power (or energy) based methods is discussed. The effectiveness and advantages of the presented method in such cases is also pointed out.

- A brief example on the effects of different inputs on the selection of reduced order physical models is presented.
- The Hankel Singular Values' (HSV) relation to partial fraction expansion (PFE) residues and thus the relation between balanced truncation method and the physical based model reduction is provided.
- It is shown that, "effect" matrices based on the physical representation of the system can be formed that give the relative contribution of system components' on the eigenvalues of the system.

1.3. Thesis Outline

The outline of the thesis is as follows:

Chapter 2 presents a brief survey on the current model reduction methodologies and tools that are used for model reduction, including the basics of bond graphs. In addition to the basics, a relationship between Hankel singular values (HSV) and partial fraction expansion residues is presented. This relationship provides clues for the explanation of the eigenvalues obtained from balanced truncation type of approaches.

Chapter 3 gives the methods used for obtaining eigenvalue distribution of physical linear dynamic systems and presents a procedure for physical domain model reduction. In this chapter, several physical examples are presented to illustrate the efficiency of decomposition procedures.

Chapter 4 provides several examples on the application of the physical domain model reduction procedure that is given in Chapter 3 including multi energy domain systems. In this chapter, additionally, one of the shortcomings of the power and energy method is presented. Via a simple physical example, the effectiveness of using the decomposition procedures is shown.

In Chapter 5, "effect" matrices are introduced. Based on the physical representation of the system, effect matrices are formed that give the relative contribution of system components' on the eigenvalues of the system. Furthermore, a physical based model reduction method based on effect matrices are provided. Several examples are given to illustrate the results.

Chapter 6 summarizes the contribution of the thesis and makes recommendations for further research.

2. A SURVEY ON CURRENT MODEL REDUCTION METHODOLOGIES AND TOOLS FOR MODEL REDUCTION

During modeling of a system, determining a suitable order for the model is very important. It is often easy to find a too complex model, and the issue of reducing the model without removing the important features of it, at least for a given frequency range of interest, becomes important. In recent years attempts have been made to address these issues [17, 18], by looking at the power or the energy of the whole system and the lumped parameter elements, and then to decide whether to keep an element in the system. These approaches are still not complete and are still being investigated [17].

In this thesis, before answering the above type of questions, the tools for model reduction and some of the most commonly used and effective model reduction procedures will be reviewed.

The organization of this chapter is as follows: Section 2.1 gives the commonly used mathematical background in model reduction. Section 2.2 gives brief information on bond graphs. Section 2.3 presents the frequently used model reduction methodologies. One of the most popular methods used is the balanced truncation approach, and in this section it will briefly be explained. Then, the power and energy based methods which are physically based approaches, are reviewed.

2.1. Some Basic Tools for Model Reduction

In this section a brief explanation of basic mathematical tools for model reduction are given for completeness of the thesis. For this purpose, the following concepts are stated: controllability and observability matrices, Hankel singular values, error norms, partial fraction expansion, and residues.

2.1.1. Controllability and Observability Matrices

Consider a linear time invariant (LTI) system given by:

$$\dot{\mathbf{x}} = \mathbf{A}\mathbf{x} + \mathbf{B}\mathbf{u} \quad , \quad \mathbf{x}_{t_0} = \mathbf{x}_0 \tag{2.1}$$

$$\mathbf{y} = \mathbf{C}\mathbf{x} + \mathbf{D}\mathbf{u} \tag{2.2}$$

where $\mathbf{A}$, $\mathbf{B}$, $\mathbf{C}$, $\mathbf{D}$, are the time invariant matrices of compatible sizes. Also, $\mathbf{x} \in \mathcal{R}^n$, $\mathbf{y} \in \mathcal{R}^m$, and $\mathbf{u} \in \mathcal{R}^p$ where n, m and p are the order, the number of outputs and the number of inputs of the system respectively. This representation might also be a linearization of a nonlinear system which is only a reasonable approximation within a specific region around the operating point.

It is very well known that, from this representation, a transfer function matrix, $\mathbf{G}(s)$ can be obtained by:

$$\mathbf{G}(s) = \mathbf{C}(s\mathbf{I} - \mathbf{A})^{-1}\mathbf{B} + \mathbf{D} \tag{2.3}$$

For the rest of this discussion assume that $\mathbf{D} = \mathbf{0}$.

If $\mathbf{G}(s)$ is related to $\mathbf{A}$, $\mathbf{B}$ and $\mathbf{C}$ by Equation (2.3), then $\mathbf{A}$ is minimal in dimension if and only if $(\mathbf{A}, \mathbf{B})$ is completely controllable and $(\mathbf{A}, \mathbf{C})$ is completely observable. Then the $(\mathbf{A}, \mathbf{B}, \mathbf{C})$ is called a minimal realization of $\mathbf{G}(s)$.

For a given system, the controllability and observability matrices can be expressed as follows:

$$\mathbf{W}_c(\tau) \triangleq [\mathbf{B} \;\; \mathbf{AB} \;\; \cdots \;\; \mathbf{A}^{\tau-1}\mathbf{B}] \tag{2.4}$$

$$\mathbf{W}_o(\tau) \triangleq \begin{bmatrix} \mathbf{C} \\ \mathbf{CA} \\ \vdots \\ \mathbf{CA}^{\tau-1} \end{bmatrix} \tag{2.5}$$

where τ represents the length of the horizon on which the controllability and the observability of a system are checked. Then, depending on the value of τ we have the following matrices [21]:

- When $\tau = n$, the controllability and observability matrices of the system are obtained,
- When $\infty > \tau > n$, the finite controllability and observability matrices are obtained, and
- When $\tau = \infty$, the infinite controllability and observability matrices are obtained.

Note that, besides the complete uncontrollable/unonservable states, there could exist some weakly controllable/observable states. The existence of these states can be justified by a bad conditional number of these matrices [7, 21].

2.1.1.1. Gramian Matrices. A robust way of analyzing the controllability and observability of a system is to look at the singular values of the gramian matrices. This provides some insight about the system. For instance, the number of small (compared to the rest) singular values of the controllability gramian will indicate the number of weakly controllable states in the system [7]. Some important properties of the gramians are indicated in the following discussion.

The controllability gramian, $\mathbf{P}$, of a system given by Equations (2.1) and (2.2) is:

$$\mathbf{P} \triangleq \int_0^\infty e^{\mathbf{A}t}\mathbf{B}\mathbf{B}^T e^{\mathbf{A}^T t}\, dt \tag{2.6}$$

and the observability gramian, $\mathbf{Q}$ is:

$$\mathbf{Q} \triangleq \int_0^\infty e^{\mathbf{A}^T t}\mathbf{C}^T\mathbf{C}e^{\mathbf{A}t}\,dt \tag{2.7}$$

The gramians can also be computed from the *Lyapunov* equations [7, 21]:

$$\begin{aligned} \mathbf{A}\mathbf{P} + \mathbf{P}\mathbf{A}^T + \mathbf{B}\mathbf{B}^T &= \mathbf{0} \\ \mathbf{A}^T\mathbf{Q} + \mathbf{Q}\mathbf{A} + \mathbf{C}^T\mathbf{C} &= \mathbf{0} \end{aligned} \tag{2.8}$$

Note that, if the system is asymptotically stable, the Lyapunov equation has a unique solution, and if the system is minimal, $\mathbf{P}$ and $\mathbf{Q}$ are nonsingular.

The positive definite character of the gramians involves some important aspects:

- $\mathbf{P} > 0 \Longleftrightarrow (\mathbf{A}, \mathbf{B})$ is completely controllable,
- $\mathbf{Q} > 0 \Longleftrightarrow (\mathbf{A}, \mathbf{C})$ is completely observable.

The above implications give a more reliable way to test the controllability and observability of a system. Basically, a zero eigenvalue in the controllability gramian $\mathbf{P}$ implies that $(\mathbf{A}, \mathbf{B})$ is uncontrollable, while a zero eigenvalue of the observability gramian $\mathbf{Q}$ implies that $(\mathbf{A}, \mathbf{C})$ is unobservable.

There is also a physical interpretation of the gramians, which will not be discussed here in great detail, but for completeness one important point needs to be given: It has been stated in the literature [7, 22] that, the controllability gramian $\mathbf{P}$ helps to represent a measure of the energy necessary to transport a system from state $\mathbf{x}_0$ to $\mathbf{x}_1$ (two different states). In this case, to assure that the energy quantities are finite, it is assumed that the input signal $\mathbf{u}(t)$ and the output signal $\mathbf{y}(t)$ are square-integrable. Then,

$$\min\left\{ \int_{-\infty}^0 \mathbf{u}^T(t)\mathbf{u}(t)\,dt \right\} = (\mathbf{x}_1 - \mathbf{x}_0)^T\mathbf{P}^{-1}(\mathbf{x}_1 - \mathbf{x}_0) \tag{2.9}$$

Also, an eigenvalue of $\mathbf{P}$ is an expression of the controllability of the system in the direction of the corresponding eigenvector. A large eigenvalue of $\mathbf{P}$ indicates that in the direction of the corresponding eigenvector, little energy is needed to transport the system in that direction. On the other hand, similarly, the observability gramian $\mathbf{Q}$ is related to the energy transmitted to the output [7, 22].

2.1.2. Hankel Singular Values

The Hankel singular values of a transfer function matrix $\mathbf{G}(s)$ are defined as the square roots of the eigenvalues, λ_i, of the product of controllability and observability gramians $(\mathbf{PQ})$:

$$\sigma_i\{\mathbf{G}\} \triangleq \sqrt{\lambda_i(\mathbf{PQ})} \quad , \quad i = 1, \ldots, n \tag{2.10}$$

The gramians are positive definite matrices, hence the eigenvalues of $(\mathbf{PQ})$ are strictly positive, $\sigma_i > 0$. They are usually ordered as $\sigma_1 \geq \sigma_2 \geq \cdots \geq \sigma_n \geq 0$. From the definition of (2.10), one can observe that the Hankel singular values give a measure of the importance of the states in the overall system transfer function matrix.

For the k'th Hankel singular value, $\frac{1}{\sigma_k}$ represents the power needed to drive the k'th state from 0 to 1 (two different state values). Also, the power from k'th state as seen at the output of the system is σ_k. So if σ_k is, let's say, 10 times greater than σ_{k+1}, then the k'th state is 10 times more observable and controllable than $(k+1)$'th state. Thus the ratio between any adjacent Hankel singular values can be compared to a user specified tolerance ε [22, 23],

$$\frac{\sigma_k}{\sigma_{k+1}} > \frac{1}{\varepsilon} \quad , \quad k = 1, 2, \ldots, n-1$$

and by this way the states can be ordered according to their relative importance.

It should be noted that, the name Hankel singular values comes from the fact that they are the singular values of the corresponding Hankel matrix. More details on

Hankel matrices can be found in the literature [7, 16, 21, 24, 25].

2.1.3. Error Norms

When a stable high order system with a transfer function matrix $\mathbf{G}(s)$, such that $\mathbf{G}(s) \in \mathcal{C}^{m\times n}$, is to be approximated by a low order transfer function matrix $\mathbf{G}_r(s)$, the error transfer function is given by

$$\mathbf{E}(s) = \mathbf{G}(s) - \mathbf{G}_r(s) \tag{2.11}$$

where $\mathbf{E}(s)$ is the Laplace transform of $\mathbf{e}(t)$. Note that, in the reduced model, r denotes the reduced model order, but the size of $\mathbf{G}(s)$ and $\mathbf{G}_r(s)$ remains the same, which indicates that they have the same number of inputs and outputs.

Some of the most commonly used error norms are:

- H_2 norm:

$$\|\mathbf{E}\|_2 \triangleq \left[\int_{-\infty}^{\infty} \sum_{i=1}^{p} (\sigma_i(\mathbf{E}(j\omega)))^2 d\omega\right]^{\frac{1}{2}} \tag{2.12}$$

  where $p = \min\{m, n\}$.

- H_∞ norm:

$$\|\mathbf{E}\|_\infty \triangleq \sup_{\omega} \bar{\sigma}\{\mathbf{E}(j\omega)\} \qquad \text{sup: the least upper bound} \tag{2.13}$$

  where $\bar{\sigma}$, represents the largest singular value.

- Hankel norm:

$$\|\mathbf{E}\|_H \triangleq \sigma_{\max}\{\mathbf{E}(s)\} = \sqrt{\lambda_{\max}(\mathbf{PQ})} \tag{2.14}$$

where $\sigma_{\max}$ represents the largest Hankel singular value. It is noted that the

Hankel norm gives the L_2-gain from past inputs to future outputs [6, 24].

As a last note, the smallest error is achieved by the Hankel norm, in other words, $\|\mathbf{E}\|_H \leq \|\mathbf{E}\|_\infty$, [7].

2.1.4. Partial Fraction Expansion and Residues

Consider the single-input single-output (SISO) proper rational function,

$$G(s) = \frac{\sum_{i=0}^{m} b_i s^i}{\sum_{i=0}^{n} a_i s^i} \tag{2.15}$$

where $a_n = 1$ and $n \geq m$.

Suppose the denominator polynomial equation, $\sum_{i=0}^{n} a_i s^i = 0$, has n_1 roots equal to $-p_1$, n_2 roots equal to $-p_2$, ... , n_r roots equal to $-p_r$, where $\sum_{i=1}^{r} n_i = n$. Then,

$$\sum_{i=0}^{n} a_i s^i = \prod_{i=1}^{r} (s + p_i)^{n_i} \tag{2.16}$$

and $G(s)$ can be written as,

$$G(s) = \frac{\sum_{i=0}^{m} b_i s^i}{\prod_{i=1}^{r} (s + p_i)^{n_i}} \tag{2.17}$$

The partial fraction expansion representation of the rational function $G(s)$ is then,

$$G(s) = b_n + \sum_{i=1}^{r} \sum_{k=1}^{n_i} \frac{c_{ik}}{(s + p_i)^k} \tag{2.18}$$

where $b_n = 0$ unless $m = n$ and coefficients are given by[2] ,

$$c_{ik} = \frac{1}{(n_i - k)!} \left\{ \frac{d^{n_i-k}}{ds^{n_i-k}} [(s + p_i)^{n_i} G(s)] \right\} \Big|_{s=-p_i} \tag{2.19}$$

Here the particular coefficients c_{i1}, $i = 1, 2, \ldots, r$, are called the *residues* of $G(s)$ at $-p_i$, $i = 1, 2, \ldots, r$.

Some important properties of residues are:

- A residue c_{i1} at pole $-p_i$ corresponds to a transient term in the time domain, $c_{i1}e^{(-p_i t)}$, so the significance of the residue is that its magnitude is the initial size of the transient corresponding to the pole.
- If a zero is close to a pole, the residue at that pole tends to be small, so the transient is probably small.
- If the zero coincides with the pole, it cancels it, and the transient term is zero.

The same idea of residues can also be extended to multi-input multi-output (MIMO) case [26] as follows:

Consider the linear time-invariant, multivariable system described by

$$\frac{d\mathbf{x}(t)}{dt} = \mathbf{A}\mathbf{x}(t) + \mathbf{B}\mathbf{u}(t) \tag{2.20}$$

$$\mathbf{y}(t) = \mathbf{C}\mathbf{x}(t) \tag{2.21}$$

where $\mathbf{x}(t) \in \mathcal{R}^n$ is the state vector, $\mathbf{u}(t) \in \mathcal{R}^m$ is the control signal, and $\mathbf{y}(t) \in \mathcal{R}^p$ is the vector of output measurements. The transfer function matrix of the dynamic system is

$$\mathbf{G}(s) = \mathbf{C}\,(s\mathbf{I}_n - \mathbf{A})^{-1}\,\mathbf{B} \tag{2.22}$$

[2] This is a direct computation of coefficients, and the roots of the denominator polynomial can be real, repeated or complex.

where $(s\mathbf{I}-\mathbf{A})^{-1}$, called the resolvent matrix, is an $n \times n$ matrix, each element of which is a scalar transfer function, i.e. a ratio of two scalar polynomials.

It is often necessary to find the matrix residues of the partial fraction expansion (PFE) of scalar transfer function matrices $(s\mathbf{I}_n-\mathbf{A})^{-1}$ and $\mathbf{C}(s\mathbf{I}_n-\mathbf{A})^{-1}\mathbf{B}$. There are several well-known methods available, namely:

i. by computing the adj $(s\mathbf{I}_n-\mathbf{A})^{-1}$ by minors or the Leverrier-Faddeeva algorithm and then performing a PFE on the result,
ii. by the use of the modal matrix, taking into consideration the particular nature of the Jordan form of $\mathbf{A}$, and
iii. by the use of the function of a matrix [27, 28, 29, 30].

There are also other less known methods available;

i. using the Lagrange-Sylvester interpolation formula,
ii. using the Cayley-Hamilton theorem, and
iii. using Krylov's matrix [31, 32, 33, 34].

The procedure given here only uses a set of arithmetic operations, and it is particularly suitable for systems with repeated eigenvalues [35].

2.1.4.1. Partial Fraction Expansion of the Resolvent Matrix. The resolvent matrix can be written in two equivalent forms:

$$(s\mathbf{I}_n-\mathbf{A})^{-1} = \frac{\mathbf{B}_1 s^{n-1}+\mathbf{B}_2 s^{n-2}+\cdots+\mathbf{B}_{n-1}s+\mathbf{B}_n}{s^n+s^{n-1}+\cdots+d_{n-1}s+d_n} = \frac{\mathbf{B}(s)}{d(s)} \tag{2.23}$$

$$= \frac{\mathbf{B}_1 s^{n-1}+\mathbf{B}_2 s^{n-2}+\cdots+\mathbf{B}_{n-1}s+\mathbf{B}_n}{(s-\lambda_1)^{m_1}(s-\lambda_2)^{m_2}\cdots(s-\lambda_\sigma)^{m_\sigma}} \tag{2.24}$$

where $\mathbf{B}_i \in \mathcal{R}^{n\times n}$, λ_i is an eigenvalue of $\mathbf{A}$ and m_i its multiplicity, such that $n = \sum_{i=1}^{\sigma} m_i$, and the subscript σ is the number of distinct eigenvalues.

A third form is obtained by expanding into PFE:

$$(s\mathbf{I}_n - \mathbf{A})^{-1} = \sum_{i=1}^{\sigma} \sum_{j=1}^{m_i} \frac{\mathbf{F}_{ij}}{(s-\lambda_i)^j} \tag{2.25}$$

where the coefficients $\mathbf{F}_{ij} \in C^{n\times n}$ are to be determined.

The representation given in Equation (2.23) can also be expressed in polynomial form as $d(s)\mathbf{I}_n = \mathbf{B}(s)\,(s\mathbf{I}_n - \mathbf{A})$, where matrix polynomials of order n are obtained on both sides. By comparing the coefficients of the matrix polynomials, the following expression is obtained:

$$\begin{bmatrix} \mathbf{B}_1 \\ \mathbf{B}_2 \\ \vdots \\ \mathbf{B}_n \end{bmatrix} = \begin{bmatrix} \mathbf{I}_n & \mathbf{0}_n & \cdots & . & \mathbf{0}_n \\ d_1\mathbf{I}_n & . & \cdots & . & . \\ . & . & \cdots & . & . \\ . & . & \cdots & . & \mathbf{0}_n \\ d_{n-1}\mathbf{I}_n & . & \cdots & d_1\mathbf{I}_n & \mathbf{I}_n \end{bmatrix} \begin{bmatrix} \mathbf{I}_n \\ \mathbf{A} \\ \vdots \\ \mathbf{A}^{n-1} \end{bmatrix} \tag{2.26}$$

where $\mathbf{B}_i$ are the matrix coefficients of the numerator polynomial of Equation (2.23). To this end, recall the following well-known definition of Kronecker products:

Definition 1 *Let* $\mathbf{X}$ *be an* $n \times m$ *matrix and* $\mathbf{Y}$ *be a* $p \times q$ *matrix. Then the* $np \times mq$ *matrix*

$$\mathbf{X} \otimes \mathbf{Y} = \begin{bmatrix} X_{11}\mathbf{Y} & \cdots & X_{1m}\mathbf{Y} \\ . & \cdots & . \\ . & \cdots & . \\ X_{n1}\mathbf{Y} & \cdots & X_{nm}\mathbf{Y} \end{bmatrix} \tag{2.27}$$

is called the Kronecker product of $\mathbf{X}$ *and* $\mathbf{Y}$. *It is easily verified from the above definition that* $(\mathbf{X} \otimes \mathbf{Y})(\mathbf{T} \otimes \mathbf{S}) = (\mathbf{XT} \otimes \mathbf{YS})$ *when compatibility exists, (see [27, 36])*

Thus, Equation (2.26) is equivalent to the following Kronecker product represen-

tation:

$$\begin{bmatrix} \mathbf{B}_1 \\ \mathbf{B}_2 \\ \vdots \\ \mathbf{B}_n \end{bmatrix} = (\mathbf{D} \otimes \mathbf{I}_n) \begin{bmatrix} \mathbf{I}_n \\ \mathbf{A} \\ \vdots \\ \mathbf{A}^{n-1} \end{bmatrix} \tag{2.28}$$

where $\mathbf{D}$ is a lower Toeplitz matrix that contains the coefficients of $d(s)$.

The following formula for the matrix residues was derived in [37], which links Equations (2.23) and (2.25):

$$\begin{bmatrix} \mathbf{F}_{11} \\ \mathbf{F}_{21} \\ \vdots \\ \mathbf{F}_{n1} \end{bmatrix} = (\mathbf{V}^{-1}\mathbf{D}^{-1} \otimes \mathbf{I}_n) \begin{bmatrix} \mathbf{B}_1 \\ \mathbf{B}_2 \\ \vdots \\ \mathbf{B}_n \end{bmatrix} \tag{2.29}$$

where on the left-hand side are the desired matrix residues, and the matrix $\mathbf{V}$ is the Vandermonde matrix formed from the eigenvalues of $\mathbf{A}$. For nonrepeated eigenvalues, this matrix is given by:

$$\mathbf{V} = \begin{bmatrix} 1 & 1 & \cdots & 1 \\ \lambda_1 & \lambda_2 & \cdots & \lambda_n \\ \lambda_1^2 & \lambda_2^2 & \cdots & \lambda_n^2 \\ . & . & \cdots & . \\ . & . & \cdots & . \\ \lambda_1^{n-1} & \lambda_2^{n-1} & \cdots & \lambda_n^{n-1} \end{bmatrix} \tag{2.30}$$

The coefficients $\mathbf{F}_{ij}$ of Equation (2.25) are obtained by combining Equations (2.28)

and (2.29); thus, it is seen that

$$\begin{bmatrix} \mathbf{F}_{11} \\ \mathbf{F}_{21} \\ \vdots \\ \mathbf{F}_{n1} \end{bmatrix} = (\mathbf{V}^{-1} \otimes \mathbf{I}_n) \begin{bmatrix} \mathbf{I}_n \\ \mathbf{A} \\ \vdots \\ \mathbf{A}^{n-1} \end{bmatrix} \tag{2.31}$$

which is the desired result for obtaining the matrix residues of PFE of the resolvent matrix $(s\mathbf{I}_n - \mathbf{A})^{-1}$.

For the multiple root case, the Vandermonde matrix in Equation (2.30) is changed to the generalized Vandermonde matrix, defined as follows for an eigenvalue λ_i with multiplicity m_i:

$$\mathbf{V} = \begin{bmatrix} 1 & \cdots & 1 & 0 & 0 & \cdots & 0 & \cdots & 1 \\ \lambda_1 & \cdots & \lambda_i & 1 & 0 & \cdots & 0 & \cdots & \lambda_\sigma \\ \lambda_1^2 & \cdots & \lambda_i^2 & 2\lambda_i & 1 & \cdots & 0 & \cdots & \lambda_\sigma^2 \\ . & \cdots & . & . & . & \cdots & . & \cdots & . \\ . & \cdots & . & . & . & \cdots & . & \cdots & . \\ \lambda_1^{n-1} & \cdots & \lambda_i^{n-1} & \binom{n-1}{1}\lambda_i^{n-2} & \binom{n-1}{2}\lambda_i^{n-3} & \cdots & \binom{n-1}{m_i-1}\lambda_i^{n-m_i} & \cdots & \lambda_\sigma^{n-1} \end{bmatrix}$$

The result given in Equation (2.31) shows that the residues are a linear combination of the powers of $\mathbf{A}$, if $\mathbf{V}^{-1} = \mathbf{\Omega}$; then, the combination for the i'th residue is:

$$\mathbf{F}_{i1} = \omega_{i1}\mathbf{I}_n + \omega_{i2}\mathbf{A} + \cdots + \omega_{in}\mathbf{A}^{n-1} \tag{2.32}$$

2.1.4.2. Partial Fraction Expansion of Transfer Function Matrices. The matrix residues for the PFE of the transfer function matrix (Equation (2.22)) can now be obtained by

pre and post multiplication of Equation (2.25) by $\mathbf{C}$ and $\mathbf{B}$, i.e. the residues $\mathbf{F}_{ij}$

$$\mathbf{C}\left(s\mathbf{I}_n - \mathbf{A}\right)^{-1}\mathbf{B} = \sum_{i=1}^{\sigma}\sum_{j=1}^{m_i}\frac{\mathbf{R}_{ij}}{(s-\lambda_i)^j} \tag{2.33}$$

then the residues in Equation (2.33) become

$$\mathbf{R}_{i1} = \omega_{i1}\mathbf{CB} + \omega_{i2}\mathbf{CAB} + \cdots + \omega_{in}\mathbf{CA}^{n-1}\mathbf{B} \tag{2.34}$$

The above relation shows that the matrix residues are a linear combination of the Markov parameters [29], i.e., $\mathbf{h}_i = \mathbf{CA}^{i-1}\mathbf{B}$ up to order $i = 1, \ldots, n$.

The expression given in Equation (2.34) can be expressed in closed form as

$$\begin{bmatrix} \mathbf{R}_{11} \\ \mathbf{R}_{21} \\ \vdots \\ \mathbf{R}_{n1} \end{bmatrix} = \left(\mathbf{V}^{-1} \otimes \mathbf{I}_p\right) \begin{bmatrix} \mathbf{CB} \\ \mathbf{CAB} \\ \vdots \\ \mathbf{CA}^{n-1}\mathbf{B} \end{bmatrix} \tag{2.35}$$

or equivalently by:

$$\begin{bmatrix} \mathbf{R}_{11} \\ \mathbf{R}_{21} \\ \vdots \\ \mathbf{R}_{n1} \end{bmatrix} = \left(\mathbf{V}^{-1} \otimes \mathbf{C}\right) \begin{bmatrix} \mathbf{B} \\ \mathbf{AB} \\ \vdots \\ \mathbf{A}^{n-1}\mathbf{B} \end{bmatrix} \tag{2.36}$$

In Equation (2.36), the last matrix on the right hand side is the same as the finite controllability matrix $\mathbf{W}_c$ in column form. A rigorous proof which is completely different from the approach shown above can be obtained from the block observability realization as given in [35], or by the use of the well-known Leverrier-Faddeeva algorithm and the formula for PFE of matrix transfer functions [38].

As a result, the three steps for computing the residues of the PFE of $\mathbf{G}(s)$ can be stated as follows:

1. Determine the set of eigenvalues of $\mathbf{A}$ with multiplicities m_i for $i = 1, 2, \ldots, \sigma$.
2. Construct the Vandermonde matrix (or the generalized Vandermonde matrix) $\mathbf{V}$ using the structure given in Equation (2.30).
3. Use formula of Equation (2.35) or (2.36) to calculate the matrix residues.

2.1.4.3. Numerical Example. Consider the 3^{rd} order multi-input multi-output (MIMO) system described by

$$\frac{d\mathbf{x}(t)}{dt} = \begin{bmatrix} 1 & -1 & 0 \\ 3 & -4 & 1 \\ 5 & -6 & 1 \end{bmatrix} \mathbf{x}(t) + \begin{bmatrix} 1 & 2 \\ 0 & 3 \\ 1 & 0 \end{bmatrix} \mathbf{u}(t) \tag{2.37}$$

$$\mathbf{y}(t) = \begin{bmatrix} 1 & 5 & 0 \\ 4 & 1 & 2 \end{bmatrix} \mathbf{x}(t) \tag{2.38}$$

Here, $\det(s\mathbf{I} - \mathbf{A}) = s(s + 1 \pm 1i)$; therefore, the three eigenvalues are distinct with two complex conjugates. Then the matrix residues will be complex for the complex eigenvalues. The Vandermonde matrix has its simplest form (Equation (2.30), and upon applying the formula in Equation (2.36), the matrix coefficients of the PFE can be obtained from

$$\begin{pmatrix} \mathbf{G}_{11} \\ \mathbf{G}_{21} \\ \mathbf{G}_{31} \end{pmatrix} = \left(\begin{bmatrix} 1 & 1 & 1 \\ 0 & -1+i & -1-i \\ 0 & -2i & 2i \end{bmatrix}^{-1} \otimes \begin{bmatrix} 1 & 5 & 0 \\ 4 & 1 & 2 \end{bmatrix} \right) \begin{pmatrix} \mathbf{B} \\ \mathbf{AB} \\ \mathbf{A^2B} \end{pmatrix}$$

Carrying out the multiplication gives the expansion as

$$\mathbf{G}(s) = \frac{\begin{bmatrix} 3.0000 & 21.0000 \\ 3.5000 & 24.5000 \end{bmatrix}}{s} + \frac{\begin{bmatrix} -1.0000 & -2.0000 \\ 1.2500 & -6.7500 \end{bmatrix} + i \begin{bmatrix} -9.5000 & 17.5000 \\ -11.2500 & 19.7500 \end{bmatrix}}{s+1-i}$$
$$+ \frac{\begin{bmatrix} -1.0000 & -2.0000 \\ 1.2500 & -6.7500 \end{bmatrix} - i \begin{bmatrix} -9.5000 & 17.5000 \\ -11.2500 & 19.7500 \end{bmatrix}}{s+1+i}$$

This concludes the example.

Using the Kronecker algebra calculation[3] of the controllability gramian, observability gramian and the cross gramian[4] can be written as

$$\text{vec}(\mathbf{P}) = -[\mathbf{I} \otimes \mathbf{A} + \mathbf{A} \otimes \mathbf{I}]^{-1} \text{vec}(\mathbf{B}\mathbf{B}^T) \tag{2.39}$$

$$\text{vec}(\mathbf{Q}) = -[\mathbf{I} \otimes \mathbf{A}^T + \mathbf{A}^T \otimes \mathbf{I}]^{-1} \text{vec}(\mathbf{C}^T\mathbf{C}) \tag{2.40}$$

$$\text{vec}(\mathbf{W}_{co}) = -[\mathbf{I} \otimes \mathbf{A} + \mathbf{A}^T \otimes \mathbf{I}]^{-1} \text{vec}(\mathbf{B}\mathbf{C}) \tag{2.41}$$

The calculation of the cross gramian for a second order stable system with real and distinct eigenvalues in Jordan form reveals the following result:

A second order system with real and distinct eigenvalues has the following state-space representation:

$$\mathbf{A} = \begin{bmatrix} \lambda_1 & 0 \\ 0 & \lambda_2 \end{bmatrix} \tag{2.42}$$

$$\mathbf{B} = \begin{bmatrix} 1 \\ 1 \end{bmatrix} \tag{2.43}$$

$$\mathbf{C} = \begin{bmatrix} R_1 & R_2 \end{bmatrix} \tag{2.44}$$

[3] More information on Kronecker algebra is given in Appendix A.

[4] See [39] for its definition.

where λ_1 and λ_2 are the eigenvalues and R_1 and R_2 are the corresponding residues, respectively. As $\mathbf{A} = \mathbf{A}^T$, the calculation of the cross-gramian $\mathbf{W}_{co}$ as in Equation (2.41) is as follows:

$$\begin{aligned} \text{vec}(\mathbf{W}_{co}) &= -[\mathbf{I} \otimes \mathbf{A} + \mathbf{A}^T \otimes \mathbf{I}]^{-1}\text{vec}(\mathbf{BC}) && (2.45)\\ &= -(\mathbf{A} \oplus \mathbf{A})\text{vec}(\mathbf{BC}) && (2.46)\\ &= \begin{bmatrix} -\frac{1}{2\lambda_1} & 0 & 0 & 0 \\ 0 & -\frac{1}{\lambda_1+\lambda_2} & 0 & 0 \\ 0 & 0 & -\frac{1}{\lambda_1+\lambda_2} & 0 \\ 0 & 0 & 0 & -\frac{1}{2\lambda_2} \end{bmatrix} \begin{bmatrix} R_1 \\ R_1 \\ R_2 \\ R_2 \end{bmatrix} && (2.47) \end{aligned}$$

$$\mathbf{W}_{co} = \begin{bmatrix} -\frac{R_1}{2\lambda_1} & -\frac{R_2}{\lambda_1+\lambda_2} \\ -\frac{R_1}{\lambda_1+\lambda_2} & -\frac{R_2}{2\lambda_2} \end{bmatrix} \qquad (2.48)$$

It is observed that

$$2 \times \text{trace}(\mathbf{W}_{co}) = -\sum_{i=1}^{2} \frac{R_i}{\lambda_i} \qquad (2.49)$$

which is the DC gain of the system. Additionally the eigenvalues of $\mathbf{W}_{co}$ gives the Hankel singular values of the system (with a corresponding sign). It should be indicated that, without this sign the argument of $\sum_i$(Hankel singular values) = |DC|/2 will become erroneous.

Additionally, a careful analysis of the cross gramian gives some insight on the sign of the corresponding Hankel singular values of the system. Thus for the special case of second order systems with real and distinct eigenvalues the following holds:

$$\text{sign (Hankel singular value)}_i = \text{sign}(-\frac{R}{\lambda})_i \qquad (2.50)$$

An example of this calculation is as follows:

Consider the simple second order system with the transfer function of

$$G(s) = \frac{s+1}{s^2+5s+6} \tag{2.51}$$

This system has the following Jordan form:

$$\mathbf{A} = \begin{bmatrix} -3 & 0 \\ 0 & -2 \end{bmatrix} \tag{2.52}$$

$$\mathbf{B} = \begin{bmatrix} 1 \\ 1 \end{bmatrix} \tag{2.53}$$

$$\mathbf{C} = \begin{bmatrix} 2 & -1 \end{bmatrix} \tag{2.54}$$

The calculation of Hankel singular values using the cross-grammian gives 0.1129, and -0.0295 respectively. With these values, it is verified that Equation (2.50) holds. Additionally the DC gain of the system is calculated as $[0.1129+(-0.0295)]/2 = 0.1667$ which is the correct value.

2.2. Bond Graphs

Modeling and analysis of dynamic system behavior is the key to successful control of complex engineering systems. The bond graph modeling language developed by Paynter provides a systematic framework for compositional modeling of dynamic physical systems from physical principles [40, 41, 42, 43]. This modeling technique facilitates the explanation of causal interactions and temporal relations between parameters by drawing upon fundamental laws of energy conservation and continuity. In

this section brief information on bond graphs is given.

2.2.1. Bond Graph Elements

The bond graphs were originally developed by Paynter [40]. The idea was further developed by Karnopp and Rosenberg in their textbooks [41, 42, 43, 44], such that it could be used in practice [45, 46]. By means of the formulation by Breedveld [47, 48] of a framework based on thermodynamics, bond-graph model description evolved to a systems theory.

Bond graphs are a domain-independent graphical description tool for dynamic behavior of physical systems. This means that systems from different domains (such as electrical, mechanical, hydraulic, acoustical, thermodynamic, material) can be described in the same manner. Bond graphs are based on energy and energy exchange. Analogies between domains are more than just equations being analogous: the used physical concepts are analogous [43].

Bond graph modeling is a powerful tool for modeling engineering systems, especially when different physical domains are involved. Furthermore, bond graph submodels can be reused elegantly, because bond-graph models are non-causal. The submodels can be seen as objects, thus bond graph modeling is a form of object-oriented physical systems modeling.

Bond graphs are labelled and directed graphs, in which the vertices represent submodels and the edges represent an ideal energy connection between power ports. The vertices are idealized descriptions of physical phenomena: they are concepts, denoting the relevant (i.e. dominant and usually interesting) aspects of the dynamic behavior of the system.

To introduce bond graphs, consider the simple RLC circuit of the electrical domain as shown in Figure 2.1.

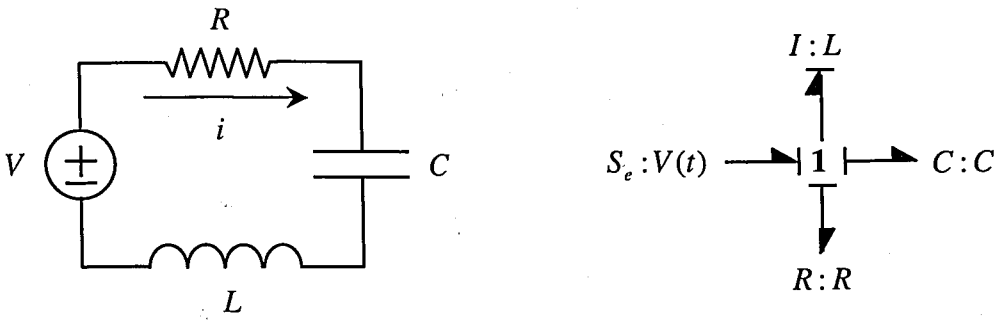

Figure 2.1. Simple RLC circuit

In electrical networks, the port variables of the bond graph elements are the electrical voltage over the element port and electrical current through the element port. Note that a port is an interface of an element to other elements, thus it is the connection point of the bonds. The power being exchanged by a port with the rest of the system is the product of voltage and current: $P = Vi$. The equations of a resistor, capacitor and inductor are:

$$V_R = iR \tag{2.55}$$

$$V_C = \frac{1}{C}\int i dt \tag{2.56}$$

$$V_L = L\frac{di}{dt} \text{ or } I_L = \frac{1}{L}\int V dt \tag{2.57}$$

In order to facilitate the conversion to bond graphs, the different elements of the electrical system are drawn in such a way that their ports become visible. To this port, a *power bond* (or *bond* for short) is connected. This bond denotes the energy exchange between the elements. A bond is drawn as an edge with half an arrow. The direction of this half arrow denotes the positive direction of the energy (power) flow. In principle, the voltage source delivers power and the other elements absorb this power. For this simple RLC circuit, it can be seen that the voltage over the elements are different and through all elements flows the same current. The current is indicated with i and the bonds of all elements are connected with this current. Changing the electrical symbols into corresponding bond graph mnemonics, result in the bond graph of the electrical circuit as shown in Figure 2.1. The common i is changed to a '1', a so-called 1-junction. Writing the specific variables along the bonds makes the bond graph an electrical bond

graph. The voltage is mapped into the domain-independent effort variable and the current maps onto the domain-independent flow variable (the current always on the side of the arrow). The 1-junction means that the current (flow) through all connected bonds is the same, and that the voltages (efforts) sum to zero, considering the sign. This sign is related to the power direction (i.e. direction of the half arrow) of the bond. This summing equation is the Kirchhoff's voltage law.

Parallel connections, on the other hand, in which the voltage over all connected elements is the same, are denoted by a V in the port-symbol network. The bond graph mnemonic is a '0', the so-called 0-junction. A 0-junction means that the voltage (effort) over all connected bonds is the same, and that the currents (flows) add up to zero, considering the sign. The summing equation is the Kirchhoff's current law.

Using similar arguments, analogies between different domains can be drawn. For example, the following analogies exist between mechanical and electrical elements:

- A damper is analogous to an electrical resistor.
- A spring is analogous to a capacitor; the mechanical compliance corresponds to the electrical capacity.
- A mass is analogous to an inductor.
- A force source is analogous to a voltage source.
- A common velocity is analogous to a loop current.

Through the presented RLC example, we have indicated most bond graph symbols and showed how in two physical domains the elements are transformed into bond graph mnemonics. There is one more group of bond graph elements that has not yet been introduced, namely, the transducers. To represent ideal scalings or transformations, bond graphs have two ideal basic elements, transformers and gyrators. They both have two power ports and they are power continuous, i.e., at any instant the power coming in from one of the two ports is equal to the power going out of the other port. For a transformer, the transformation can be within the same domain (toothed wheel, lever) or between different domains (electromotor, winch). Through a

transformer, efforts are transduced to efforts and flows to flows. On the other hand, a gyrator is used for domain transformation. Examples for gyrators are electromotors , pumps and turbines. Detailed information on these elements will be skipped for simplicity. In conclusion, the most important elements of bond graphs are as shown in Table 2.1.

Table 2.1. Important bond graph elements

C	storage element for a generalized displacement-type variable, e.g. capacitor (stores charge), spring (stores displacement)
I	storage element for a generalized momentum-type variable, e.g. inductor (stores flux linkage), mass (stores momentum)
R	resistor dissipating free energy, e.g. electrical resistor, mechanical friction
S_e, S_f	sources, e.g. electrical mains (voltage source), gravity (force source), pump (flow source)
TF	transformer, e.g. an electrical transformer, toothed wheels, lever
GY	gyrator, e.g. electromotor, centrifugal pump
0, 1	0- and 1-junctions, for connecting two or more elements

Once an ideal physical model, i.e. the bond graph elements and power directions are identified, a systematic procedure can be employed to derive a bond graph model. This procedure consists of the identification of the domains and basic elements, the generation of the connection structure (called the junction structure), the placement of the elements, and possibly simplifying the graph. The procedure is different for the mechanical domain compared to the other domains. In the procedure below, these differences are indicated by the statements between the parenthesis. This is because the elements need to be connected to difference variables or across variables. The across variables are the efforts in the non-mechanical domains and the velocities (flows) in the mechanical domains. The eight step procedure for constructing the bond graph of a physical system is as follows:

1. Determine which physical domains exist in the system and identify all basic el-

ements like C, I, R, S_e, S_f, TF and GY. Give every element a unique name to distinguish them from each other.

2. Indicate a reference effort (reference velocity with positive direction for the mechanical domain) in the physical model. Note that only the references in the mechanical domains have a direction.
3. Identify all other efforts (mechanical domains: velocities) and give them unique names.
4. Draw these efforts (mechanical: velocities), and not the references, graphically by 0-junctions (mechanical: 1-junctions). Keep if possible, the same layout as the ideal physical model.
5. Identify all effort differences (mechanical: velocity (= flow) differences) needed to connect the ports of all elements enumerated in Step 1 to the junction structure. Give these differences a unique name, preferably showing the difference nature. As an example, the difference between e_1 and e_2 can be indicated by e_{12}.
6. Construct the effort differences using a 1-junction (mechanical: flow differences with a 0-junction). The junction structure is now ready and the elements can be connected.
7. Connect the port of all elements found at Step 1 with the 0-junctions of the corresponding efforts or effort differences (mechanical: 1-junctions of the corresponding flows or flow differences).
8. Simplify the resulting graph by applying the following rules:
   - A junction between two bonds can be skipped, if the bonds have a 'through' power direction (one bond incoming, the other outgoing).
   - A bond between two of the same junctions can be skipped, and the junctions can join into one junction.
   - Two separately constructed identical effort or flow differences can join into one effort or flow difference.

In this procedure, Steps 1 and 2 concern the identification of the domains and elements and Steps 3 through 6 describe the generation of the connection structure (called the junction structure).

The procedure above is not the only method for deriving bond graphs from physical models. Another one is the so-called inspection method, where parts of the ideal physical model are recognized that can be represented by one junction [43]. An example is a series connection in an electrical network, which is drawn as one 1-junction. Although the inspection method is shorter than the systematic method, it may be error prone [47].

Once the bond graph model is obtained, the next important step is the causality assignment, which is also called as the causal analysis [43, 47].

2.2.2. Causal Analysis

Causal analysis is the determination of the signal direction of the bonds [43]. The energetic connection (bond) is now interpreted as a bi-directional signal flow. The result is a causal bond graph, which can be viewed as a compact block diagram. Besides derivation of equations, causal analysis can give insight in the correctness and competency of the model. These issues especially motivate the discussion of causal analysis in this section.

Depending on the kind of equations of the elements, the element ports can impose constraints on the connected bonds. There are four different causality constraints [4]:

i. *Fixed causality.* Fixed causality is the case, when the equations only allow one of the two port variables to be the outgoing variable. This occurs at sources: an effort source (S_e) has by definition always its effort variable as signal output, and has the causal stroke outwards. This causality is called effort-out causality or effort causality. A flow source (S_f) clearly has a flow-out causality or flow causality. Another situation where fixed causality occurs is at nonlinear elements, where the equations for that port cannot be inverted (for example, division by zero). This is possible at R, GY, TF, C and I elements. Thus, there are two reasons to impose a fixed causality:

   - There is no relation between the port variables.

- The equations are not invertible ('singular').

ii. *Constrained causality.* At TF, GY, 0- and 1-junction, relations exist between the causalities of the different ports of the element. These relations are causal constraints, since the causality of a particular port imposes the causality of the other ports. In a TF, one of the ports has effort-out causality and the other has flow-out causality. In a GY, both ports have either effort-out causality or flow-out causality. At a 0-junction, where all efforts are the same, exactly one bond must bring in the effort. This implies that 0-junctions always have exactly one causal stroke at the side of the junction. The causal condition at a 1-junction is the dual form of the 0-junction. All flows are equal, thus exactly one bond will bring in the flow, implying that exactly one bond has the causal stroke away from the 1-junction.

iii. *Preferred causality.* At the storage elements, the causality determines whether an integration or differentiation with respect to time will be the case. Integration has preference above a differentiation. At the integrating form, an initial condition must be specified [43]. Besides, integration with respect to time is a process, which can be realized physically. Numerical differentiation is not physically realizable, since information at future time points is needed. Another drawback of differentiation occurs when the input contains a step function: the output will then become infinite. Therefore, integrating causality is seen as the preferred causality. This implies that a C-element has effort-out causality and an I-element has flow-out causality at its preference.

iv. *Indifferent causality.* Indifferent causality is used, when there are no causal constraints. As an example, at a linear R, it does not matter which of the port variables is the output.

Therefore we have the following: The S_e and S_f have a fixed causality, the C and I have a preferred causality, the TF, GY, 0 and 1 have constrained causality, and the R has an indifferent causality (provided that the equations of these basic elements all are invertible).

The procedure for assigning causality on a bond graph starts with those elements

that have the strongest causality constraint namely fixed causality (deviation of the causality condition cannot be granted by rewriting the equations, since rewriting is not possible). Via the bonds in the graph, one causality assignment can cause other causalities to be assigned. This effect is called causality propagation: after one assignment, the causality propagates through the bond graph due to the causal constraints.

The three step causality assignment procedure is as follows [43]:

1. i. Choose a fixed causality of a source element, assign its causality, and propagate this assignment through the graph using the causal constraints. Go on until all sources have their causalities assigned.
   ii. Choose an unassigned causal port with fixed causality (non-invertible equations), assign its causality, and propagate this assignment through the graph using the causal constraints. Go on until all ports with fixed causality have their causalities assigned.
2. Choose an unassigned causal port with preferred causality (storage elements), assign its causality, and propagate this assignment through the graph using the causal constraints. Go on until all ports with preferred causality have their causalities assigned.
3. Choose a not yet causal port with indifferent causality, assign its causality, and propagate this assignment through the graph using the causal constraints. Continue until all ports with indifferent causality have their causalities assigned.

Often, the bond graph is completely causal after Step 2, without any causal conflict (all causal conditions are satisfied). If this is not the case, then the place on the bond graph where a conflict occurs can give insight in the correctness and competence of the model [43].

2.2.3. Generation of Equations

A causal bond graph contains all the information to derive the system equations. The model is made up of either a set of ordinary first-order differential equations,

ODEs, when the model is explicit (no causal conflicts), or a set of differential and algebraic equations, DAEs, when the model is implicit (a causal conflict in Step 2 or Step 3 of the causality assignment procedure is necessary).

The procedure to derive the equations is covered by available bond graph software such as Enport [1], MS1 [2], CAMP [3] and 20 - SIM [4, 5]. Therefore, in practice, generation of equations need not be done by hand. However, we shall discuss the generation of equations for the sake of completeness.

The following procedure is used to generate equations [43, 47]:

i. The set of mixed differential and algebraic equations are written. These are the constitutive relations of all elements in computational form, or causal form. This comprises of $2n$ equations of a bond graph having n bonds. n equations compute an effort and n equations compute a flow, or derivatives of them.
ii. The algebraic equations are eliminated. This elimination process can be done by first eliminating the identities coming from the sources and junctions. Thereafter, the multiplications with a parameter, stemming from resistors and transducers (TF, GY) are substituted. At last, the summation equations of the junctions into the differential equations of the storage elements are substituted. During this process, it is efficient to mark the state variables. In principle, the state variables are the contents of the storage elements. However, if the constitutive relations of storage elements are written as one differential equation, the efforts at C-elements and flows at I-elements can also be used. The different choices of state variables are shown in Table 2.2.

If the equations are going to be generated by hand, the first elimination step can be taken into account while formulating the equations at the sources by directly using the signal function at the bond. Furthermore, the variable determining the junction along all bonds connected to that junction can be written. The variable determining the junction is the variable that gets assigned to bond variables of all the other bonds connected to that junction via the identities of the junction equations. At a 0-junction,

Table 2.2. Choice of state variables

Chosen variables	Given name
efforts and flows	Power variables
generalized displacements and momenta	Energy variables (also called as Hamiltonian state variables)
flows and generalized displacements	Lagrange's state variables
efforts and generalized momenta	Complementary Lagrange variables

this is the effort of the only bond with its causal stroke towards the 0-junction. At a 1-junction, this is the flow of the only bond with its causal stroke away from the 1-junction.

In case of dependent storage elements, special care should be given not to eliminate the accompanying state variable. These are the so-called semi state variables. When the state variables are marked, including the semi state variables in this situation, on beforehand, the wrong variable can be prevented from being eliminated. In case of algebraic loops, implicit equations will be encountered. One of the variables in these loops is chosen as algebraic loop breaker and that variable becomes a semi state variable. The equation consisting of the semi state variable of a storage element is eliminated at the second elimination step: it is a multiplication. The semi state variable itself must not be substituted.

This concludes the information on bond graphs. In the next section some of the commonly used model reduction methods will be briefly given.

2.3. Commonly Used Model Reduction Methods

In this section, two of the most commonly used model reduction methodologies are reviewed. These are balanced truncation method, and power and energy methods for model reduction.

2.3.1. Balanced Truncation Model Reduction

Balanced truncation type of approaches, introduced by Moore [10], are based on the singular value decompositions and have the balanced realization as a starting point. This realization is characterized by certain symmetries between controllability and observability of the system. The reduced order model is obtained by discarding those states that are identified to have little effect on the input-output behavior of the system [10, 16, 22, 49, 50, 51, 52].

In this thesis full theory will not be given but a quick review is presented for completeness of the subject.

A balanced realization $(\mathbf{A}_b, \mathbf{B}_b, \mathbf{C}_b, \mathbf{D}_b)$ is defined as a realization where controllability, $\mathbf{P}$, and observability, $\mathbf{Q}$, gramians are equal and diagonal matrices,

$$\mathbf{P} = \mathbf{Q} = \mathbf{\Sigma} \tag{2.58}$$

where

$$\mathbf{\Sigma} = \begin{bmatrix} \sigma_1 & 0 & 0 & 0 \\ 0 & \sigma_2 & 0 & 0 \\ 0 & 0 & \ddots & 0 \\ 0 & 0 & 0 & \sigma_n \end{bmatrix} \tag{2.59}$$

with $\sigma_i,\ i = 1, \ldots, n$ are the Hankel singular values as defined earlier. The balanced realization can be obtained by a similarity transformation $(\mathbf{x}_b = \mathbf{T}\mathbf{x})$, such as,

$$\left.\begin{aligned} \mathbf{A}_b &= \mathbf{T}\mathbf{A}\mathbf{T}^{-1} \\ \mathbf{B}_b &= \mathbf{T}\mathbf{B} \\ \mathbf{C}_b &= \mathbf{C}\mathbf{T}^{-1} \\ \mathbf{D}_b &= \mathbf{D} \end{aligned}\right\} \tag{2.60}$$

with $\mathbf{T}$ being the nonsingular similarity transformation matrix. In order to find this

transformation matrix, one can refer to the following procedure [6]:

Procedure for obtaining the nonsingular transformation matrix, $\mathbf{T}$:

In the special case where $\begin{bmatrix} \mathbf{A} & \mathbf{B} \\ \mathbf{C} & \mathbf{D} \end{bmatrix}$ *is a minimal realization, a balanced realization can be obtained by:*

i. Compute $\mathbf{P} > \mathbf{0}$ *and* $\mathbf{Q} > \mathbf{0}$,

ii. Find a matrix $\mathbf{R}$ *such that* $\mathbf{P} = \mathbf{R}^T\mathbf{R}$,

iii. Diagonalize $\mathbf{RQR}^T$ *to get* $\mathbf{RQR}^T = \mathbf{U}\boldsymbol{\Sigma}^2\mathbf{U}^T$,

iv. Let $\mathbf{T}^{-1} = \mathbf{R}^T\mathbf{U}\boldsymbol{\Sigma}^{-\frac{1}{2}}$. *Then* $\mathbf{TPT}^T = \mathbf{T}^{T^{-1}}\mathbf{QT}^{-1} = \boldsymbol{\Sigma}$ *and consequently* $\begin{bmatrix} \mathbf{TAT}^{-1} & \mathbf{T}B \\ \mathbf{CT}^{-1} & \mathbf{D} \end{bmatrix}$ *is balanced.*

Note that two other closely related realizations are called "input normal realization" with $\mathbf{P} = \mathbf{I}$ and $\mathbf{Q} = \boldsymbol{\Sigma}^2$, and "output normal realization" with $\mathbf{P} = \boldsymbol{\Sigma}^2$ and $\mathbf{Q} = \mathbf{I}$ [6]. Additionally, in MATLAB, balanced realization functions use a slightly different transformation in the form of $\mathbf{x} = \mathbf{Z}\mathbf{x}_b$ where $\mathbf{Z}$ is just the inverse of the $\mathbf{T}$ matrix given here.

Then the basic idea of balance and truncate model reduction can be put in words as,

- Transform the system to an internally balanced realization,
- Neglect all the states that correspond to σ_i, $i > r$, where r is chosen to obtain an acceptable approximation. Typically r is selected somewhere where there is a gap, i.e. $\sigma_r \gg \sigma_{r+1}$.

This method of truncation gives a bound on the difference in frequency response between that of the original system and the reduced order system such that [24, 51],

$$\|\mathbf{G} - \mathbf{G}_r\|_\infty \leq 2 \sum_{i=r+1}^{n} \sigma_i \tag{2.61}$$

Here, an important note should be made. Davidson [53], introduced a new measure made up of Hankel singular values, because the usual method of balance and truncate can, sometimes, eliminate the states which are in fact the most important ones. Here is a short summary of his comments [53]:

Consider the system impulse response norm

$$\|\mathbf{y}\|_2^2 = \int_0^\infty \mathbf{y}^T\mathbf{y}\, dt \tag{2.62}$$

with $\mathbf{y}(t) = \mathbf{C}e^{\mathbf{A}t}\mathbf{B}$. Then,

$$\|\mathbf{y}\|_2^2 = \text{trace} \int_0^\infty \mathbf{y}\mathbf{y}^T\, dt = \text{trace}(\mathbf{C}^T\mathbf{C}\mathbf{P}) = \text{trace}(\mathbf{B}\mathbf{B}^T\mathbf{Q}) \tag{2.63}$$

and we know that $\mathbf{P} = \mathbf{Q} = \text{diag}(\sigma_1, \ldots, \sigma_n)$. If this is evaluated for an SISO system in balanced form $(\mathbf{A}_b, \mathbf{B}_b, \mathbf{C}_b)$ where $\mathbf{B}_b = [b_{b_1}\ b_{b_2}\ \cdots\ b_{b_n}]^T$ and $\mathbf{C}_b = [c_{b_1}\ c_{b_2}\ \cdots\ c_{b_n}]$,

$$\|\mathbf{y}\|_2^2 = \sum_{i=1}^{n} c_{b_i}^2\sigma_i = \sum_{i=1}^{n} b_{b_i}^2\sigma_i = \sum_{i=1}^{n} \mp b_{b_i}c_{b_i}\sigma_i = \sum_{i=1}^{n} d_i \tag{2.64}$$

with d_i being the new measure,

$$d_i = c_{b_i}^2\sigma_i = b_{b_i}^2\sigma_i \tag{2.65}$$

This new measure, basically, helps to reorder the balanced states according to their importance. It is noted that for MIMO systems d_i will be the diagonal elements of $(\mathbf{C}_b^T\mathbf{C}_b\mathbf{P})$.

There has been many successful applications of this method and there were attempts to make it even better in the literature [54, 55].

2.3.2. Power and Energy Methods for Model Reduction

In the past decade, an active research area for model reduction in the physical domain was the development of procedures based on power criteria [17, 18, 56, 57, 58]. The underlying intuition of the power criteria is the conjecture that components associated with small power flow makes small contribution to a system's dynamic behavior. The existing model reduction approaches based on power criteria are composed of the following three major steps,

i. Calculate system's time response under certain input with numerical simulation,
ii. Use various indices to measure the power flow into and/or out of a component,
iii. Remove the components associated with low power flow level.

The idea is to evaluate the individual energy elements of generalized inertance, capacitance and resistance of a full model under a stereotypic set of input and initial conditions. One of the major indices used for the measure of power flow is the use of activity. The activity for each element in the model is calculated by computing the absolute value time integral of the element power over some characteristic time,

$$\text{Activity} = \int_0^T |P_i(t)|dt \tag{2.66}$$

Louca et. al. [17] utilized bond graphs for representing the models of the system. While strictly speaking, the bond graphs are not required by their technique, they clearly are a natural choice due to their explicit representation of the system power topography. In addition, the bond graph junction structure automatically preserves the system configuration or structure.

However, despite of more than ten years of research, no strict mathematical proof has been presented for this approach.

3. INFORMATION FROM PHYSICAL DOMAIN

Obtaining information from physical domain is the most important part in physical domain model reduction procedures. In this chapter the decomposition of linear dynamics will be presented, and a procedure for physical domain model reduction will be given. The decomposition procedures are used to identify fast-slow dynamics, high-low frequency oscillation modes, and heavily-lightly damped dynamic subsystems for the purpose of physical model reduction. Then, these subsystems are associated to the partial fraction expansion residues and eigenvalues of the system. As a last step the relevant physical subsystems are retained by considering the absolute values of the residues (norm in MIMO case) of the full model for obtaining a reduced order model.

3.1. Relation of Eigenvalues to Physical Parameters

The eigenvalues of a given linear system are the most essential dynamic feature in the analysis and design considerations. From the design point of view, the eigenvalues determine the open-loop system behavior and contribute to the performance limits of feedback systems. In the analysis process, the eigenvalues can be easily computed by existing softwares. However, for the purpose of design and physical model reduction, these numerical values do not indicate any possible improvement toward better system performance unless by a huge number of trial-and-error iterations as it is almost impossible to build a direct connection between the eigenvalues and the physical parameters of a system. Therefore, it is important to build this direct relation between the components and the system eigenvalues in order to perform a systematic model reduction procedure.

It is known that the symbolic solutions for the eigenvalues of high order systems are not available. Specifically, it is theoretically impossible to symbolically represent eigenvalues of a system of order six or more. Even if the exact solutions exist, they may be too complicated, and therefore do not point out useful directions. So, instead of using the exact solutions, the use of the approximations (or the bounds) of the

eigenvalues may be feasible. If they can be found by simple computations, the influences of the system components would be shown effectively. In the literature, efforts have been made to find the numerical bounds of the eigenvalues [59]. In addition, a variety of matrix theories have been proposed to find the bounds of the eigenvalues in terms of the matrix components [60]. A method has been proposed by [61] to obtain the formulas of the eigenvalues for a class of systems with uniform parameters[5] . However, in many cases, these approaches still do not provide a satisfactory result.

In this chapter, the difficulty of directly using the existing approaches for building a direct relation between eigenvalues and the physical system is examined. Several decomposition procedures are presented to improve the results. These procedures identify the physical components which influence certain eigenvalues. Using the available matrix theories and other existing approaches, the bounds of each eigenvalue group can be represented in terms of the component parameters [62]. Additionally, physical domain based model reduction schemes can use these results.

In Section 3.2, currently available methods are examined. In this section, Subsection 3.2.1 describes the decomposition procedure for fast-slow dynamics. Section 3.3 shows the decomposition procedure for high-low frequency oscillation modes. Section 3.4 shows the decomposition procedure for the heavily damped modes and the lightly damped modes. The eigenvalue estimations for general systems are discussed in Section 3.5. Several examples are shown in Section 3.6. In Section 3.7, a physical domain model reduction procedure based on decompositions and partial fraction expansion residues is given. The conclusions are stated in Section 3.8.

3.2. Currently Available Methods

The currently available methods for eigenvalue estimation can be divided into two main categories: One of these main categories is the use of the matrix theories such as the Gersĝorin's theorem and its altered versions [60]. These approaches give a

[5] A system has uniform parameters if all the inertance elements, capacitance elements and dissipation elements in the system have the same numeric parameter values respectively.

simple estimate of the bounds in terms of matrix components. As an example, given a complex $n \times n$ matrix $\mathbf{A}$,

$$\mathbf{A} = \begin{bmatrix} a_{11} & a_{12} & \cdots & \cdots & a_{1n} \\ \cdots & \cdots & \cdots & \cdots & \cdots \\ a_{j1} & a_{j2} & \cdots & \cdots & a_{jn} \\ \cdots & \cdots & \cdots & \cdots & \cdots \\ a_{n1} & a_{n2} & \cdots & \cdots & a_{nn} \end{bmatrix} \tag{3.1}$$

a set of Gersĝorin discs $D_j(\mathbf{A})$ can be formed on the s-plane by choosing the diagonal terms as the center and the absolute sum of the off-diagonal terms in each row as the radius [60],

$$D_j(\mathbf{A}) = \left\{ z \in \mathbf{C} : |z - a_{jj}| \leq \sum_{j \neq \ell} |a_{j\ell}| \right\}, \quad \text{for } j = 1, 2, \ldots, n \tag{3.2}$$

The Gersĝorin theorem further proves that each eigenvalue of $\mathbf{A}$ lies in some Gersĝorin's disc of $\mathbf{A}$.

Although this theorem is easy to apply, it cannot be directly used for system design or for model reduction. One obvious reason is that since the physical system parameters are real numbers, the $\mathbf{A}$ matrices of the state equations are real. In this case, the center of the Gersĝorin's discs will be real. If the system possesses complex eigenvalues, the radii of some discs have to be very large to include the eigenvalues in these discs. Therefore, the bounds will be too conservative. To solve this problem, the $\mathbf{A}$ matrices need to be pre-conditioned so that the diagonal terms contain more of the system parameters that affect the characteristics as explained in [63].

The second category of eigenvalue estimation approaches assume that the system has uniform parameters. In that case, it is easier to obtain the eigenmodes of the physical systems. Then the eigenvalues can be easily calculated and simple symbolic expressions can be formed. To explain this concept consider the following example. Figure 3.1 shows the first oscillation mode of a mass-spring system. Since the system

has uniform parameters, there must be a node at exactly the center of the system. Therefore, the eigenvalue of this mode can be determined by either one of the subsystems separated by the node. Similarly, the highest frequency oscillation mode of the same system is shown in Figure 3.2. In this case, there is a node in the middle of each adjacent mass pair. The eigenvalue of each subsystem should be the same and equal to the eigenvalue of this mode. So the exact positions of the nodes can be easily identified and an expression for the eigenvalue of this mode can be obtained.

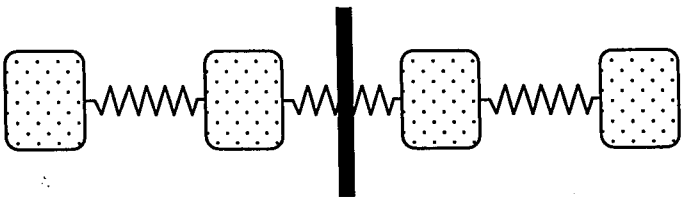

Figure 3.1. The first oscillation mode of a mass-spring system

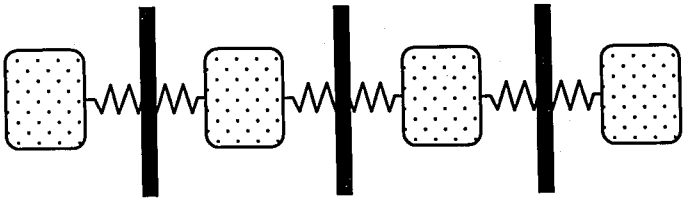

Figure 3.2. The highest frequency oscillation mode of a mass-spring system

However, for general systems with non-uniform parameters, the only result this method can provide is certain bounds on the eigenvalues [62]. These bounds are obtained by forming systems with the uniform parameters which generate the largest and the smallest possible eigenvalues. It is apparent that if the elements of a system has sparse parametric values, these bounds would be very large.

Therefore, to obtain meaningful bounds for the eigenvalues, the physical systems should be decomposed in a way that each subsystem represents a compact group of eigenvalues, if possible. Then, certain methods can be used to estimate the eigenvalues. Since these bounds are closely related to the characteristics of physical elements, the estimated eigenvalues can be directly used in physical model reduction processes.

In the following sections, three decomposition procedures are presented individually for certain categories of dynamic systems. Then, the considerations for general systems will follow.

3.2.1. Decomposition of Fast-Slow Dynamics

One common technique in the application of eigenvalues is the decomposition of fast-slow dynamics. When a system contains fast and slow dynamics, the slow dynamics dominate the system behavior. Therefore, the eigenvalues corresponding to the fast dynamics can be safely ignored in further analysis. However, this process cannot be related to the identification of physical elements which contribute to the fast and slow dynamics. If a design or model reduction task needs to modify the eigenvalues of the dominant (or important) dynamics, such a numerical decomposition does not help and a physical decomposition is necessary.

3.2.2. Singular Perturbation Theory

According to the singular perturbation theory [64], if a system has dynamics with different time scales, the state equations can be decomposed as follows,

$$\dot{\mathbf{x}} = \mathbf{A}\mathbf{x} \Rightarrow \begin{pmatrix} \dot{\mathbf{x}}_1 \\ \epsilon\dot{\mathbf{x}}_2 \end{pmatrix} = \begin{bmatrix} \mathbf{A}_{11} & \mathbf{A}_{12} \\ \mathbf{A}_{21} & \mathbf{A}_{22} \end{bmatrix} \begin{pmatrix} \mathbf{x}_1 \\ \mathbf{x}_2 \end{pmatrix}, \quad \epsilon \ll 1 \tag{3.3}$$

where $\mathbf{x}_1$ is the state vector of the slow dynamics, $\mathbf{x}_2$ is the state vector of the fast dynamics, and ϵ is a normalization factor. In this representation, all the components in the $\mathbf{A}$ matrix have the values with the same order of magnitude.

From the fast dynamics point of view, the states of the slow dynamics are quasi-static. Therefore, the fast dynamics can be represented as

$$\epsilon\dot{\mathbf{x}}_2 = \mathbf{A}_{22}\mathbf{x}_2 \tag{3.4}$$

Since the fast dynamics has much faster transient response, the slow dynamics will evolve with the states $\mathbf{x}_2$ at equilibrium status, i.e. $\dot{\mathbf{x}}_2 = 0$. So the slow dynamics can be derived as

$$\dot{\mathbf{x}}_1 = [\mathbf{A}_{11} - \mathbf{A}_{12}\mathbf{A}_{22}^{-1}\mathbf{A}_{21}]\mathbf{x}_1 \tag{3.5}$$

With this approach, if the computation can be carried out with symbolic descriptions, the system elements which contribute to the fast and slow dynamics can be identified individually. However, this method fails to explore the influence of the system's structure to the eigenvalues.

3.2.3. Decomposition in the Physical Domain

To include the system structure information and obtain useful results the decomposition should be carried out in the physical domain. Namely, this decomposition should be performed directly on a system model such as bond graph models. For a class of systems, this is particularly easy. If the system contains only R, C elements or R, I elements, the eigenvalues will always be real. Thus, the elements that are involved with the fast dynamics or the slow dynamics can be identified as in [19], i.e. the system can be decomposed into two time scales. This identification is carried out using reciprocal bond graphs and by decomposing the system into fast reduced and slow reduced bond graphs using the local loop gain concept. Local loops are the loops between the physical components of a bond graph that have a causal relationship.

As and example consider a simple $R-C$ circuit and its corresponding bond graph as shown in Figures 3.3 and 3.4. In this model, the element C_1 imposes effort to the zero junction, then through the one junction to the element R_1. The element R_1 imposes flow to the one junction and through the zero junction to the element C_1. Therefore, a causal loop is formed between these two elements. Local loop gains are calculated as follows: For an $I-R$ loop, the loop gain is equal to $\frac{I}{R}$, for an $R-C$ loop, the loop gain is equal to $\frac{1}{RC}$, and for an $I-C$ loop, the loop gain is equal to $\frac{1}{IC}$. The $I-R$ or $R-C$ loop gains represent the energy dissipation rates in the local loops

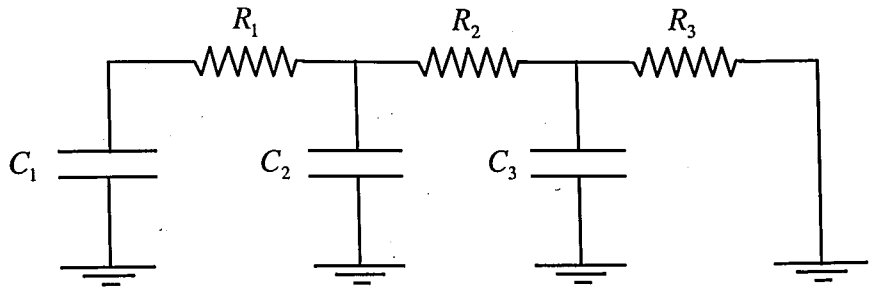

Figure 3.3. An $R-C$ circuit

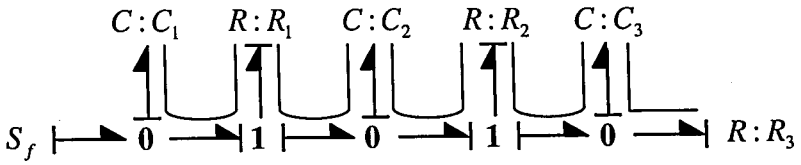

Figure 3.4. The bond graph model of an $R-C$ system

for the corresponding energy storage elements. On the other hand, the square roots of the $I-C$ loop gains represent the energy exchange rates in the local loops. Thus, the loop gain of the above causal path is computed as $\frac{1}{R_1C_1}$. Similarly, a causal loop is formed between the elements R_1 and C_2, C_2 and R_2, R_2 and C_3, C_3 and R_3. Now, the information for the two time scales can be extracted as follows: Suppose the element C_2 has a particularly small value, then the loop gains $\frac{1}{R_1C_2}$ and $\frac{1}{R_2C_2}$ will become much larger than the others. This means that the energy stored in the capacitance C_2 will be dissipated by the resistances R_1 and R_2 very quickly. Therefore, the elements R_1, C_2 and R_2 together with the junctions that the causal loops pass through represent the fast dynamics as shown in Figure 3.5. Once the fast dynamics reaches its equilibrium status ($\dot{q}_2 = 0$), the element C_2 plays no role in the slow dynamics. Replacing the element C_2 with a flow source of zero value can realize this condition [62]. Thus, the model shown in Figure 3.6 represents the slow dynamics.

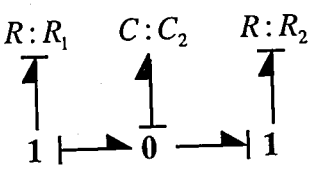

Figure 3.5. The bond graph model of the fast dynamics

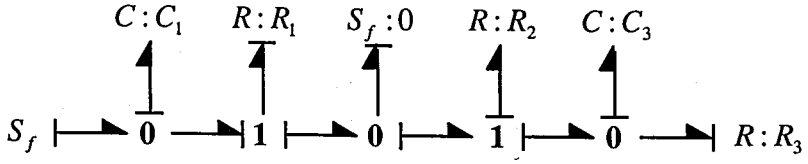

Figure 3.6. The bond graph model of the slow dynamics

It is important to note that, if the equations are derived according to the models in Figures 3.5 and 3.6, they will be exactly the same as those derived from perturbation theory. The inverse of the matrix $\mathbf{A}_{22}$ in Equation (3.5) is automatically solved by the manipulation of the causality [62]. With this approach, the physical elements and the system structures that are responsible for the fast and the slow dynamics can be clearly identified.

Furthermore, if this method is applied to electrical circuits, it provides identical solutions as the well-known 'open-circuit', 'closed-circuit' manipulations. As an example, if a local loop is isolated, the subsystems that do not belong to this loop are 'open-circuited'. As indicated in Figure 3.7, the local loop is formed when R_2, C_2 are isolated. Also, when an inertance element is replaced by an effort source with zero value, it is equivalent to the case where the two ends of this element are 'short-circuited' [62] as shown in Figure 3.8.

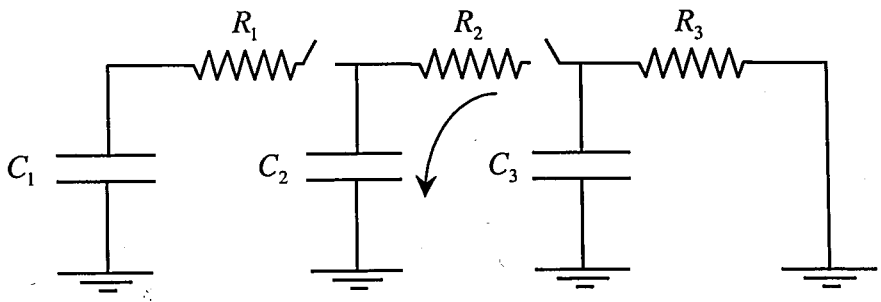

Figure 3.7. An isolated $R-C$ loop

In [62] it is noted that, using this method, even if the system becomes large, the number of loop gains which need to be examined will not grow fast and become difficult to handle. This is because, for each energy storage element, only the elements which

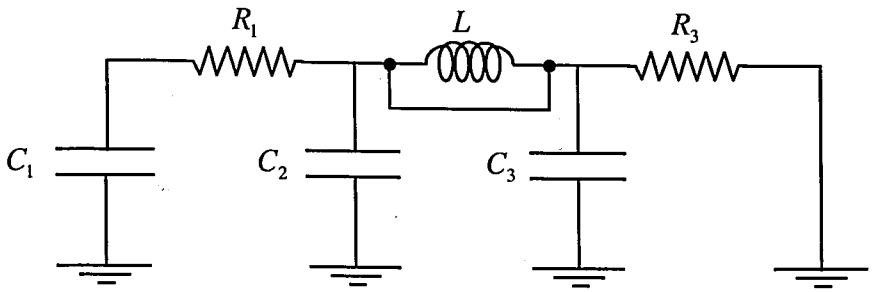

Figure 3.8. A short-circuited I element

are directly casually related to it form local loops. Thus, if the system contains, say, N elements, the number of loop gains which need to be examined will be kN, where k is a positive constant, and not N^2 or C_2^N. The last expression is the number of all possible combinations of any two elements in the system.

3.2.4. A Numerical Example

To verify the results of this decomposition, the state equations corresponding to the fast and slow dynamics of the above $R-C$ circuit are derived as follows (see Figures 3.5 and 3.6):

$$\dot{q}_2 = -\frac{R_1 + R_2}{C_2(R_1 R_2)} q_2 \tag{3.6}$$

$$\begin{pmatrix} \dot{q}_1 \\ \dot{q}_3 \end{pmatrix} = \begin{bmatrix} -\frac{1}{C_1(R_1+R_2)} & \frac{1}{C_3(R_1+R_2)} \\ \frac{1}{C_1(R_1+R_2)} & -\frac{R_1+R_2+R_3}{C_3R_3(R_2+R_3)} \end{bmatrix} \begin{pmatrix} q_1 \\ q_3 \end{pmatrix} \tag{3.7}$$

If the system parameters are assumed to be $C_1 = C_3 = 1$, $C_2 = 0.1$ and $R_1 = R_2 = R_3 = 1$, the numerical $\mathbf{A}$ matrix of the slow dynamics becomes

$$\mathbf{A} = \begin{bmatrix} -0.5 & 0.5 \\ 0.5 & -1.5 \end{bmatrix} \tag{3.8}$$

The eigenvalue of the fast dynamics is -20. The bounds obtained by the Gersĝorin's theorem is shown in Figure 3.9. This result shows that although the decomposed systems represent only the approximations of the eigenvalues, the bounds provide a good estimation on the influences of the physical elements. The symbolic bounds obtained from Equation (3.7) and the approximated eigenvalue obtained from Equation (3.6) can be directly used for either system design or model reduction. In fact for a fast and simple physical model reduction this decomposition may be used [19].

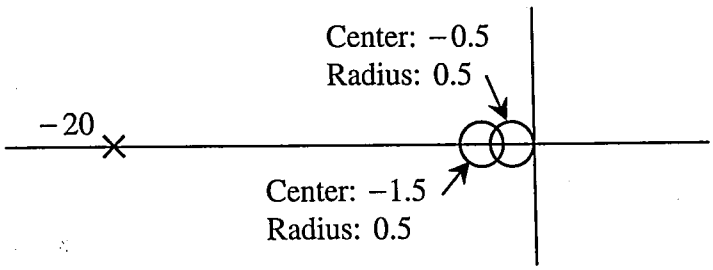

Figure 3.9. The bounds of the eigenvalues

3.3. Decomposition of High-Low Frequency Oscillation Modes

If a system contains only energy storage elements, i.e. inertial I elements and capacitance C elements, all of the eigenvalues of the system will be on the imaginary axis, and the system will exhibit pure oscillations. In this case, the singular perturbation theory fails to provide any conclusion. In this case, as an $I-C$ network can be transformed into a fictitious $R-C$ or $R-I$ network [62], the the decomposition explained to obtain fast and slow dynamics could be extended to $I-C$ systems without any modification. Thus, the subsystems that are responsible for the high and low frequency oscillation modes can be identified if the system contains well separated eigenvalues. For completeness of this subject, the auxiliary transformation of [62] is given below.

3.3.1. An Auxiliary Transformation

The state equations of an $I-C$ system can always be represented in the following general form if they are derived from a bond graph model [62],

$$\begin{pmatrix} \dot{\mathbf{e}} \\ \dot{\mathbf{f}} \end{pmatrix} = \begin{bmatrix} \mathbf{0} & \mathbf{C} \\ \mathbf{I} & \mathbf{0} \end{bmatrix} \begin{pmatrix} \mathbf{e} \\ \mathbf{f} \end{pmatrix} \tag{3.9}$$

where $\mathbf{e}$ is the state vector representing the efforts associated with the C elements, $\mathbf{f}$ is the state vector representing the flows associated with the I elements, $\mathbf{C}$ is a submatrix containing the parameters associated with C elements, and $\mathbf{I}$ is a submatrix containing the parameters associated with I elements. This set of state equations can also be represented as the following alternative forms

$$\ddot{\mathbf{e}} = \mathbf{CIe} \quad \text{or} \quad \ddot{\mathbf{f}} = \mathbf{ICf} \tag{3.10}$$

Note that from this representation, it is clear that the nontrivial eigenvalues of Equation (3.9) will be the square roots of the eigenvalues of matrices **CI** or matrix **IC**.

For the general $I-C$ systems, if all the I elements are replaced by R elements with the same parameters, the following equations can be derived from the bond graph model in a similar manner:

$$\begin{pmatrix} \dot{\mathbf{e}} \\ \mathbf{f} \end{pmatrix} = \begin{bmatrix} \mathbf{0} & \mathbf{C} \\ \mathbf{R} & \mathbf{0} \end{bmatrix} \begin{pmatrix} \mathbf{e} \\ \mathbf{f} \end{pmatrix} \tag{3.11}$$

The state equations can then be represented as

$$\ddot{\mathbf{e}} = \mathbf{CRe} \tag{3.12}$$

Note that the matrix **CR** will be exactly the same as the matrix **CI** of the original system [62].

Similarly, if all the C elements are replaced by R elements with the same parameters, the following equations can be derived from the bond graph model:

$$\begin{pmatrix} \mathbf{e} \\ \dot{\mathbf{f}} \end{pmatrix} = \begin{bmatrix} \mathbf{0} & \mathbf{R} \\ \mathbf{I} & \mathbf{0} \end{bmatrix} \begin{pmatrix} \mathbf{e} \\ \mathbf{f} \end{pmatrix} \tag{3.13}$$

The state equations can be represented as

$$\ddot{\mathbf{f}} = \mathbf{IRf} \tag{3.14}$$

Once more, note that the **IR** will be exactly the same as the matrix **IC** of the original system.

By the above derivations, it can be concluded that if the eigenvalues of matrix **CR** (or equivalently **CI**) can be separated into two groups representing fast and slow dynamics, the eigenvalues of Equation (3.9) can be separated into two groups which are responsible for the high and low frequency oscillation modes. Similarly, if the eigenvalues of matrix **IR** (or equivalently **IC**) can be separated into two groups which represent fast-slow dynamics, the eigenvalues of Equation (3.9) can be separated into two groups which are responsible for the high-low oscillation modes. This transformation procedure simply replaces all the I or C elements in an $I-C$ system by R elements with the same parameters. The effect of such a transformation can be visualized by Figure 3.10. This transformation brings the eigenvalues of the original systems from the imaginary axis to the real axis by a one-on-one mapping. Note that in the actual implementations, such a derivation or transformation is not necessary. Since this transformation is always possible, the application of the decomposition procedure discussed in the previous section is extended to $I-C$ systems without any modification.

3.3.2. Physical Interpretations

By applying the decomposition procedure, the elements and structures that are responsible for the high-low frequency oscillation modes can be identified in a system-

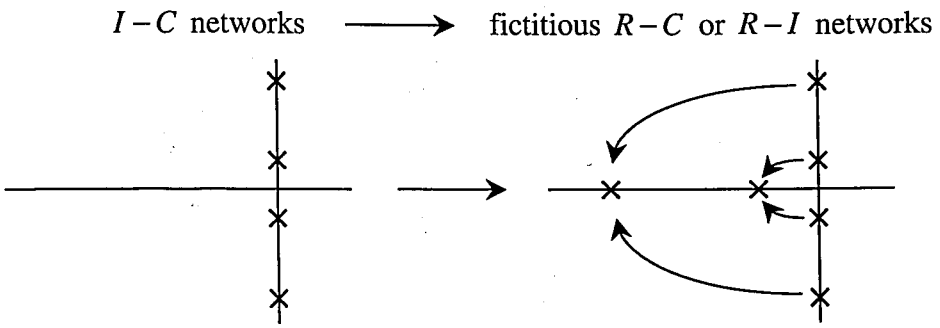

Figure 3.10. The effects of the auxiliary transformation

atic way. These results have physical interpretations, which cannot be obtained by a routine analysis of systems' characteristics. In the following, two examples are used to illustrate the physical interpretations of the decomposition results [62].

A simple cascaded mass-spring system is shown in Figure 3.11. For this system two cases may be examined: In the first case, suppose that the element C_2 has a much smaller value, i.e. this spring is much stiffer than others, and the other elements have values with the same order of magnitude. By examining the local loop gains, it will be found that the loop gain associated with elements C_2, I_1 $(\frac{k_2}{m_1})$ and the one associated with C_2, I_2 $(\frac{k_2}{m_2})$ are much larger than the others $(\frac{k_1}{m_1}, \frac{k_3}{m_2}, \frac{k_3}{m_3})$. The decomposition procedure indicates that the subsystem shown in Figure 3.12 represents the high frequency oscillation mode, and the subsystem shown in Figure 3.13 represents the low frequency oscillation mode. In the low frequency oscillation mode, since the elements I_1 and I_2 are directly casually connected, these elements can be grouped and represented by an equivalent I element as shown in Figure 3.14. The physical interpretation of this decomposition is that in the high frequency oscillation mode, the soft springs have only minor effects on the system behavior. Therefore, they do not appear in the model. However, the stiff spring behaves like a rigid link in the low frequency oscillation mode. The effects of elements I_1 and I_2 are therefore difficult to distinguish.

As a second case, assume that the mass m_2 has a much smaller value than the other two masses, and the other elements have values with the same order of magnitude.

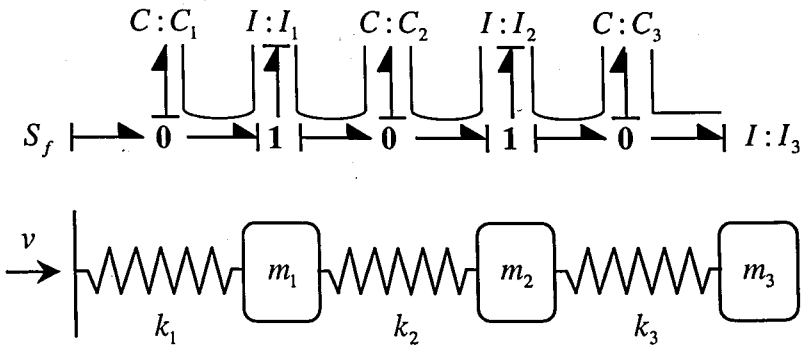

Figure 3.11. An $I - C$ system

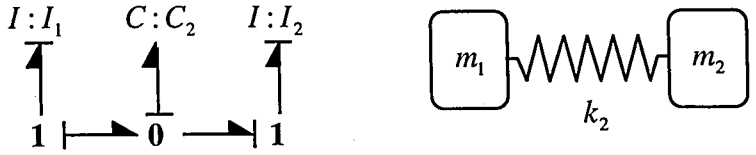

Figure 3.12. High frequency oscillation mode of case 1

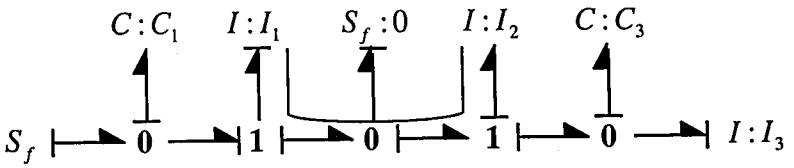

Figure 3.13. Low frequency oscillation mode of case 1

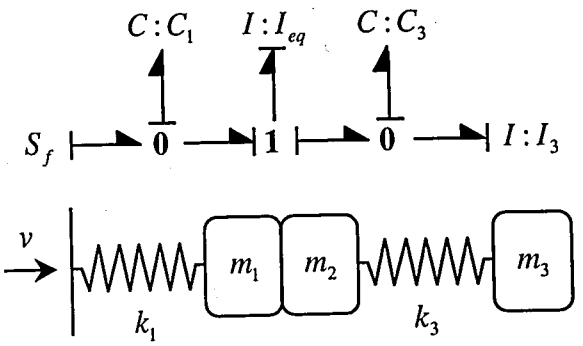

Figure 3.14. Low frequency oscillation mode of case 1 with equivalent I element

Figure 3.15. High frequency oscillation mode of case 2

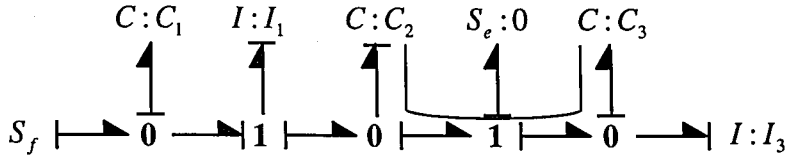

Figure 3.16. Low frequency oscillation mode of case 2

In this case, since the loop gains $\frac{k_1}{m_2}$ and $\frac{k_2}{m_2}$ are much smaller than $\frac{k_1}{m_1}$, $\frac{k_2}{m_3}$, and $\frac{k_3}{m_3}$, the subsystem representing the high frequency oscillation mode will be as shown in Figure 3.15. Consequently, the subsystem representing the low frequency oscillation mode is formed by replacing I_2 with an effort source of zero value as shown in Figure 3.16. In this subsystem, since the elements C_2 and C_3 are directly casually connected, they can be grouped into and equivalent C element as shown in Figure 3.17. The physical interpretation of this decomposition is that in the high frequency oscillation mode, the large inertance elements behave like rigid boundaries. On the other hand, the small mass has almost no effect on the dynamics in the low frequency oscillation mode. Thus, it does not appear in the model.

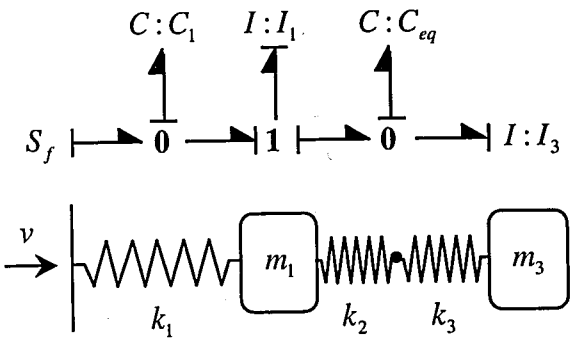

Figure 3.17. Low frequency oscillation mode of case 2 with equivalent C element

3.4. Decomposition of Heavily-damped and Lightly-damped Dynamics

In the previous sections, it is shown that for $R-C$, $R-I$ or $I-C$ networks, a simple procedure can be employed to decompose the physical systems according to their eigenvalue distributions. For general systems, I, R, C elements will be present at the same time. However, under certain assumptions, the presented decomposition procedure can be reasonably applied. For example, if a system contains very little dissipation, the eigenvalues will be very close to the imaginary axis. Therefore, the system can be legitimately considered as an $I-C$ network and given procedure can be applied. On the other hand, if a system contains very large dissipation everywhere, the eigenvalues will be separated into two groups on the real axis. One group represents the faster dynamics. The physical system behaves like an $I-R$ network. The C elements contribute very little to these modes. Another group will be close to the origin and the physical system behaves like an $R-C$ network. Since this dynamics is slow, the I elements have no obvious effect. For example, in the case of simple second order system, $m\ddot{x}+b\dot{x}+kx=0$, the two roots approach to $\frac{b}{m}$ and $\frac{k}{b}$ when b gets large. For each group, the presented procedure can be applied.

In this section, the decomposition procedure is extended for the systems which contain both light and heavy dissipations [62, 65]. The eigenvalue distribution of such systems is shown in Figure 3.18. The eigenvalues will be either close to the imaginary axis or to the real axis. The purpose of this decomposition is to identify the subsystems that are responsible for these two groups of eigenvalues.

3.4.1. The Decomposition Procedure

The decomposition procedure is still based on the local loop gains as discussed before. Additionally, for each energy storage element, instead of a single loop gain, the local damping ratios should also be calculated as that become dominant. For each directly casually related $I-C$ pair in the system (with R elements casually connected to either I or C or both elements), the local damping ratios are calculated as $\frac{G_{RC}}{2\sqrt{G_{IC}}}$ and $\frac{G_{RI}}{2\sqrt{G_{IC}}}$ for the C and I elements respectively. In these formulae, G_{IC} represents

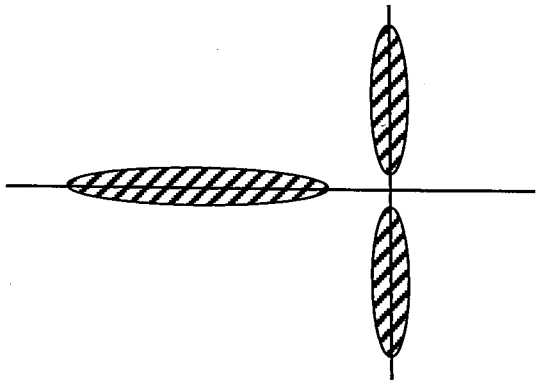

Figure 3.18. The eigenvalue distribution of the systems with both light and heavy dissipations

the $I-C$ loop gain, G_{RC} represents the sum of the $R-C$ loop gains of $R-C$ pairs, and G_{RI} represents the sum of the $R-I$ loop gains of $R-I$ pairs. Notice that this calculation is equivalent to determining the damping ratio of a second order system. In the following, two procedures are presented to decompose the physical system into a subsystem $\mathcal{H}$, which represents the heavily damped eigenmodes and a subsystem $\mathcal{L}$, which represents the lightly damped eigenmodes.

3.4.2. Identification of Heavily Damped Subsystems

The identification of heavily damped subsystems consists of the following ten steps:

1. Replace all the C elements by flow sources with zero value, identify the remaining $R-I$ pairs which are directly casually related. Denote these $R-I$ elements and and the involved junctions as part of the subsystem $\mathcal{H}$.
2. Restore the C elements which are replaced in the previous step. Identify the C elements which are directly casually related to the above I elements. If $\sqrt{G_{IC}} \gg G_{IR}$, then replace the C elements by flow sources with zero value. Denote these flow sources as part of the subsystem $\mathcal{H}$. If the inequality is reversed, neglect the identified C elements.
3. Identify the I elements that become dependent due to the causalities imposed by

the above sources, and denote these I elements as part of the subsystem $\mathcal{H}$.

4. Replace all the I elements by effort sources with zero value, identify the remaining $R-C$ pairs which are directly casually related. Denote these $R-C$ elements and the involved junctions as part of the subsystem $\mathcal{H}$.
5. Restore the I elements that are replaced in the previous step, identify the I elements which are directly causally related to the above C elements. If $\sqrt{G_{IC}} \gg G_{RC}$, then replace the I elements by effort sources with zero value and denote these effort sources as part of the subsystem $\mathcal{H}$. If the inequality is reversed, neglect the identified I elements.
6. Identify the C elements that become dependent due to the causalities imposed by the above sources; denote these C elements as part of the subsystem $\mathcal{H}$.
7. Identify the resistances, which are involved in heavily damped local loops (loops with very large local damping ratios). Denote these R elements and the involved $I-C$ pairs and junctions as part of the subsystem $\mathcal{H}$.
8. Identify the C elements that are not involved in Step 7, but are directly causally related to the above I elements. If $\sqrt{G_{IC}} \gg G_{IR}$, replace the C elements by flow sources with zero value and denote these flow sources and the involved junctions as part of the subsystem $\mathcal{H}$. If the inequality is reversed, neglect the identified C elements.
9. Identify the I elements that are not involved in Step 7, but are directly causally related to the above C elements. If $\sqrt{G_{IC}} \gg G_{RC}$, replace the I elements by effort sources with zero value. Denote these effort sources as part of the subsystem $\mathcal{H}$. If the inequality is reversed, neglect the identified I elements.
10. Remove the elements that are not denoted as part of the subsystem $\mathcal{H}$. The remaining subsystem is the heavily damped subsystem $\mathcal{H}$.

In the above procedure, Step 1 identifies the R and I elements that are responsible for the heavily damped modes given that they affect the dynamics even if all of the capacitances are disabled. Step 2 and Step 3 identify the I elements that are involved in the heavily damped modes by the power transmission through $I-C$ loops. Step 4 to Step 6 repeat the same procedure for $R-C$ elements. Step 7 includes the over-damped subsystems. Steps 8 and 9 identify the I or C elements that affect the heavily damped

modes by the power transmission through other $I - C$ loops.

Similarly, the decomposition procedure for the identification of lightly damped subsystems is explained in the following section.

3.4.3. Identification of Lightly Damped Subsystems

The identification of lightly damped subsystems consists of the following four steps:

1. Identify the $I - C$ pairs, which are involved in lightly damped local loops (loops with small local damping ratios), denote these $I - C$ elements as part of the subsystem $\mathcal{L}$.
2. Identify the R elements which are not involved in Step 1, but are directly causally related to the above I or C elements. If $\sqrt{G_{IC}} \ll G_{RI}$ or $\sqrt{G_{IC}} \ll G_{RC}$, replace the *resistive* R elements by flow sources with zero value and *conductive* R elements by effort sources with zero value, denote these sources as part of the subsystem $\mathcal{L}$.
3. Identify the energy storage elements which become dependent due to the causalities imposed by the above sources; denote these elements as part of the subsystem $\mathcal{L}$.
4. Remove the elements that are not denoted as part of the subsystem $\mathcal{L}$. The remaining subsystem is the lightly damped subsystem $\mathcal{L}$.

In this procedure, Step 1 detects the lightly damped subsystems. Step 2 and Step 3 identify the I or C elements that are involved in the lightly damped modes by considering the power transmission through other $I - R$ loops.

It should be noted that, if multiple paths connect two elements casually, then the effective loop gain is different from the sum of the loop gains corresponding to each individual path. In the latter case, the coupling between the multiple paths is not taken into account. Otherwise, implementation of these procedures remains unchanged.

3.4.4. Example on Identification of Heavily-Lightly Damped Dynamics

Consider the system shown in Figure 3.19. The bond graph representation is shown in Figure 3.20. By applying Steps 1 and 4 of the procedure for heavily damped subsystems, it is found out that there are no remaining $R-I$ or $R-C$ pairs that are directly casually related. Therefore, only Step 7 to Step 9 need to be considered for this example.

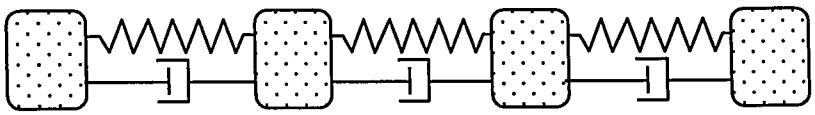

Figure 3.19. A simple mass-spring-damper system

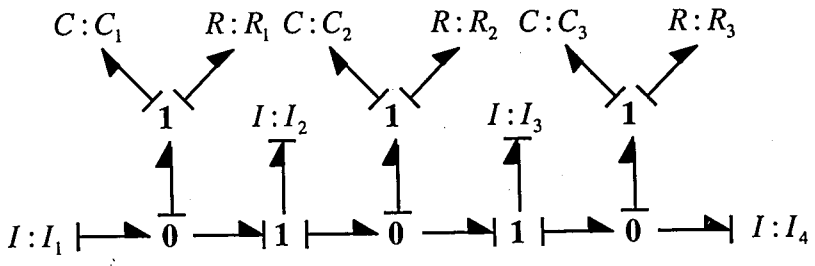

Figure 3.20. The corresponding bond graph model

Suppose that in this system, R_2 has a large value, and R_1 and R_3 are very small. Furthermore, the other elements has the values with the same order of magnitude. In this case, the $I-C$ pairs which are casually related to the element R_2 are involved in the heavily damped modes. Since the natural motion of the lightly damped subsystems is oscillatory, their effects on the heavily damped modes are negligible unless the loop gains of the elements I_2-C_1 and I_3-C_3 are particularly large. Thus, the subsystem shown in Figure 3.21 represents the heavily damped dynamics.

On the other hand, when the system is dominated by the oscillation modes, the subsystem associated with the resistance R_2 cannot follow the motion easily since its natural motion is heavily damped. As a result, this part of system behaves like a rigid mass in the oscillation modes. This constraint can be represented by replacing

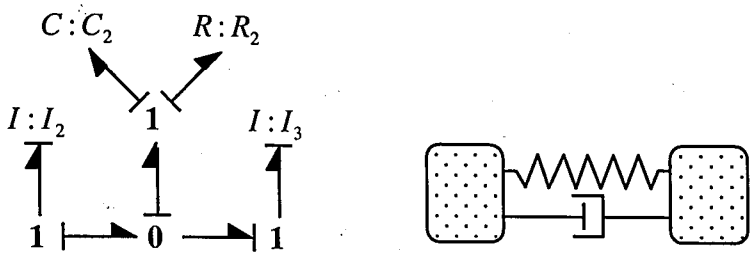

Figure 3.21. The bond graph model representing the heavily damped modes

the resistance R_2 with a flow source with a zero value as shown in the second step of procedure for lightly damped modes. The resulting model is shown in Figure 3.22. The model can also be represented as Figure 3.23, since the element C_2 plays no role in this system. According to Step 2 of procedure for lightly damped subsystems, if the subsystem associated with the resistance R_2 has a large damping ratio due to large R_2 and almost negligible C_2, the model representing the oscillation modes becomes two separate subsystems as shown in Figure 3.24.

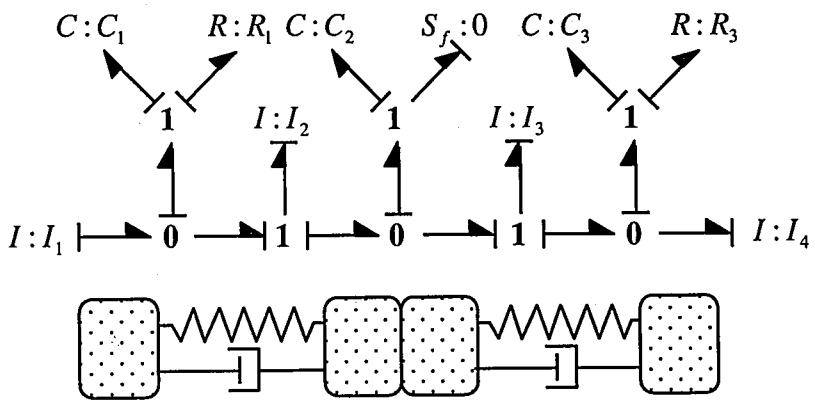

Figure 3.22. The bond graph model representing the lightly damped modes

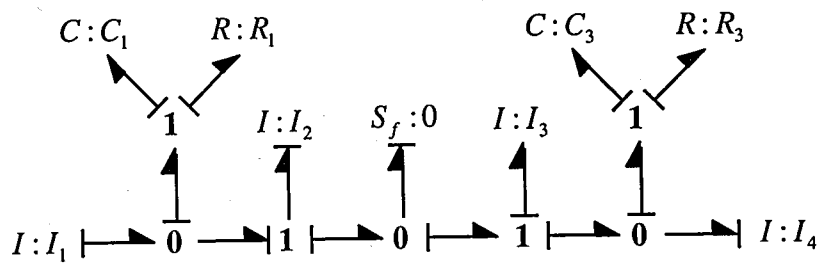

Figure 3.23. The equivalent bond graph model representing the lightly damped modes

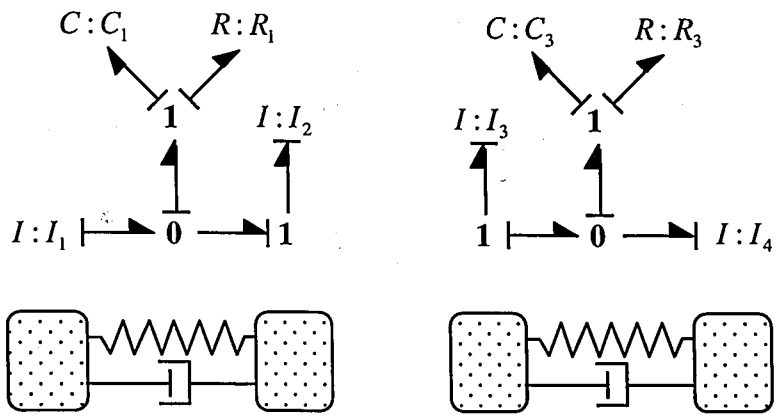

Figure 3.24. The bond graph model representing the lightly damped modes

3.4.5. A Numerical Example

As discussed before, the results from the decomposition procedures are approximations. To demonstrate the accuracy of such approximations, a numerical example is presented in the following. Note that, the purpose of the decomposition is to obtain approximation of the eigenvalues and to use them for physical based model reduction and for system design.

Suppose that in the system of Figure 3.19, $m_1 = m_2 = m_3 = m_4 = 1\,kg$, and $k_1 = k_2 = k_3 = 1\,\frac{N}{m}$. Under this assumption, all of the $I - C$ pairs have the same loop gains. Additionally there are only three different damping ratios; $\zeta_1 = \frac{R_1}{2\sqrt{m_1 k_1}}$ (from the local loops formed by R_1, I_1 and C_1, I_1 as can be seen in Figure 3.20), or $\frac{R_1}{2\sqrt{m_2 k_1}}$, $\zeta_2 = \frac{R_2}{2\sqrt{m_2 k_2}} = \frac{R_2}{2\sqrt{m_3 k_2}}$, and $\zeta_3 = \frac{R_3}{2\sqrt{m_3 k_3}} = \frac{R_3}{2\sqrt{m_4 k_3}}$. Figure 3.25 shows the eigenvalue distribution of two cases: case 1 with $\zeta_1 = \zeta_3 = 0.25$ and $\zeta_2 = 0.7$ and case 2 with $\zeta_1 = \zeta_3 = 0.25$ and $\zeta_2 = 1.4$.

Note that in the first case, the imaginary parts of the estimated eigenvalues with heavier damping ratio are off about 70%. This is because the damping ratio ζ_2 is not large enough. As a result, the coupling of these eigenvalues is not negligible. In the second case, the distribution of the eigenvalues shows the pattern as Figure 3.18, and the estimations are much closer to the true eigenvalues.

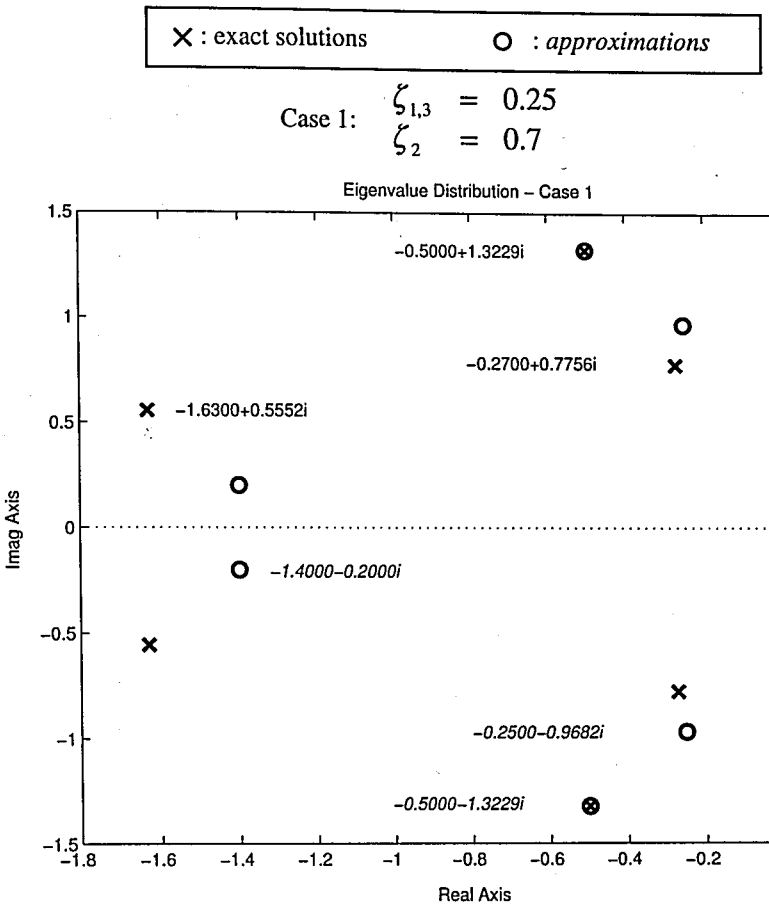

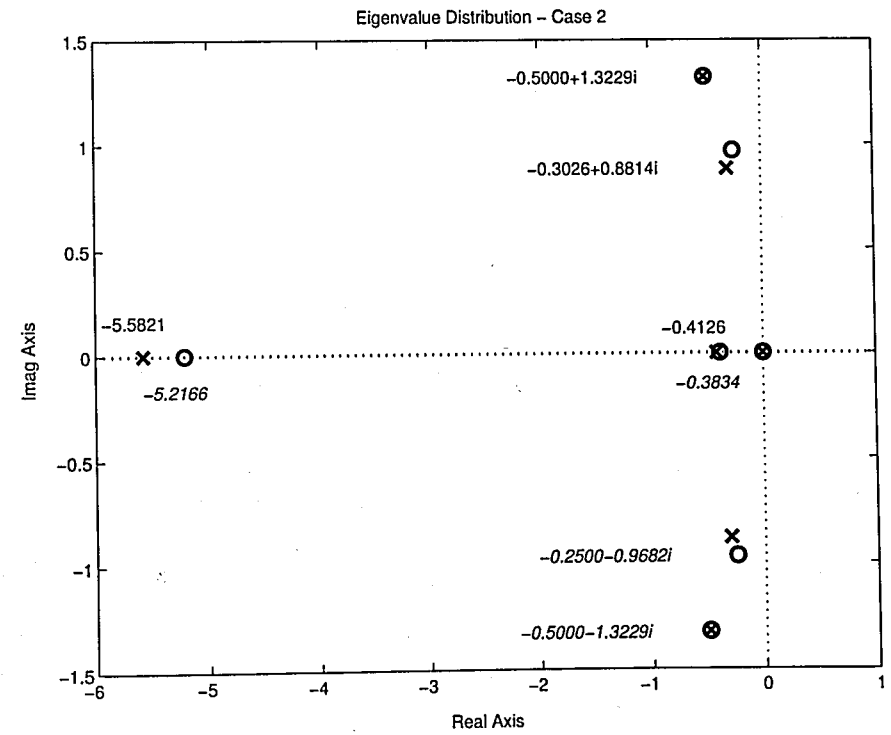

Figure 3.25. The decomposition results for $\zeta_2 = 0.7$ and $\zeta_2 = 1.4$

3.5. Eigenvalue Estimation for General Systems

The presented decomposition procedures can be schematized as in Figure 3.26. If all the local damping ratios are large, the system can be decomposed into an $R-C$ and an $R-I$ network[6] . The procedure described in Section 3.2.1 can be applied to both networks. On the other hand, if all the local damping ratios are small, the system can be treated as an $I-C$ network. The procedure in Section 3.3 can be applied. If the system contains both large and small local damping ratios, the procedure in Section 3.4 can be applied. Also, the decomposed heavily damped subsystems can be decomposed further into $R-C$ and $R-I$ networks and be processed by the procedure in Section 3.2.1.

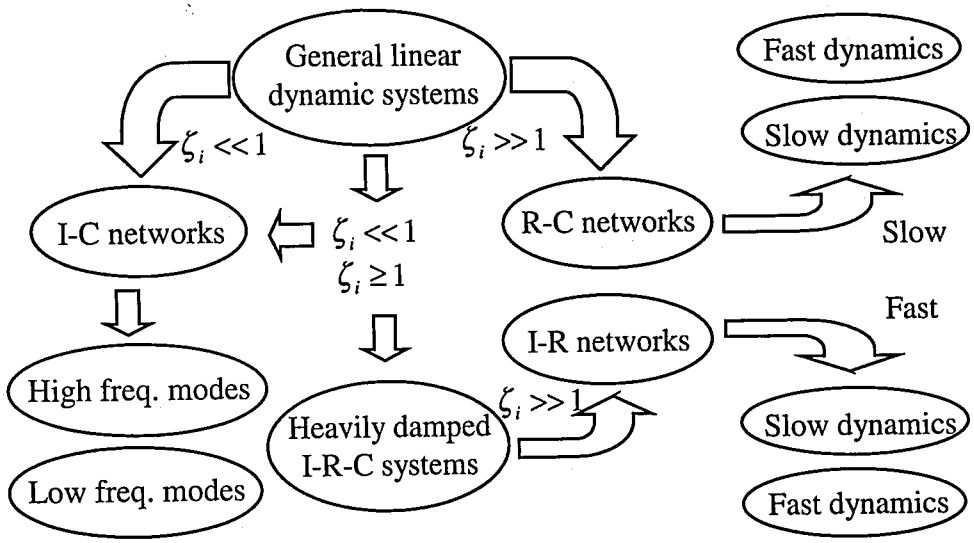

Figure 3.26. A summary of the presented decomposition procedures

By applying these procedures, it is possible to extract only a few eigenvalues out of a large system. In this case, whether the results provide useful information depends on the system characteristics. If the extracted eigenvalues are the dominant eigenvalues, the system's performance can be improved by only modifying the characteristics of very few elements which are strongly related to the dominant eigenvalues and an efficient reduced order model can be obtained. On the contrary, if the extracted eigenvalues are

[6] This includes the case where only one type of energy storage elements appear in part of the system. In that case, the corresponding local damping ratios would be infinitely large.

far from the origin, the result would provide only a limited model reduction.

3.5.1. Undecomposable Systems

A missing link in dealing with the general systems is the following: if a system contains subsystems with local damping ratios around 0.5, none of the presented procedures would directly apply. However, this does not mean that a decomposition is impossible for systems with moderate local damping ratios. For example, if the system eigenvalues have the distribution shown in Figure 3.27, it can be processed by a modified procedure from the results of the previous sections [62]. On the other hand,

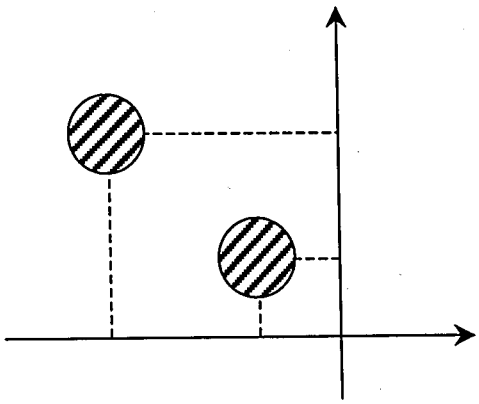

Figure 3.27. A decomposable distribution of eigenvalues

it is almost impossible to provide a decomposition for the distribution in Figure 3.28. In this case, some physical elements may have significant influences in more than one

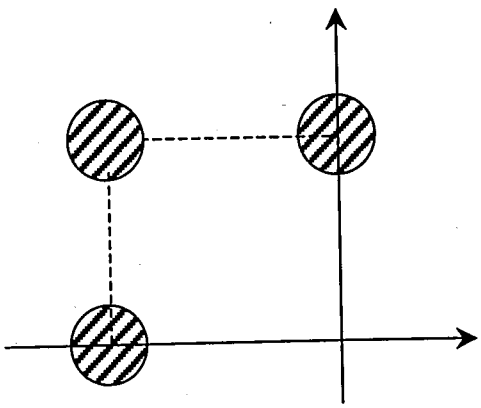

Figure 3.28. An undecomposable distribution of eigenvalues

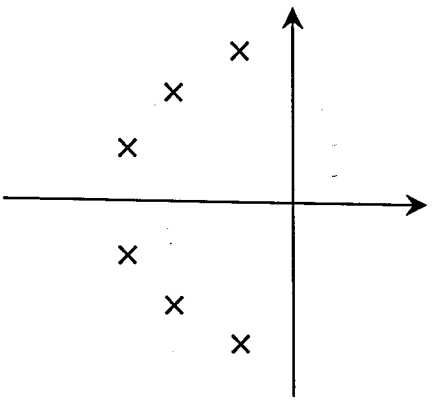

Figure 3.29. The eigenvalue distribution of a Butterworth type filter

group of eigenvalues. As a result, almost all the physical elements are important in every eigenmode. None of the subsystems can be considered individually responsible for a certain eigenmode. For such systems a numerical procedure is provided in Chapter 5. This situation indicates that for such kinds of systems, it is not easy to change the dynamic behavior by modifying only a few elements or subsystems. It may only be possible to move the whole group of eigenvalues by modifying the characteristics of all the energy storage elements or all the dissipative elements. As shown by the eigenvalue distribution of Figure 3.29, Butterworth type of filters are examples of such undecomposable systems. For this category of systems, the best information that can be obtained for model reduction and design is the effects of individual components on the eigenvalues. This issue will be investigated in Chapter 5.

3.6. Examples of Decomposition Procedures

To illustrate the effectiveness of the presented procedures, several numerical examples are given in this section.

3.6.1. A Mechanical Structure

Consider the mechanical system and its bond graph representation shown in Figures 3.30 and 3.31.

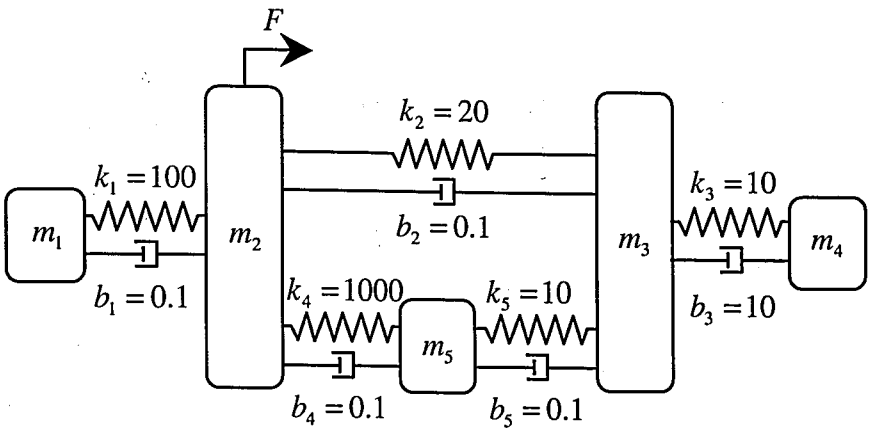

Figure 3.30. A mechanical structure

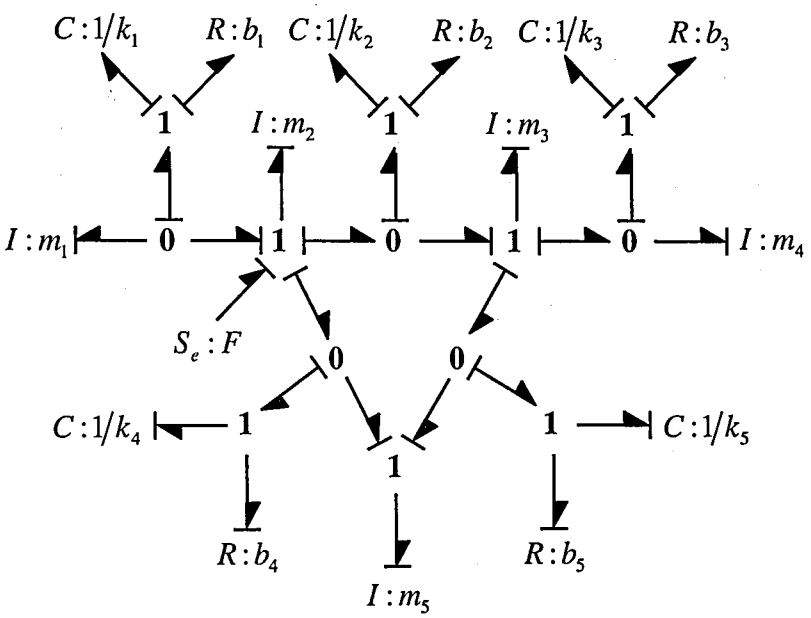

Figure 3.31. The corresponding bond graph model

There are ten independent energy storage elements in integral causality, hence, the order of the system is ten. Assume that in this system, $m_1 = m_2 = m_3 = m_4 = m_5 = 1\,kg$, and the other parameters are as shown on Figure 3.30 with springs having the unit of $\frac{N}{m}$ and dampers having the unit of $\frac{Nsec}{m}$. It is noted that the local damping ratio $\zeta_{3-4} = \frac{b_3}{2\sqrt{k_3 m_3}} = 1.581$ is much larger than the others (maximum $\zeta_{5-3} = 0.01581$, minimum $\zeta_{2-5} = 1.581 \times 10^{-3}$). This suggests that the system can be decomposed into two subsystems representing the heavily damped modes and the lightly damped modes as shown in Figure 3.32. Additionally, in the lightly damped subsystem (as shown in Figure 3.32(b), the local loop gain $\frac{k_4}{m_5} = 1000\ \frac{rad}{sec^2}$ is much larger than the others

(maximum $\frac{k_1}{m_1} = \frac{k_1}{m_2} = 100\ \frac{rad}{sec^2}$, minimum $\frac{k_3}{m_3} = \frac{k_3}{m_4} = 10\ \frac{rad}{sec^2}$). Thus, this subsystem can be decomposed into two subsystems, namely, high frequency and low frequency oscillation modes. as shown in Figure 3.33. Finally, as mentioned before, the two roots of a second order system $m\ddot{x} + b\dot{x} + kx = 0$ approach to $\frac{b}{m}$ and $\frac{k}{b}$ when b is large. Therefore, the heavily damped subsystem consisting of m_3, k_3, b_3 and m_4 can further be decomposed into fast and slow dynamical subsystems as shown in Figure 3.34.

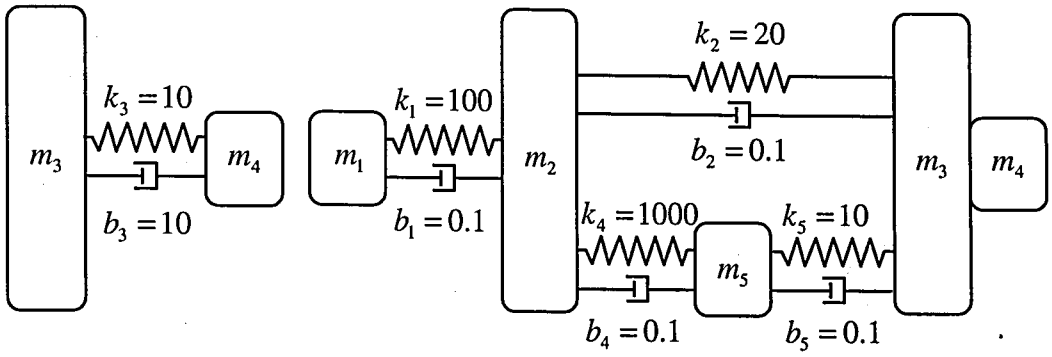

Figure 3.32. The decomposition of heavily damped (a) and lightly damped (b) modes

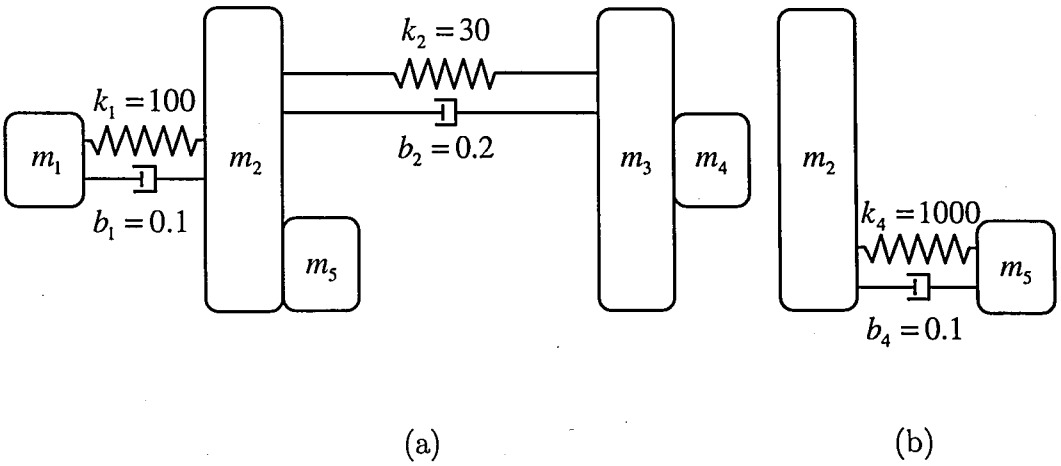

Figure 3.33. The decomposition of high (a) -low (b) frequency oscillation modes

The decomposed subsystems and the numerical eigenvalues are shown in Figure 3.35. One remarks the closeness of these values indicating the effectiveness of the decomposition technique used in the model reduction method. It is possible to quantify the closeness by selecting a norm based on eigenvalues or on the full and reduced order model responses. Suppose that for a design task, the focus is only on the dominant

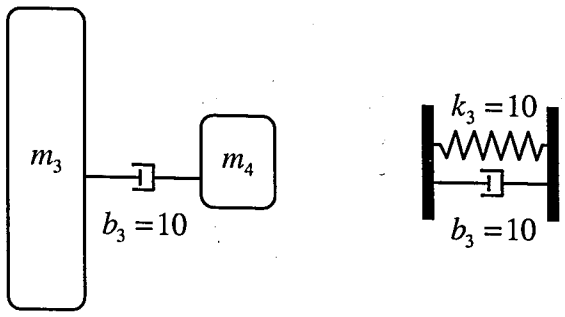

(a) (b)

Figure 3.34. The decomposition of fast (a) -slow (b) dynamics

dynamics as encircled in Figure 3.35. The considered physical system should include the low frequency oscillation mode, subsystem 1, and the slow dynamics, subsystem 4. As a result, the complex system in Figure 3.30 can be simplified into the system in Figure 3.36. Since the simplified model reasonably approximates the behavior of the original system, further analysis can be performed on it.

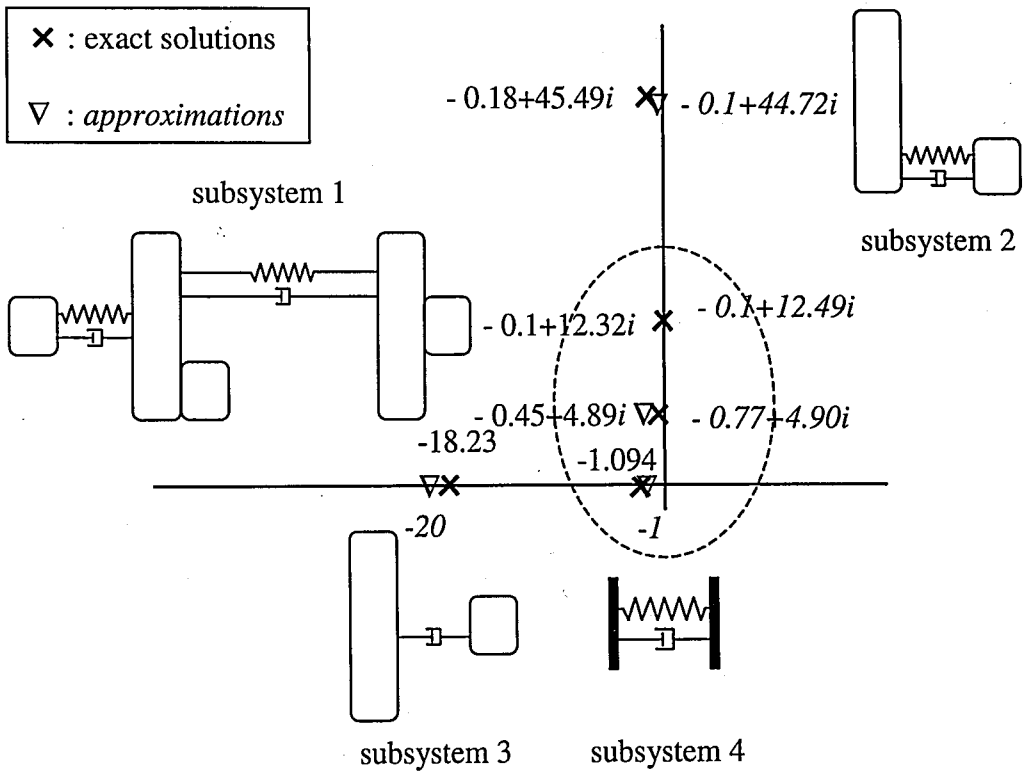

Figure 3.35. The estimated eigenvalues from the decomposed subsystems

As discussed in Section 3.3, the state equations of an $I-C$ system can be written

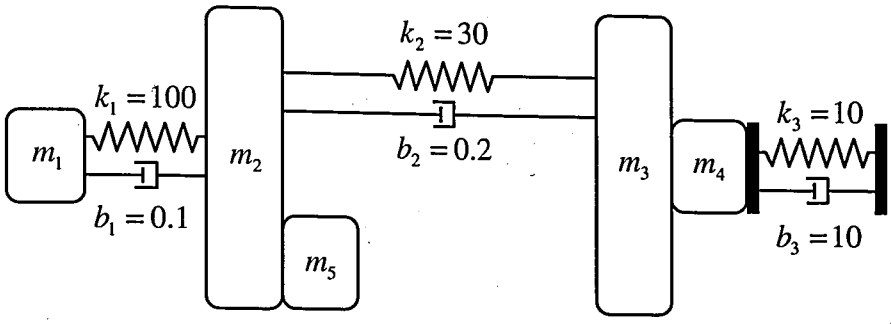

Figure 3.36. The physical subsystems representing the dominant dynamics

in the form of Equation 3.9. In this case, the A matrix of subsystem 1 in Figure 3.35 can be written as [62]:

$$\mathbf{A} = \left[\begin{array}{cc|ccc} 0 & 0 & \frac{1}{m_1} & -\frac{1}{m_2+m_5} & 0 \\ 0 & 0 & 0 & \frac{1}{m_2+m_5} & -\frac{1}{m_3+m_4} \\ \hline -k_1 & 0 & 0 & 0 & 0 \\ k_1 & -(k_2+k_5) & 0 & 0 & 0 \\ 0 & (k_2+k_5) & 0 & 0 & 0 \end{array}\right] \tag{3.15}$$

Let $m_2' = m_2 + m_5$, $m_3' = m_3 + m_4$, $k_2' = k_2 + k_5$ and $b_2' = b_2 + b_5$. Then the eigenvalues of this matrix will be the square roots of the eigenvalues of the matrix

$$\begin{bmatrix} \frac{1}{m_1} & -\frac{1}{m_2'} & 0 \\ 0 & \frac{1}{m_2'} & -\frac{1}{m_3'} \end{bmatrix} \begin{bmatrix} -k_1 & 0 \\ k_1 & -k_2' \\ 0 & k_2' \end{bmatrix} = \begin{bmatrix} -\frac{k_1}{m_1} - \frac{k_1}{m_2'} & \frac{k_2'}{m_2'} \\ \frac{k_1}{m_2'} & -\frac{k_2'}{m_2'} - \frac{k_2'}{m_3'} \end{bmatrix} \tag{3.16}$$

By applying the Gersĝorin's theorem, the bounds of the eigenvalues are calculated and they are shown in Figure 3.37. Examining the symbolic bounds, it can be concluded that the most efficient way to increase the lower bound of the oscillation frequency is to increase the value of element k_2. On the other hand, the most efficient way to tighten the upper bound is to reduce the value of k_1. However, when k_2' becomes too large and k_1 becomes too small, their roles switch. Note that k_3 and b_3 have very little effect on the oscillation modes. They are mostly responsible for the overdamped mode. This kind of physical information can only be obtained by the physical examination of the

system.

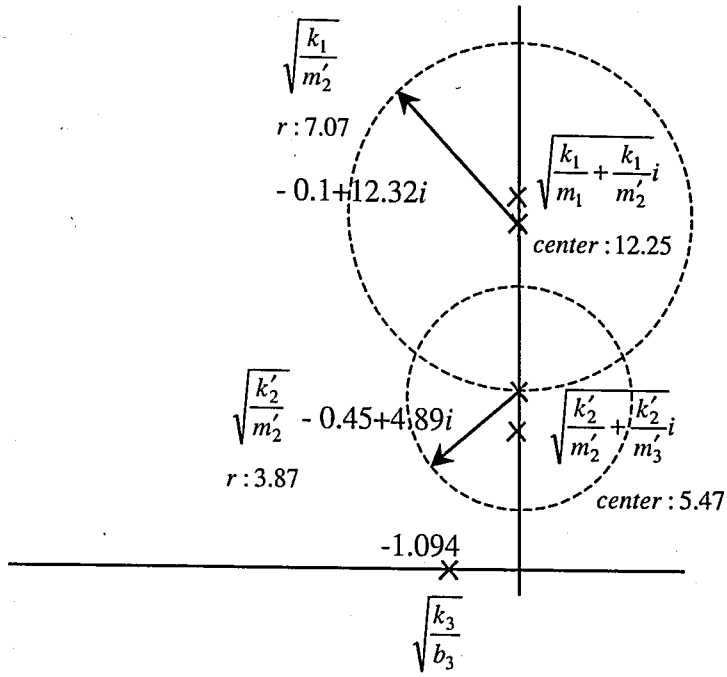

Figure 3.37. The oscillation modes for the dominant dynamics

3.6.2. An Arm Prosthesis

A schematic of a simple arm prosthesis mechanism [66] is shown in Figure 3.38. It can be observed that this system is a multi energy domain system. The input of this system is the current to the motor and the output is the angular velocity of the arm prosthesis. The bond graph of the arm prosthesis is shown in Figure 3.39. Note that due to kinematic relations, the model contains a junction loop [62, 66]. The **A** matrix of this system is shown below:

$$\mathbf{A} = \begin{bmatrix} 0 & -\frac{(\frac{1}{T_1}+\frac{1}{T_2})}{I_f} & \frac{1}{I_m T_1} \\ \frac{(\frac{1}{T_1}+\frac{1}{T_2})}{C_b} & -\frac{(R_m+\frac{R_i}{T_2^2}+R_f)}{I_f} & \frac{R_m}{I_m} \\ -\frac{1}{C_b T_1} & \frac{R_m}{I_f} & -\frac{R_m}{I_m} \end{bmatrix} \tag{3.17}$$

The eigenvalue locations of this system are in a pattern shown in Figure 3.40, assuming that the dissipations are reasonably small [62].

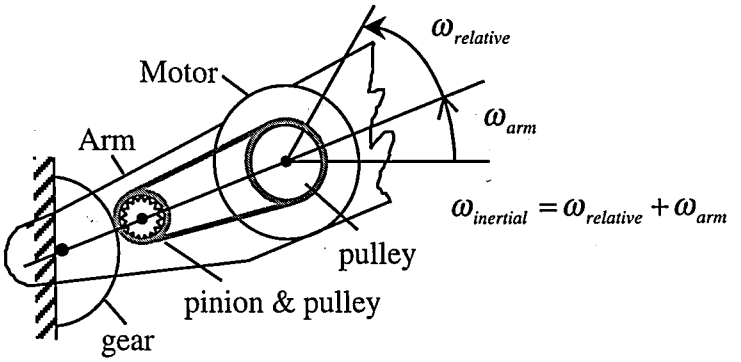

Figure 3.38. The schematic of an arm prosthesis

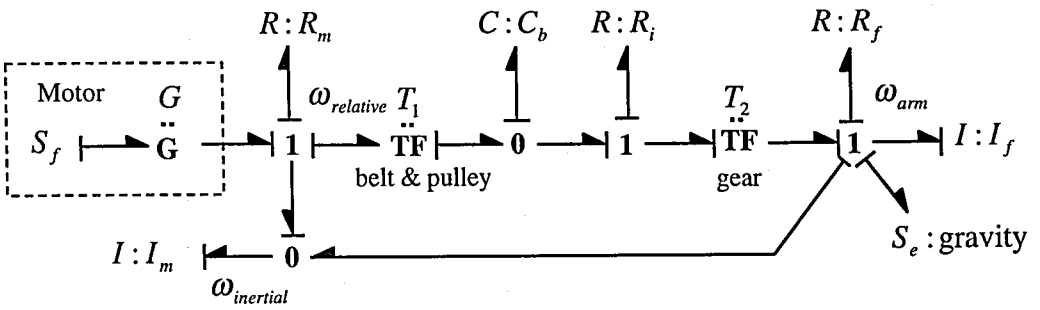

Figure 3.39. The bond graph of an arm prosthesis

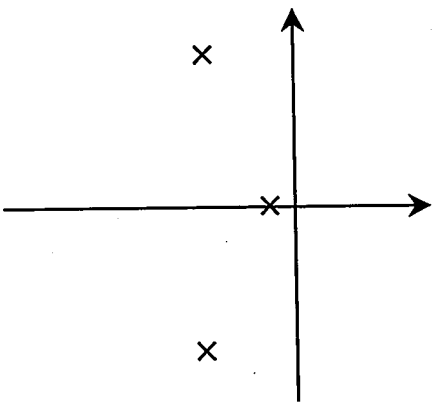

Figure 3.40. The eigenvalue distribution of the arm prosthesis

Although this is only a 3^{rd} order system, there is no simple way to address the influence of the system parameters to its eigenvalues. On the other hand, the decomposition procedures discussed in this chapter can be employed to provide a useful insight about the relation between the system parameters / structures and the eigenvalues.

First of all, by examining the causal relations, it can be found that the capacitance

C_b has multiple causal paths leading to the inertance I_f. This does not change the fact that local loop gains serve as a guide line for decompositions. In this case, the effective loop gain associated with the multiple causal paths must be calculated. Such a loop gain associated with C_b and I_f is $(\frac{1}{T_1}+\frac{1}{T_2})^2\frac{1}{C_bI_f}$ as indicated by the dashed loop shown in Figure 3.41. Note that this gain is not just the sum of the loop gains associated with each single causal path: $(\frac{1}{T_1^2}+\frac{1}{T_2^2})\frac{1}{C_bI_f}$. The coupling between the two causal paths should also be considered.

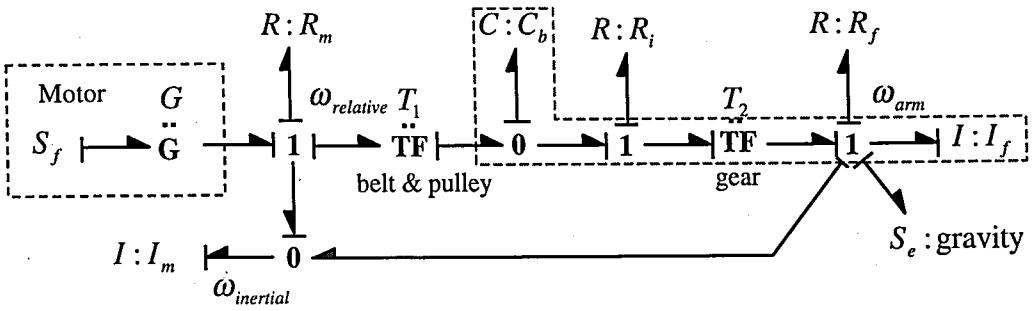

Figure 3.41. The local loop of C_b, I_f

On the other hand, since the capacitance C_b is also casually related to the inertance I_m (the loop gain is $\frac{1}{T_1^2}\frac{1}{C_bI_m}$ as indicated by the dashed loop shown in Figure 3.42), the elements C_b, I_m, and I_f are all responsible for an oscillation eigenmode unless the dissipations are extremely large. If I_m is much larger than I_f or T_2 is particularly small,

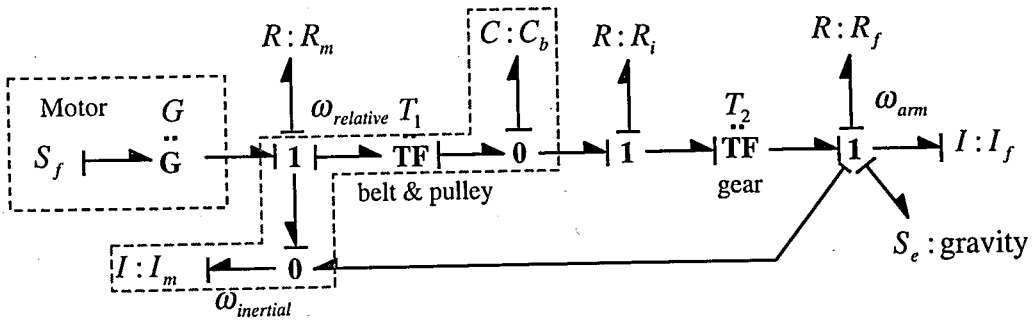

Figure 3.42. The local loop of C_b, I_m

the C_b, I_f loop will dominate. In this case, the frequency of the oscillation mode would be close to $\sqrt{(\frac{1}{T_1}+\frac{1}{T_2})^2\frac{1}{C_bI_f}}$. On the contrary, if I_f is particularly large, the frequency would be close to $\sqrt{\frac{1}{T_1^2}\frac{1}{C_bI_m}}$. On the other hand, if the loop gains concerning C_b, I_f

and C_b, I_m are about the same order of magnitude, the coupling between these three elements can not be neglected.

Figure 3.43 shows the bond graph model corresponding to the pure oscillation eigenmode by removing the dissipations and the inputs. Note that, from the properties of bond graphs, the subsystem enclosed by the dashed line can be represented by an equivalent inertance. Figure 3.44 shows the revised model. From this model, the frequency of the oscillation mode is calculated to be $\sqrt{\frac{1}{T_1^2}\frac{1}{C_b I_m} + (\frac{1}{T_1} + \frac{1}{T_2})^2 \frac{1}{C_b I_f}}$. Since this is only an approximation, the exact value would be smaller due to dissipation. However, this expression is already useful in determining the oscillation and in designing the parameters to increase or decrease the frequency of the oscillation mode.

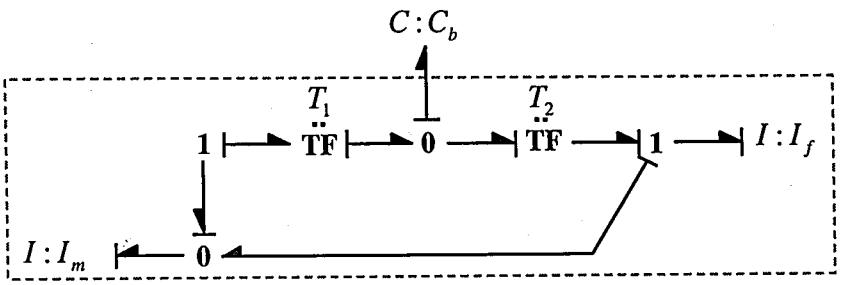

Figure 3.43. The bond graph model representing the pure oscillation eigenmode

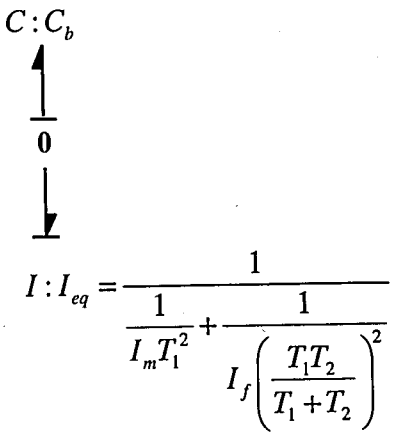

Figure 3.44. The equivalent bond graph model representing the pure oscillation eigenmode

The system under consideration is a 3^{rd} order system. Therefore, the last eigen-

value must be a real number. In Section 3.4, it is shown that a system with lightly damped and heavily damped modes can be effectively decomposed. A single real eigenvalue can be treated as an extreme case of heavily damped modes. Also, in this arm prosthesis model, there is no dissipative elements directly casually connected to the capacitance C_b. So this real eigenvalue must be from the R and I elements. Assuming all the R elements are reasonably small, by applying Step 1 to 3 of the first procedure in Section 3.4, this real mode can be represented by replacing the capacitance using a flow source with zero value. This model is shown in Figure 3.45. From the causality, it can be concluded that this system has only one eigenvalue. The model can be simplified step by step as shown from Figure 3.46 to Figure 3.49. Finally, from Figure 3.49, the eigenvalue can be obtained as $\lambda = \frac{R_m+R_iT_1^2+R_fT_1^2T_2^2}{I_m(1+T_1T_2)^2+I_fT_1^2T_2^2}$.

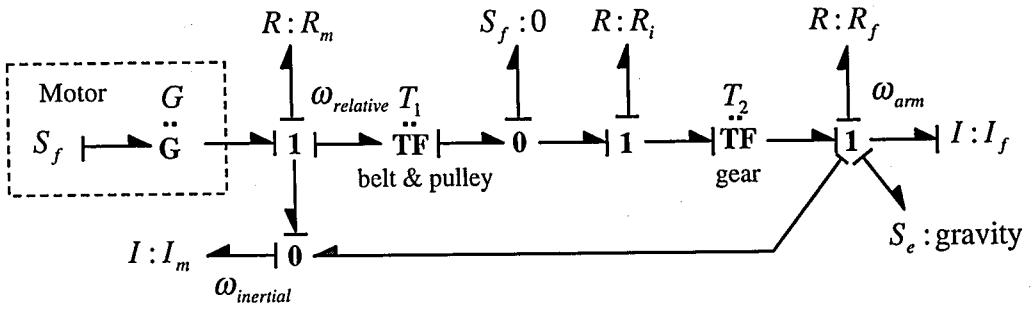

Figure 3.45. The bond graph model corresponding to the real eigenvalue

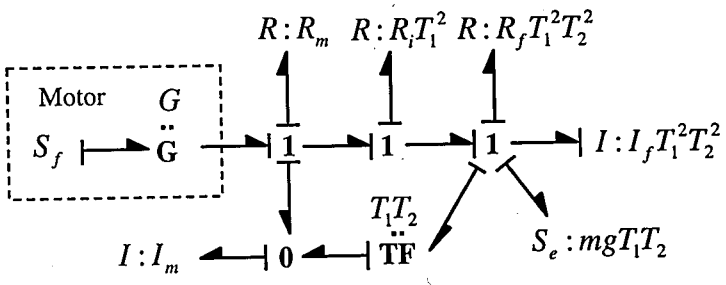

Figure 3.46. A simplified bond graph model

To evaluate the accuracy of the above approximations, several numerical calculations are presented in Table 3.1. In these calculations, the errors of the oscillation frequencies increase when the local damping ratios increase. However, if the values of the dissipative elements are held the same, the approximated oscillation frequencies

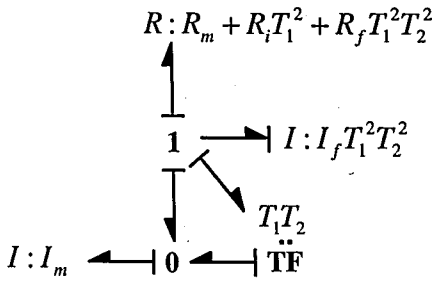

Figure 3.47. A simplified bond graph model

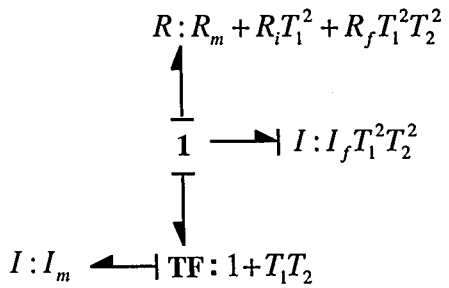

Figure 3.48. A simplified bond graph model

are roughly proportional to the true frequencies. On the other hand, the approximated real eigenvalues are very close to the true values when the values of R's are within a range. These results consequently means that a reduced order model will be very close to the original model with these values.

Note that, using the decomposition procedures the influence of the element characteristics such as the transformer parameters T_1 and T_2 on the eigenvalues are effectively shown by the symbolic approximate eigenvalue expressions. The result shows that T_1 and T_2 are coupled with other elements in particular ways for different group

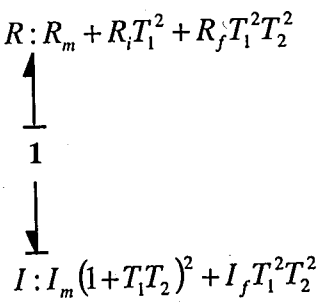

Figure 3.49. A bond graph model representing the real eigenmode

Table 3.1. Numerical evaluations of the approximated eigenmode models

I_f	I_m	C_b	T_1	T_2	R_m	R_i	R_f	True Eigenvalues	Approximated Eigenvalues
0.2	0.1	0.05	2	1.5	0.1	0.1	0.2	$-1.0775 \pm 13.5996i$	$\pm 13.6423i$
								-0.5672	-0.6775
0.2	0.1	0.05	2	1.5	0.4	0.6	0.4	$-3.7386 \pm 13.0992i$	$\pm 13.6423i$
								-1.8562	-1.8824
0.2	0.1	0.1	2	1.5	0.4	0.6	0.4	$-3.7355 \pm 8.8612i$	$\pm 9.6465i$
								-1.8624	-1.8824
1.0	1.0	1.0	2	1.5	0.4	0.6	0.4	$-0.6263 \pm 1.1034i$	$\pm 1.2693i$
								-0.2140	-0.2560

of eigenvalues. Also, it is shown that C_b has very little influence on the eigenvalue on the real axis. These are very useful guidelines for the reduction and future design of this system, which cannot be obtained by other approaches.

3.7. Physical Domain Model Reduction Procedure

Based on the decomposition procedures explained in the previous sections, a physical domain model reduction method is established of four steps as follows:

1. Obtain the linear lumped parameter model of the system and then draw the bond graph model.
2. Identify the major subsystems of the model using the decomposition procedures described above and calculate their eigenvalues.
3. It is well known from basic control theory that the residues and the eigenvalues are the parameters to assess in order to find the dominant modes of a linear system. The largest residue and the eigenvalue nearest to the imaginary axis contribute most to the dominant part of the time domain response of a linear system. Hence, in Step 3 the eigenvalues and the partial fraction expansion residues of the full order model are computed.
4. Match the eigenvalues that must be retained according to Step 3 together with

2, and consequently determine the subsystems to be retained and eliminated.

In the resulting reduced order model, there can be a DC gain discrepancy between the reduced and the full order models that can be corrected easily. The DC gain difference may occur in cases where some parameters are eliminated without compensating their effects on the system. This is related to the various sensitivities of the system with respect to each of the parameters [67]. As an example consider that the DC gain of the full order model of a given system is $DC_{FM} = a_1 a_2$ and that $a_1 = 1$, $a_2 = 10$. If the model reduction leads to the elimination of $a_1 = 1$, then the DC gains of the full and reduced order models would be unchanged as $DC_{FM} = DC_{RM} = 10$. If the model reduction had led to the elimination of $a_2 = 10$, then there would be a DC gain discrepancy of order 10 between the $DC_{FM} = a_1 a_2 = 10$ and $DC_{RM} = a_1 = 1$. It should also be noted that if the output were chosen as a flow variable such as velocity in a mechanical system that would have a zero steady-state value for a stable system then the reduced model would not have any DC gain error. A physical interpretation of steady-state considerations is given in Appendix B for completeness.

3.8. Conclusion

In this chapter, several decomposition procedures are discussed to identify the physical elements or structures which are responsible for separate groups of eigenvalues. For a category of systems, the bounds of the estimated eigenvalues are improved by the decomposition results. Since these bounds are represented by the physical parameters, they can directly contribute to the error of the reduced models and to the design of physical systems. Several examples are presented to illustrate the use of the procedures.

In addition to the decomposition procedures, a physical domain model reduction procedure is presented that utilizes the decomposition procedures. In the next chapter, implementation of this model reduction procedure will be illustrated.

4. MODEL REDUCTION IMPLEMENTATIONS

In this chapter, several examples of physical decomposition based model reduction procedure will be presented. There will be examples for both SISO and MIMO systems. In these examples, it will also be indicated , where appropriate, how other reduction techniques, such as balanced realizations may benefit from physical analysis. Additionally, use of the model reduction procedure in multi energy domain or unstable systems is noted as necessary.

4.1. A 5th Order SISO System

Consider the system shown in Figure 4.1 and its bond graph representation shown in Figure 4.2. The system is of order 4. However, considering the bond graph modelling method it has five energy storage elements in integral causality. Hence, the system is of order 5 having one state in excess. The excess state is due to the structure of the system since the spring k_2 does not generate an independent state. In this example the following values are chosen for the parameters: $m_1 = m_2 = 1\ kg$, $k_1 = k_3 = 1\ \frac{N}{m}$, $k_2 = 15\ \frac{N}{m}$, $b_1 = b_3 = 0.2\ \frac{Nsec}{m}$, $b_2 = 1\ \frac{Nsec}{m}$. Defining the power variables $\mathbf{x} = [F_{k_1}, F_{k_2}, F_{k_3}, \dot{x}_1, \dot{x}_2]^T$ where F_{k_i} etc. represents the force in the i'th spring, and $u = F$ as the input to the system then the state-space equations become:

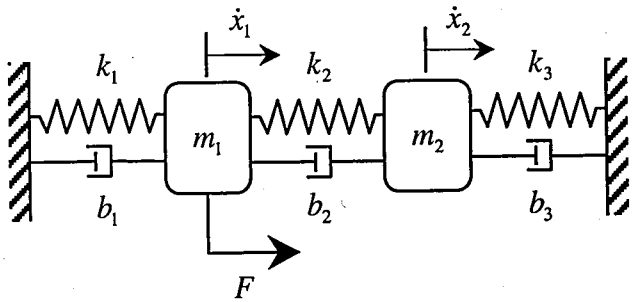

Figure 4.1. A 5th order physical system

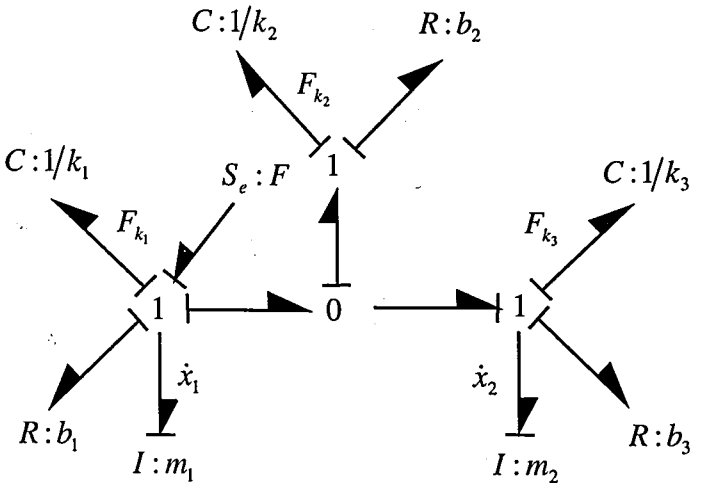

Figure 4.2. Bond graph representation of the 5th order system

$$\frac{d}{dt}\begin{pmatrix} F_{k_1} \\ F_{k_2} \\ F_{k_3} \\ \dot{x}_1 \\ \dot{x}_2 \end{pmatrix} = \underbrace{\begin{bmatrix} 0 & 0 & 0 & k_1 & 0 \\ 0 & 0 & 0 & k_2 & -k_2 \\ 0 & 0 & 0 & 0 & k_3 \\ -\frac{1}{m_1} & -\frac{1}{m_1} & 0 & -\frac{b_1+b_2}{m_1} & \frac{b_2}{m_1} \\ 0 & \frac{1}{m_2} & -\frac{1}{m_2} & \frac{b_2}{m_2} & -\frac{b_2+b_3}{m_2} \end{bmatrix}}_{\mathbf{A}} \begin{pmatrix} F_{k_1} \\ F_{k_2} \\ F_{k_3} \\ \dot{x}_1 \\ \dot{x}_2 \end{pmatrix} + \underbrace{\begin{bmatrix} 0 \\ 0 \\ 0 \\ \frac{1}{m_1} \\ 0 \end{bmatrix}}_{\mathbf{B}} F \quad (4.1)$$

If one is interested in the force F_{k_1} as the output variable then the output equation becomes:

$$y = \underbrace{\begin{bmatrix} 1 & 0 & 0 & 0 & 0 \end{bmatrix}}_{\mathbf{C}} \begin{pmatrix} F_{k_1} \\ F_{k_2} \\ F_{k_3} \\ \dot{x}_1 \\ \dot{x}_2 \end{pmatrix} \quad (4.2)$$

The model reduction procedure is applied as follows:

Step 1) **Modelling**: The bond graph model of the system is displayed in Fig-

ure 4.2.

Step 2) **Decomposition:** To perform the decomposition, the following local damping ratios and significant loop gains are calculated: Local damping ratios are $\frac{b_1}{2\sqrt{m_1 k_1}} = \frac{b_3}{2\sqrt{m_2 k_3}} = 0.1$ and $\frac{b_2}{2\sqrt{m_1 k_2}} = \frac{b_2}{2\sqrt{m_2 k_2}} = 0.1291$, and in this case the most important local loop gains are calculated as $\frac{k_2}{m_1} = \frac{k_2}{m_2} = 15\ \frac{rad}{sec^2}$ and $\frac{k_1}{m_1} = \frac{k_3}{m_2} = 1\ \frac{rad}{sec^2}$ (these values also show the symmetry of the system).

It is noted that the local damping ratios are fairly close to each other. Thus, it is not possible to immediately divide the system into two subsystems as a heavily damped and a lightly damped subsystem. However, it is possible to identify the high frequency and low frequency oscillation modes. The decomposition results into the two subsystems shown in Figure 4.3. In this figure subsystem 1 represents the low frequency oscillation mode, and subsystem 2 represents the high frequency oscillation mode.

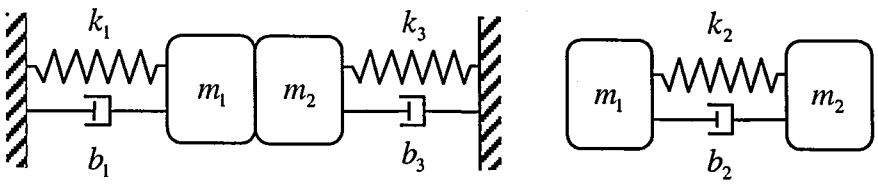

(a) Subsystem 1 (b) Subsystem 2

Figure 4.3. Subsystems of the 5th order system

Step 3) **Relevant modes:** The calculated residues, their absolute values (i.e. magnitudes) and the corresponding eigenvalues of the full order system are shown in Table 4.1. The largest residue indicates the mode that contributes most to the dynamics of the system. Therefore, the eigenvalues that correspond to the bold-slanted residues should be retained in the reduced model of order 2.

Step 4) **Matching modes to subsystems:** Now, the subsystems to be retained have to be identified. To this end, one computes the eigenvalues of subsystem 1 as $\lambda_{1,2} = -0.1 \pm 0.9950i$, and the eigenvalues of subsystem 2 as $\lambda_{3,4} = -1 \pm 5.3852i$,

Table 4.1. Residues and eigenvalues of the 5th order system

Original system			Subsystems
Residues	**Absolute values**	**Eigenvalues**	**Eigenvalues**
$-0.0000 \mp 0.2513i$	***0.2513***	$-0.1000 \pm 0.9950i$	$-0.1000 \pm 0.9950i$
$-0.0000 \mp 0.0458i$	0.0458	$-1.1000 \pm 5.4580i$	$-1.0000 \pm 5.3852i$, 0
-0.0000	0.0000	0.0000	

$\lambda_5 = 0$, which are shown in Table 4.1. We conclude that for a second order reduced model, the subsystem 1 should be retained and the subsystem 2 should be eliminated. Therefore, the subsystem 1 is selected as the reduced second order model.

The time and frequency domain responses of the full order and reduced order models and their errors are shown in Figures 4.4 and 4.5. These plots indicate that the patterns are in good agreement. In Figure 4.4(a) it is seen that the time domain responses have a very small absolute error of 0.0161 at steady-state which can be eliminated by a constant calibration factor. The frequency response plot shown in Figure 4.4(b) indicates that the mode at $\omega \cong 5.46$ rad/sec is eliminated from the two-mode full order model that justifies the proposed model reduction method.

For this example, it will also be shown how to incorporate the decomposition ideas into existing methodologies, such as balanced truncation approaches[7] . As it is discussed earlier, if it is desired to use balance and truncate approaches, the first thing that needs to be done is to calculate the Hankel singular values. For this example, the Hankel singular values are calculated as 1.3945, 1.1407, 0.2897, 0.0534, 0. These values suggest that, a reduced order model of order 2, 3 or 4 can be obtained. Choosing an order of 3 will have a smaller error than order of 2 as discussed earlier, but the resulting reduced order model will not have any resemblance to the full order system eigenvalues. Simulations for 2nd, 3rd and 4th order reduced models were performed

[7] For this example, balance and truncate approach was used with the modified criterion.

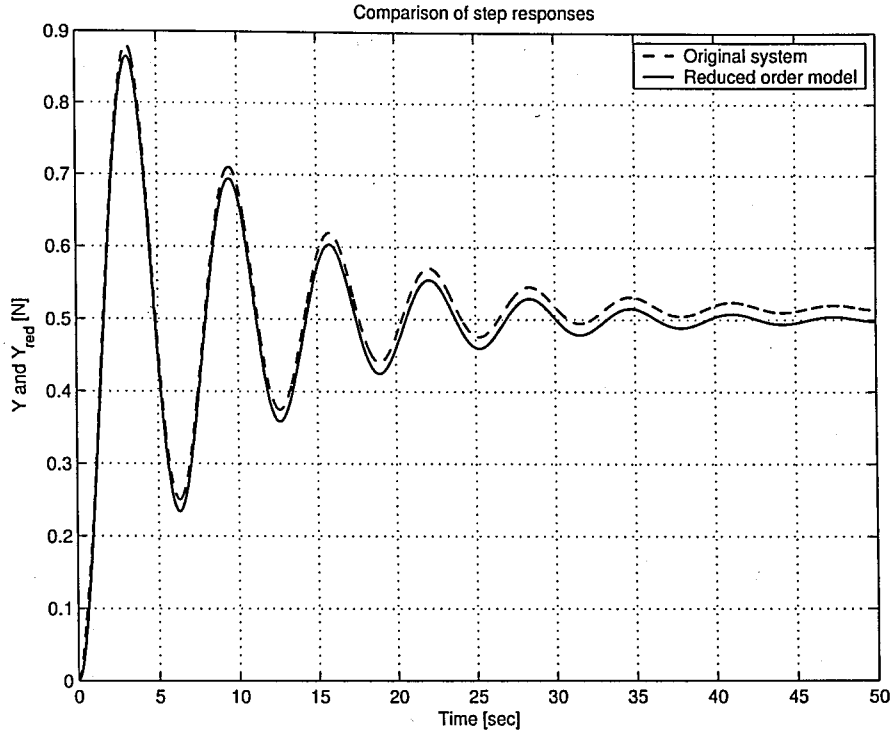

(a) Comparison of step responses

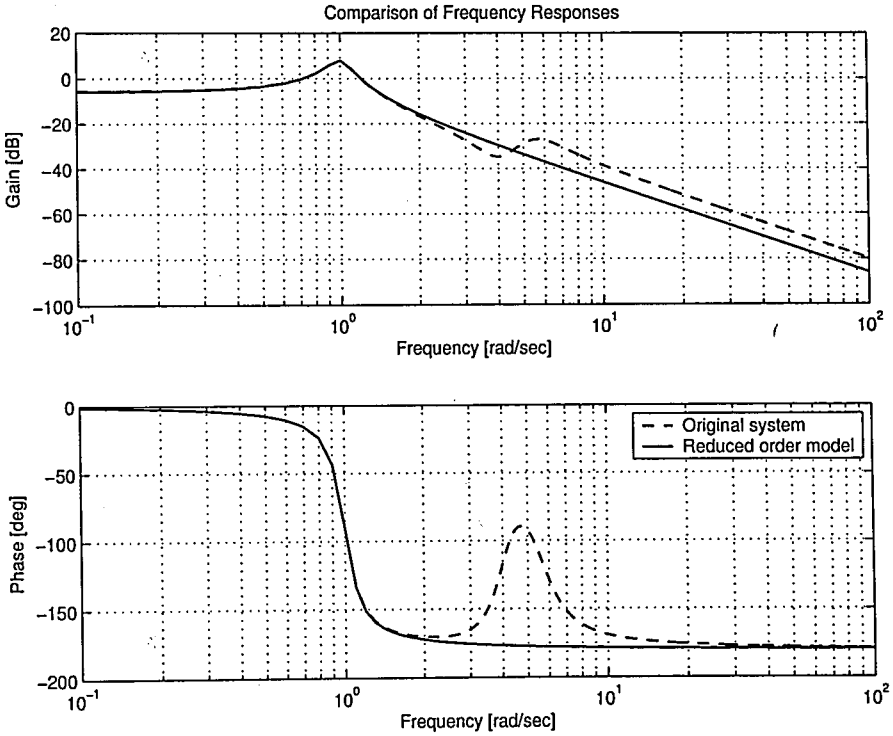

(b) Comparison of Bode plots

Figure 4.4. Comparison of responses (using subsystems)

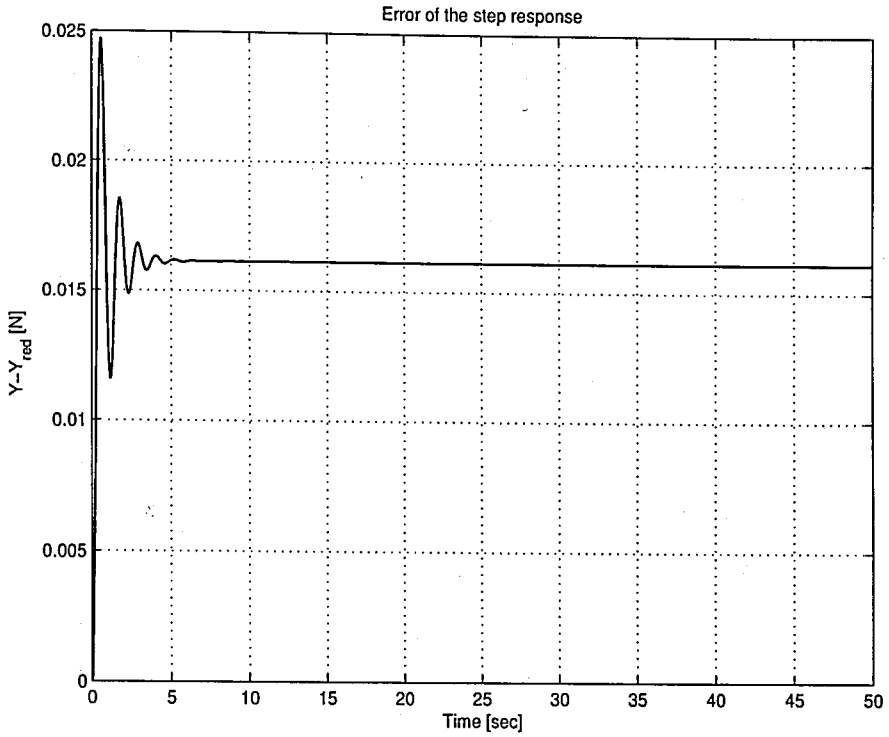

(a) Error in step response

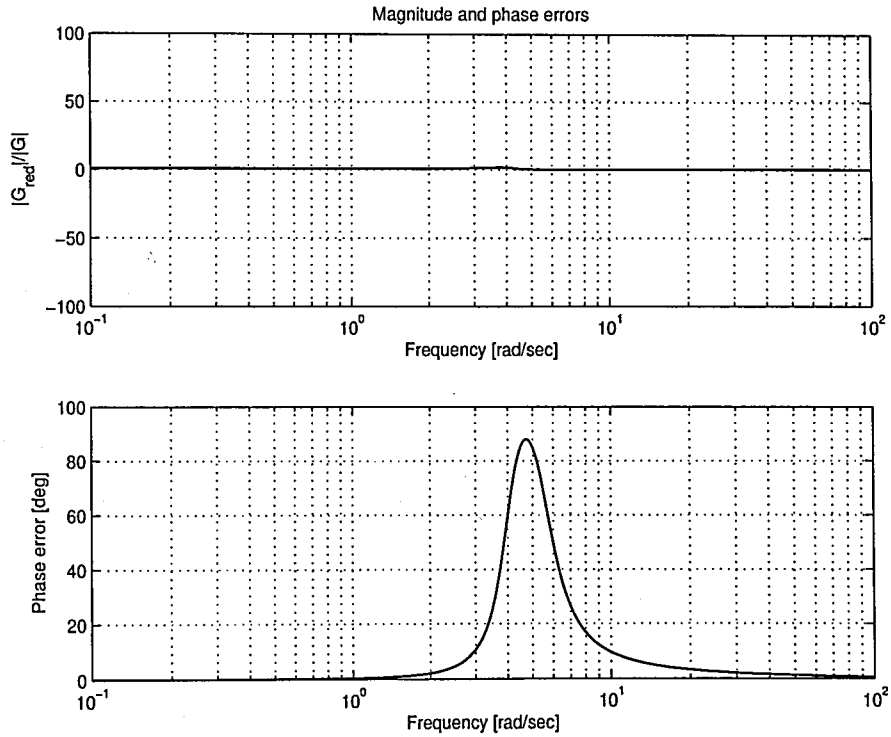

(b) Error in magnitude and phase

Figure 4.5. Error responses (using subsystems)

and the following eigenvalues were obtained[8] :

- For a 2nd order reduction $\longrightarrow -0.1030 \pm 0.9939i$.
- For a 3rd order reduction $\longrightarrow -0.1040 \pm 0.9847i$, -1.7193.
- For a 4th order reduction $\longrightarrow -0.1000 \pm 0.9950i$, $-1.1000 \pm 5.4580i$.

The results support the discussion above. It should be emphasized once more that if the new measure had not been used, the results would be even worse, meaning that the usual balance and truncate approach would miss the important states.

In this thesis, it is observed that by looking at the absolute values of the residues of the original system's eigenvalues, one can obtain similar information about the reduced model order as obtained by the Hankel singular values. Additionally, if one uses the modified criterion that was explained in Section 2.3.1, he/she can have reliable information about the resulting reduced order system and its eigenvalues. Because of balancing the resulting eigenvalues may not be exactly the same as the original system (or a subset of the original system or the subsystems), but they will be reasonably close. It is also found out that, this approach works if the absolute value of the residues have a significant value change (gap) similar to the Hankel singular value case. If there is no significant gap between the values, it means that the corresponding eigenvalues are equally important.

Additionally, the information from the decomposition procedure discussed above can be incorporated to improve the reduction of balance and truncate methods. For this purpose, one can first look at the residues, and the corresponding eigenvalues, then the matching subsystem eigenvalues and consequently decide on the reduced model order, as it is done before. After that, the reduction can be performed by truncation and the reduced order model that retains the same subsystem as discussed before is obtained. Obviously, the calculated eigenvalues will be modified because of balancing. One advantage of this approach is that, the resulting error is known beforehand.

[8] As the system is in fact of order 4, 4th order reduced model matches exactly.

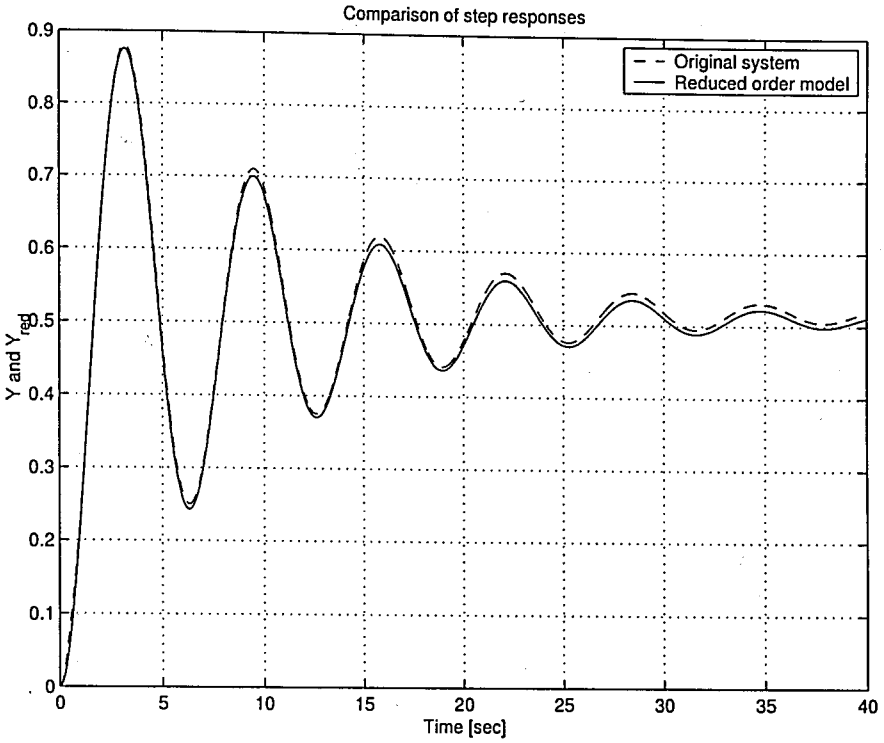

(a) Comparison of step responses

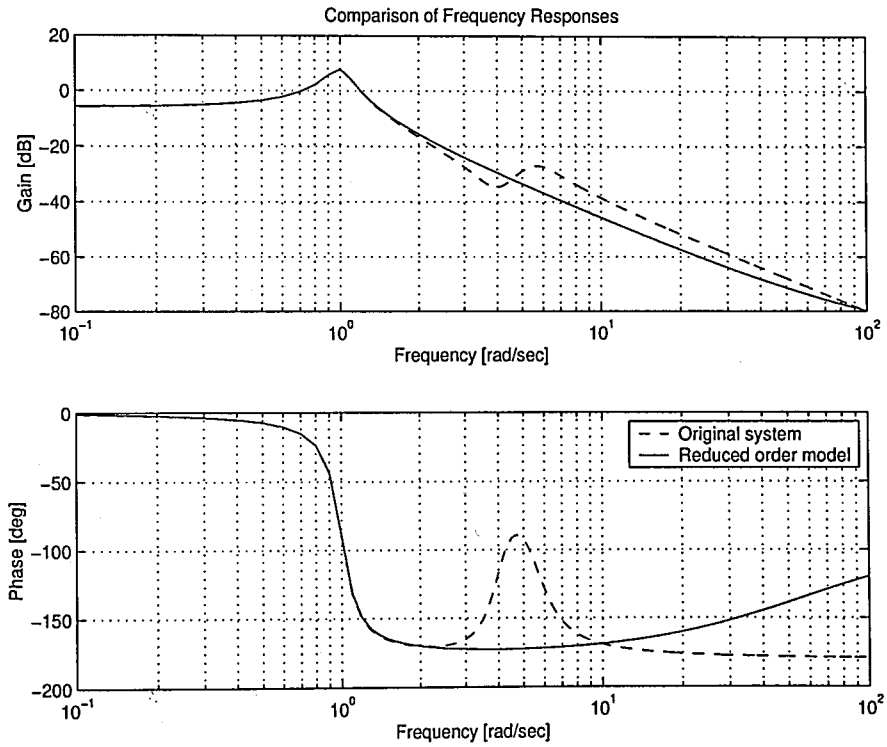

(b) Comparison of Bode plots

Figure 4.6. Comparison of responses (using balancing method)

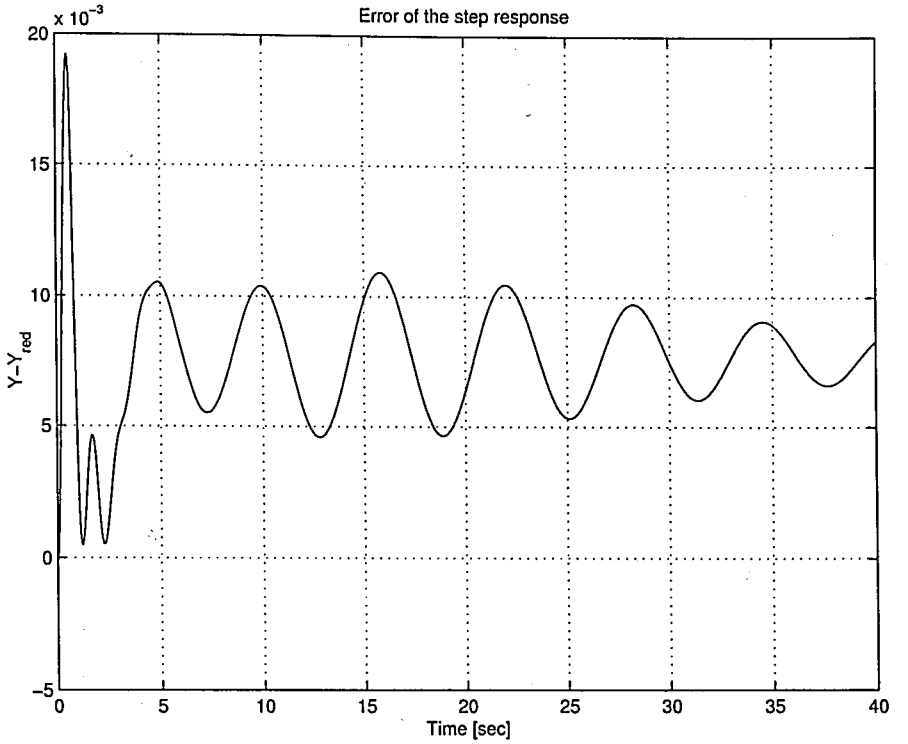

(a) Error in step response

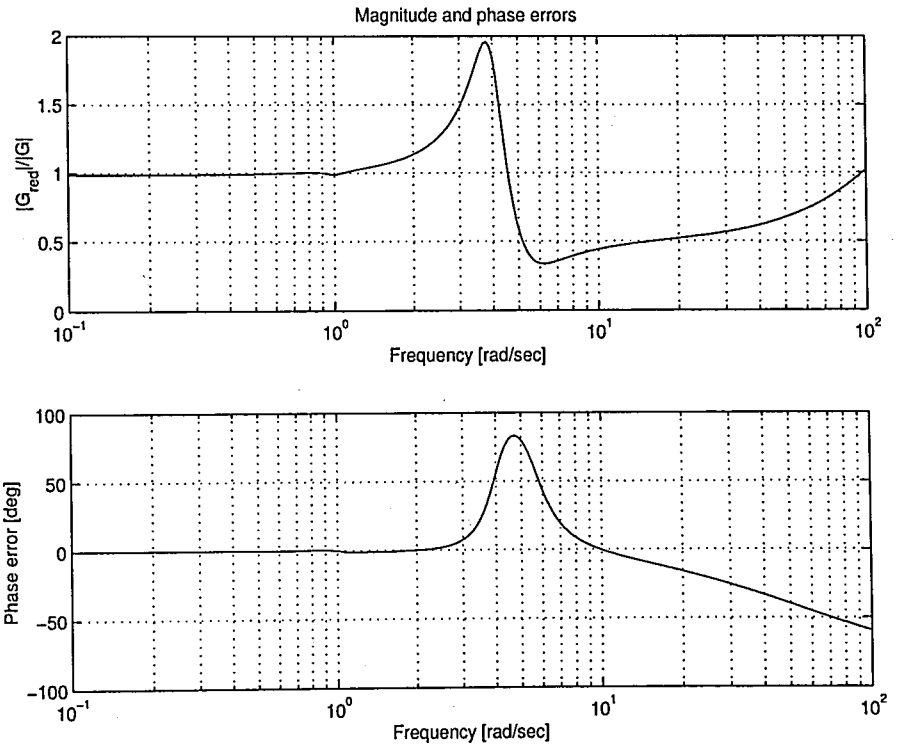

(b) Error in magnitude and phase

Figure 4.7. Error responses (using balancing method)

One can see the comparison of simulations for this system with a 2nd order reduced model using balance and truncate method with the above modifications in Figures 4.6 and 4.7. As one can see the results are in good match and the error is acceptable. Notice that, the new model reduction procedure has a better error in frequency domain (especially in phase).

4.2. A 10th Order SISO System

Now, consider the system in Figure 4.8. The bond graph representation of this system is shown in Figure 4.9. As one can see, there are 10 independent energy storage elements in integral causality, so the order of this system is 10.

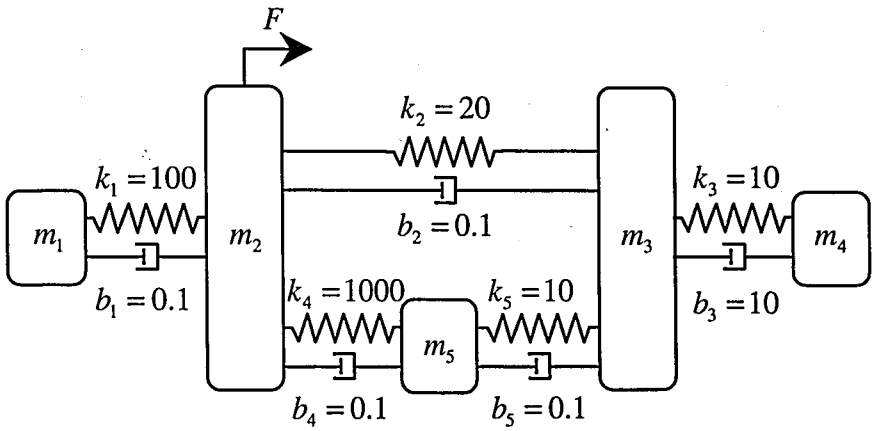

Figure 4.8. A 10th order physical system

Suppose that a 2nd order reduced model is desired. Table 4.2 shows the residues, absolute values of the residues and the corresponding eigenvalues of this 10th order system[9] , and Table 4.3 shows the eigenvalues of the subsystems obtained in Chapter 3 Section 3.6.1 and shown in Figure 4.10.

This analysis indicates that subsystems 1 and 2 together have the most important features of this system as their poles have the most significant effect in the time response according to the residues. Hence, the absolute values of the residues suggest that the

[9] In this example there are two zero eigenvalues with zero residue, so the real order of the system is 8.

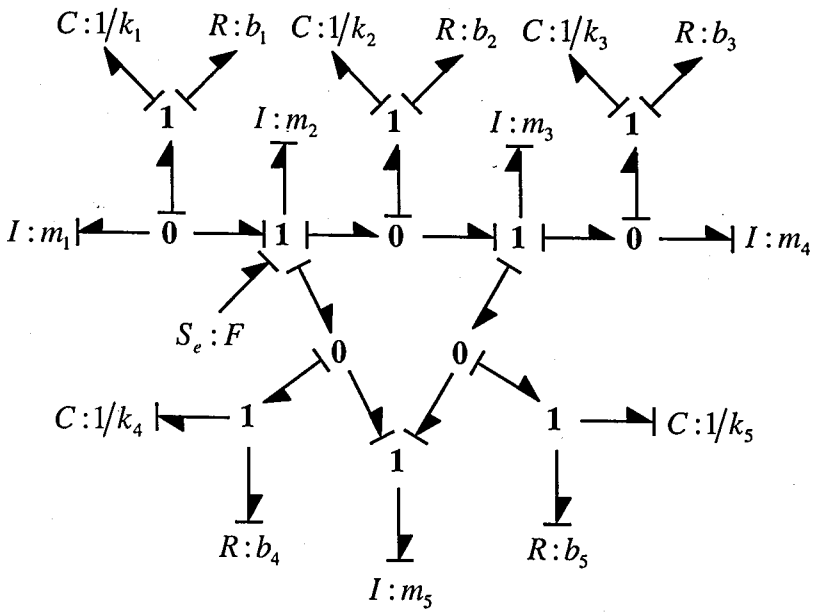

Figure 4.9. Bond graph representation of the 10th order physical system

Table 4.2. Residues and eigenvalues of the 10th order system

Residue	Absolute value of the residue	Eigenvalue
$0.0028 \mp 0.0309i$	***0.0310***	$-0.1789 \pm 45.4882i$
$0.0006 + 0.0000i$	0.0006	-18.2310
$0.0045 \mp 3.7574i$	***3.7574***	$-0.1088 \pm 12.3218i$
$0.0450 \mp 0.4727i$	***0.4749***	$-0.4498 \pm 4.8881i$
$-0.0051 + 0.0000i$	0.0051	-1.0941
$-0.0000 - 0.0000i$	0.0000	0.0000
$-0.0000 - 0.0000i$	0.0000	0.0000

eigenvalues corresponding to bold-slanted residues in Table 4.2 should be preserved in the reduced order model. Although this is the case, as a 2nd order reduced model is desired, a further decomposition is necessary. The extended decomposition reveals that the subsystem shown in Figure 4.11 should be the reduced order model.

The resulting time and frequency responses of the full order and the 2nd order reduced model can be seen in Figure 4.12. As it can be seen from these plots the

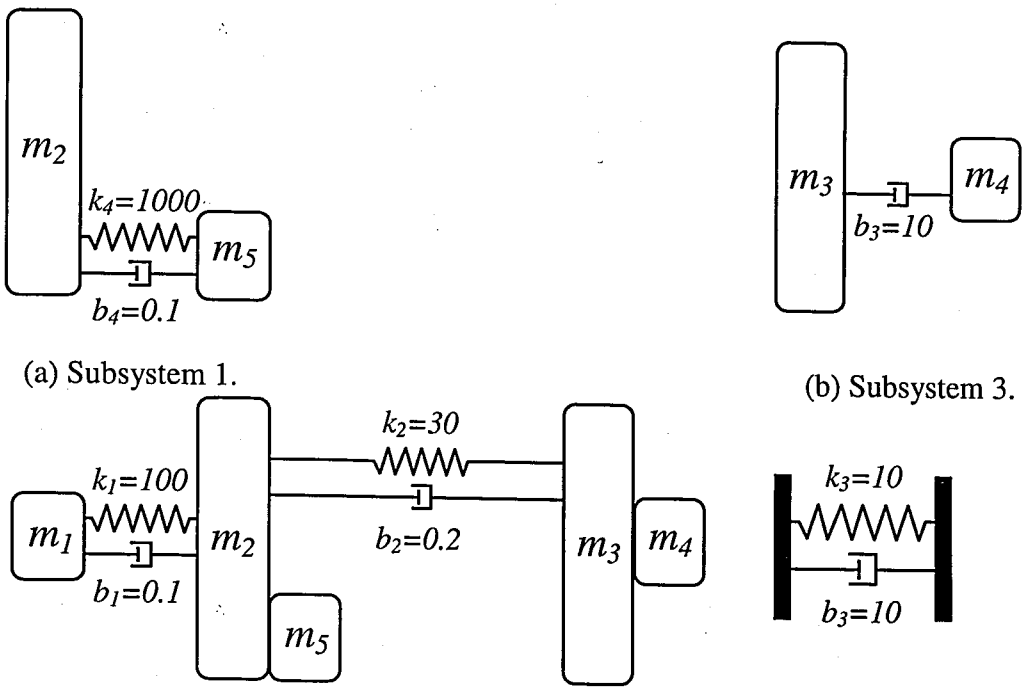

(a) Subsystem 1.

(b) Subsystem 3.

(c) Subsystem 2.

(d) Subsystem 4.

Figure 4.10. Subsystems of the 10th order mechanical structure

Table 4.3. Eigenvalues of the subsystems of the 10th order system

Eigenvalue	Subsystem Number
$-0.1000 \pm 44.7212i$	1
0	1
$-0.0979 \pm 12.4875i$	2
0	2
$-0.0771 \pm 4.9031i$	2
-20	3
-1	4

responses are in good match.

This analysis indicates that a useful procedure to obtain detailed information about the physical system and its reduced order model is determined. But this approach is mainly useful for linear systems, and for systems with residues in some kind

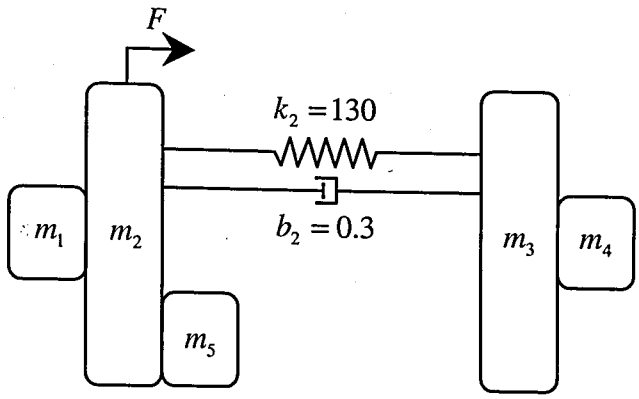

Figure 4.11. 2nd order reduced model of 10th order mechanical structure

of separated blocks as mentioned before. It is also applicable to linear MIMO systems and this will be presented in the next section.

4.3. A 7th Order MIMO System

A MIMO system can be seen in Figure 4.13, and its bond graph representation is shown in Figure 4.14. The system has seven independent energy storage elements in integral causality, thus it is of order seven. The system also has two inputs.

Using the power state variables, and representing force in spring i as F_{k_i}, the following state-space representation is obtained:

$$\dot{\mathbf{x}} = \mathbf{A}\mathbf{x} + \mathbf{B}\mathbf{u} \tag{4.3}$$

where $\mathbf{x}$, $\mathbf{A}$, $\mathbf{B}$, and $\mathbf{u}$, are given by

$$\mathbf{x} = \begin{pmatrix} \dot{x}_4 \\ F_{k_3} \\ \dot{x}_3 \\ F_{k_2} \\ \dot{x}_2 \\ F_{k_1} \\ \dot{x}_1 \end{pmatrix}, \quad \mathbf{A} = \begin{bmatrix} -\frac{b_3}{m_4} & \frac{1}{m_4} & \frac{b_3}{m_4} & 0 & 0 & 0 & 0 \\ -k_3 & 0 & k_3 & 0 & 0 & 0 & 0 \\ \frac{b_3}{m_3} & -\frac{1}{m_3} & -\frac{b_2+b_3}{m_3} & \frac{1}{m_3} & \frac{b_2}{m_3} & 0 & 0 \\ 0 & 0 & -k_2 & 0 & k_2 & 0 & 0 \\ 0 & 0 & \frac{b_2}{m_2} & -\frac{1}{m_2} & -\frac{b_1+b_2}{m_2} & \frac{1}{m_2} & \frac{b_1}{m_2} \\ 0 & 0 & 0 & 0 & -k_1 & 0 & k_1 \\ 0 & 0 & 0 & 0 & \frac{b_1}{m_1} & -\frac{1}{m_1} & -\frac{b_1}{m_1} \end{bmatrix} \tag{4.4}$$

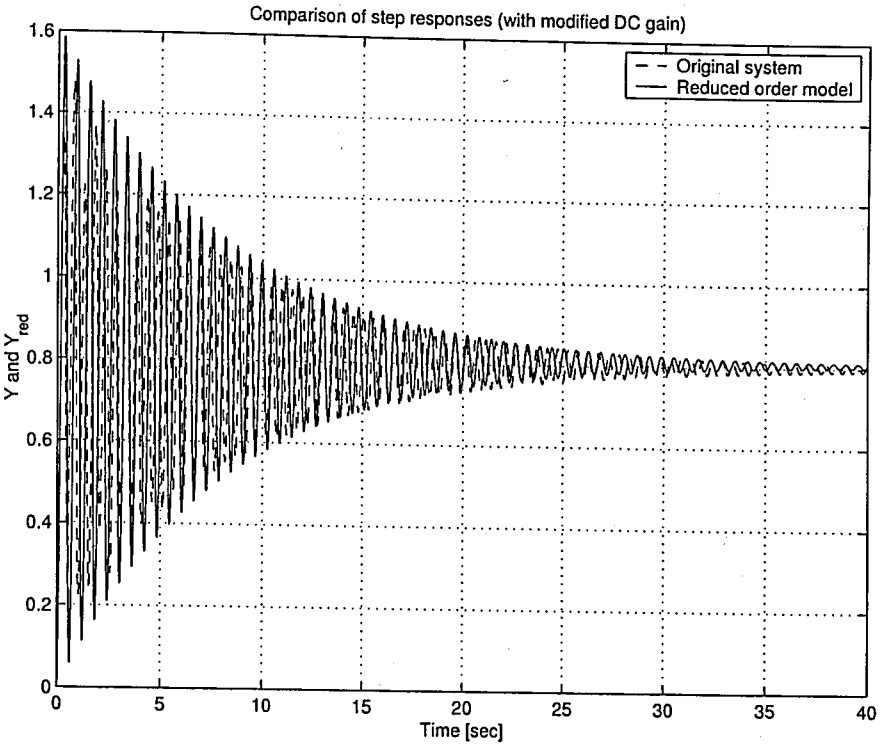

(a) Comparison of step responses

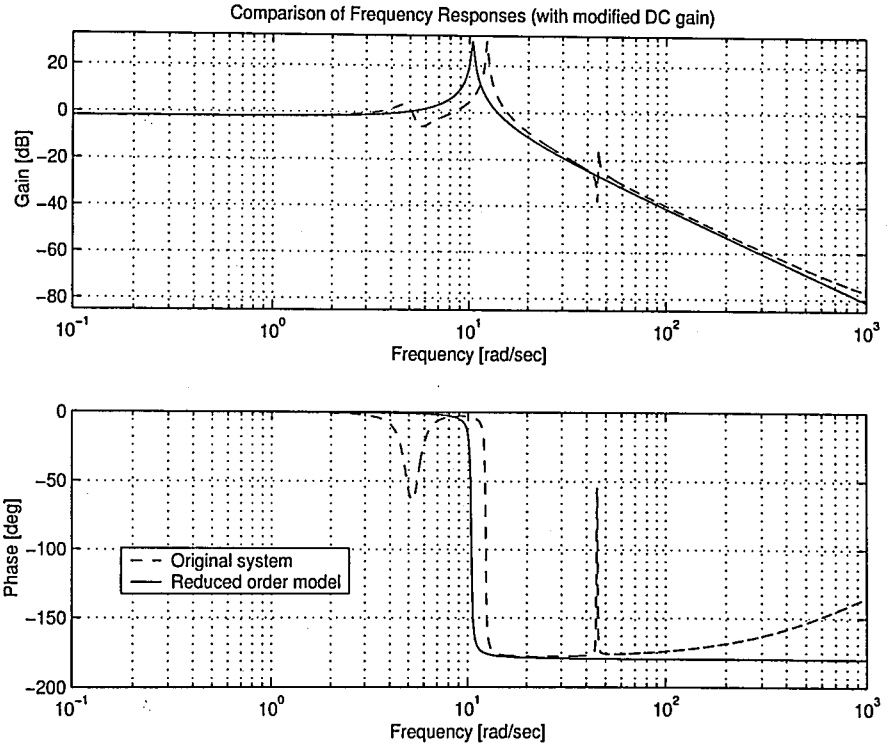

(b) Comparison of Bode plots

Figure 4.12. Comparison of responses (using subsystems)

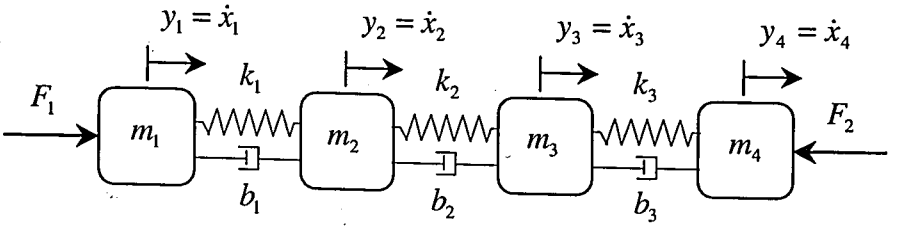

Figure 4.13. A 7th order physical system

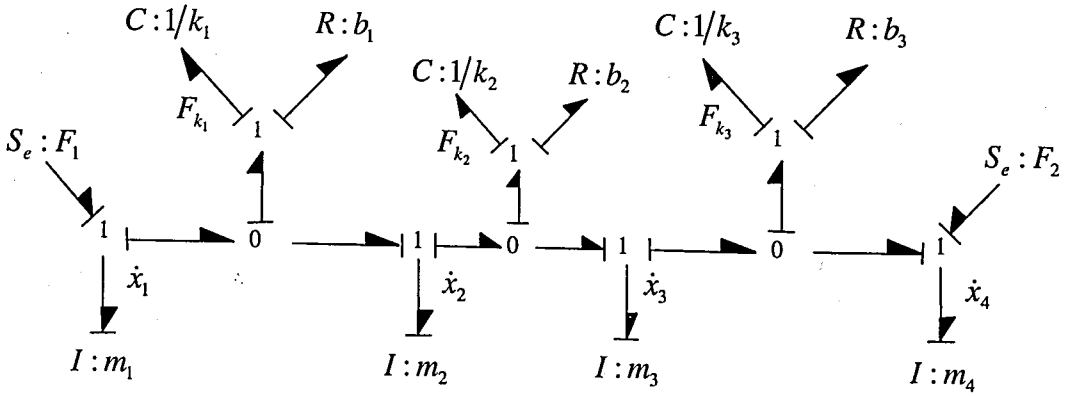

Figure 4.14. Bond graph representation of the 7th order physical system

and

$$\mathbf{B} = \begin{bmatrix} 0 & \frac{1}{m_4} \\ 0 & 0 \\ 0 & 0 \\ 0 & 0 \\ 0 & 0 \\ 0 & 0 \\ \frac{1}{m_1} & 0 \end{bmatrix}, \qquad \mathbf{u} = \begin{pmatrix} F_1 \\ F_2 \end{pmatrix} \tag{4.5}$$

Assuming the velocities $\dot{x}_1$ and $\dot{x}_2$ of masses m_1 and m_2 are of interest, the output vector equation is given by:

$$\mathbf{y} = \mathbf{C}\mathbf{x} \tag{4.6}$$

where **C** is,

$$\mathbf{C} = \begin{bmatrix} 0 & 0 & 0 & 0 & 0 & 0 & 1 \\ 0 & 0 & 0 & 0 & 1 & 0 & 0 \end{bmatrix} \tag{4.7}$$

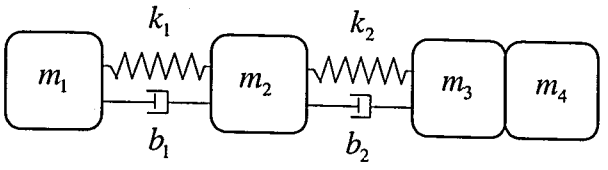

(a) Subsystem 1

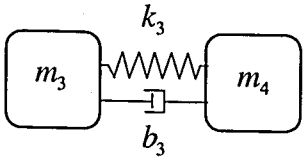

(b) Subsystem 2

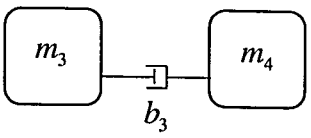

(c) Subsystem 3

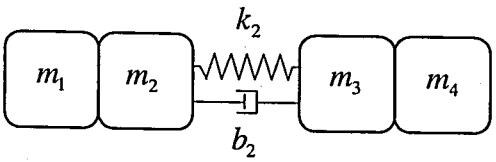

(d) Subsystem 4

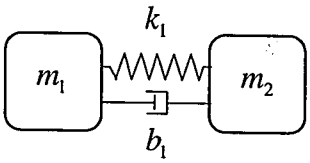

(e) Subsystem 5

Figure 4.15. Subsystems of the 7th order MIMO system

This subsystems shown in Figure 4.15 are obtained using the decomposition procedure described earlier. Assuming that $m_1 = m_2 = m_3 = m_4 = 1\ kg$, $k_1 = 4\ \frac{N}{m}$, $k_2 = 2\ \frac{N}{m}$, $k_3 = 8\ \frac{N}{m}$, $b_1 = 1\ \frac{Nsec}{m}$, $b_2 = 2\ \frac{Nsec}{m}$, and $b_3 = 4\ \frac{Nsec}{m}$, the necessary loop gains and local damping ratios are calculated as; $\frac{k_1}{m_1} = \frac{k_1}{m_2} = 4\ \frac{rad}{sec^2}$, $\frac{k_2}{m_2} = \frac{k_2}{m_3} = 2\ \frac{rad}{sec^2}$, $\frac{k_3}{m_3} = \frac{k_3}{m_4} = 8\ \frac{rad}{sec^2}$, $\frac{b_1}{2\sqrt{k_1 m_1}} = \frac{b_1}{2\sqrt{k_1 m_2}} = 0.25$, $\frac{b_2}{2\sqrt{k_2 m_2}} = \frac{b_2}{2\sqrt{k_2 m_3}} = 0.707$, $\frac{b_3}{2\sqrt{k_3 m_3}} = \frac{b_3}{2\sqrt{k_3 m_4}} = 0.707$. The subsystems 4 and 5 are obtained from the subsystem 1. The eigenvalues of the subsystems are shown in Table 4.4.

The eigenvalues of the overall system, their corresponding residues and the 2-norms are listed in Table 4.5. Notice that any norm could have been used in the model reduction process. The norms of the residues suggest that the eigenvalues corresponding to the bold-slanted residues in Table 4.5 should be retained in the reduced order model.

Table 4.4. Eigenvalues of the subsystems of the 7th order MIMO system

Eigenvalue	Subsystem Number
$-1.5775 \pm 2.0860i$	1
$-0.9225 \pm 1.2199i$	1
0	1
-4	2
-4	2
-8	3
$-1.0000 \pm 1.0000i$	4
$-1.0000 \pm 2.6458i$	5

Table 4.5. Residues and eigenvalues of the 7th order MIMO system

Residue	2-Norm	Eigenvalue
$\begin{bmatrix} 0.0005 & -0.0146 \\ -0.0075 & 0.2223 \end{bmatrix}$	0.2229	-7.14291
$\begin{bmatrix} 0.1969 \mp 0.0927i & 0.1073 \pm 0.1259i \\ -0.3039 \mp 0.0763i & -0.0047 \mp 0.2381i \end{bmatrix}$	***0.4792***	$-1.53813 \pm 2.33283i$
$\begin{bmatrix} 0.1849 \pm 0.2314i & -0.2175 \mp 0.1794i \\ 0.2082 \pm 0.0515i & -0.2040 \mp 0.0073i \end{bmatrix}$	***0.5049***	$-0.795996 \pm 1.20974i$
$\begin{bmatrix} 0.25 & 0.25 \\ 0.25 & 0.25 \end{bmatrix}$	***0.5***	0
$\begin{bmatrix} -0.0140 & -0.0150 \\ -0.0512 & -0.0548 \end{bmatrix}$	0.0778	-2.18884

The analysis shows that the subsystem 1 is the dominant one. Thus, the first subsystem is chosen as the reduced order model. Time and frequency responses of this system and its reduced order model and their errors can be seen in Figures 4.16 and 4.17. These results show that there is a good agreement between the full and the

reduced order models in the MIMO case as well[10] .

It should be noted that, while discussing SISO model reduction examples, it was indicated that the results of balance and truncate approaches can be improved by using physical information. Same improvement holds for MIMO systems.

Until this point only single domain physical systems have been analyzed. In the next sections, examples on multi energy domain dynamic systems, unstable systems, and advantages of decomposition based physical model reduction method over power and energy based model reduction procedures will be presented.

4.4. Example 4 - An Arm Prosthesis System

Consider the arm prosthesis example of Chapter 3. Using the parameter set of; $I_f = I_m = 0.1$, $C_b = 0.05$, $T_1 = 2$, $T_2 = 1.5$, and $R_m = R_f = 0.4$, $R_i = 0.6$, Table 4.6 can be constructed.

Table 4.6. Residues and eigenvalues of the arm prosthesis

Residue	Absolute value of the residue	Eigenvalue
$0.7652 \mp 0.3656i$	0.8481	$-6.2639 \mp 16.8184i$
8.4696	***8.4696***	-2.1388

Thus, by looking at the residues, it is concluded that the real root is the most dominant one. Thus, the obtained reduced order model of the arm prosthesis is as shown in Figure 4.18.

Time and frequency responses of this system and its reduced order model can be seen in Figure 4.19. As one can see, the results are in good match and the errors are acceptable.

[10] This is a MIMO system. So in the frequency domain the singular values are considered. Consequently, the error in the maximum amplification (maximum singular value) is given.

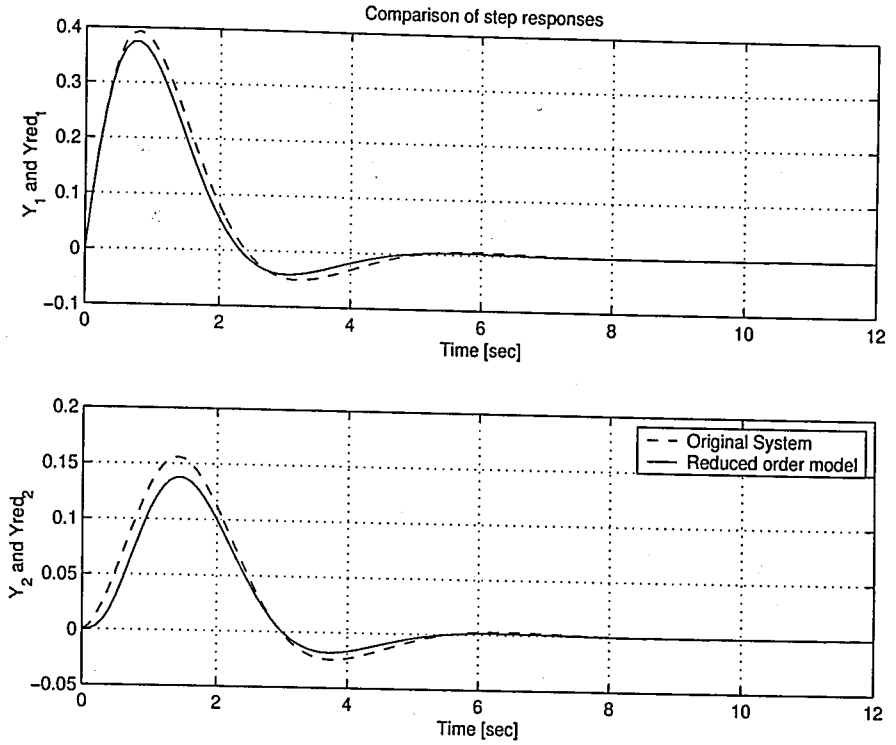

(a) Comparison of step responses

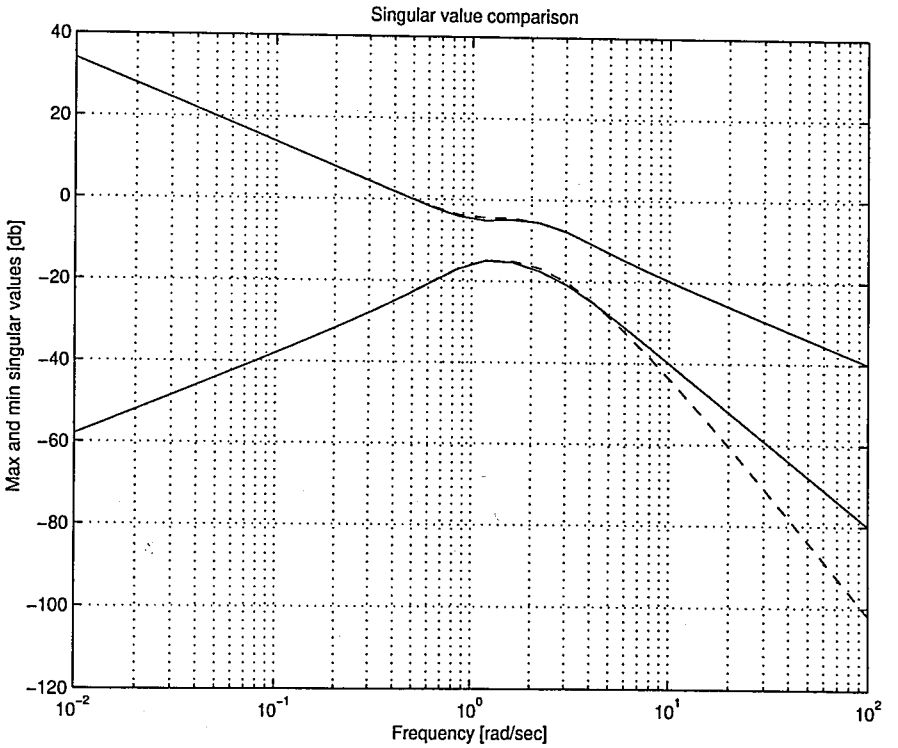

(b) Comparison of singular value plots

Figure 4.16. Comparison of responses of the MIMO system (using subsystems)

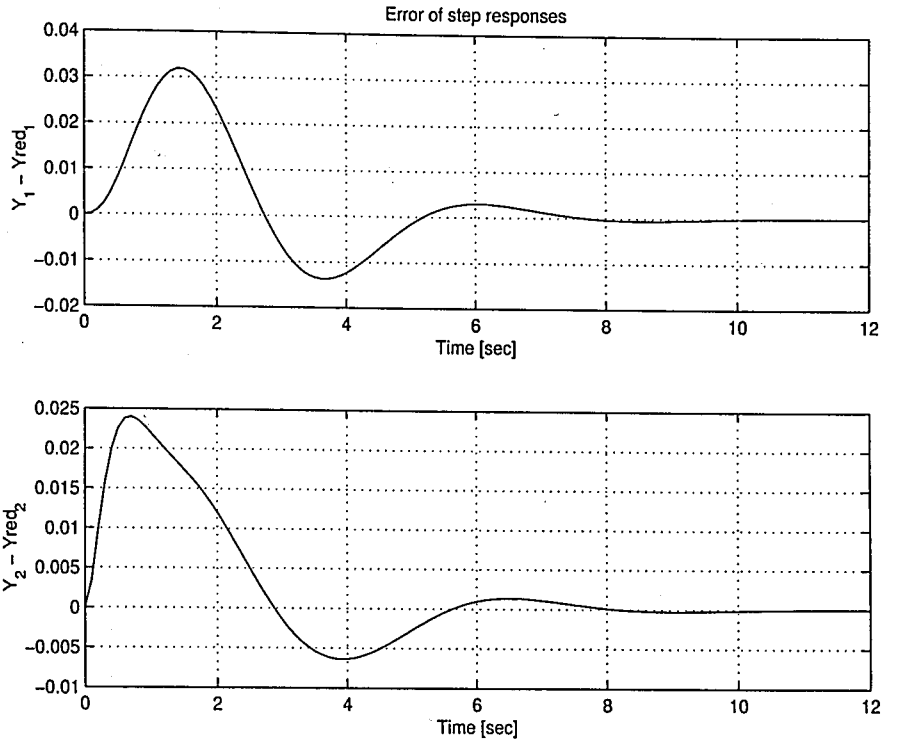

(a) Error in step responses

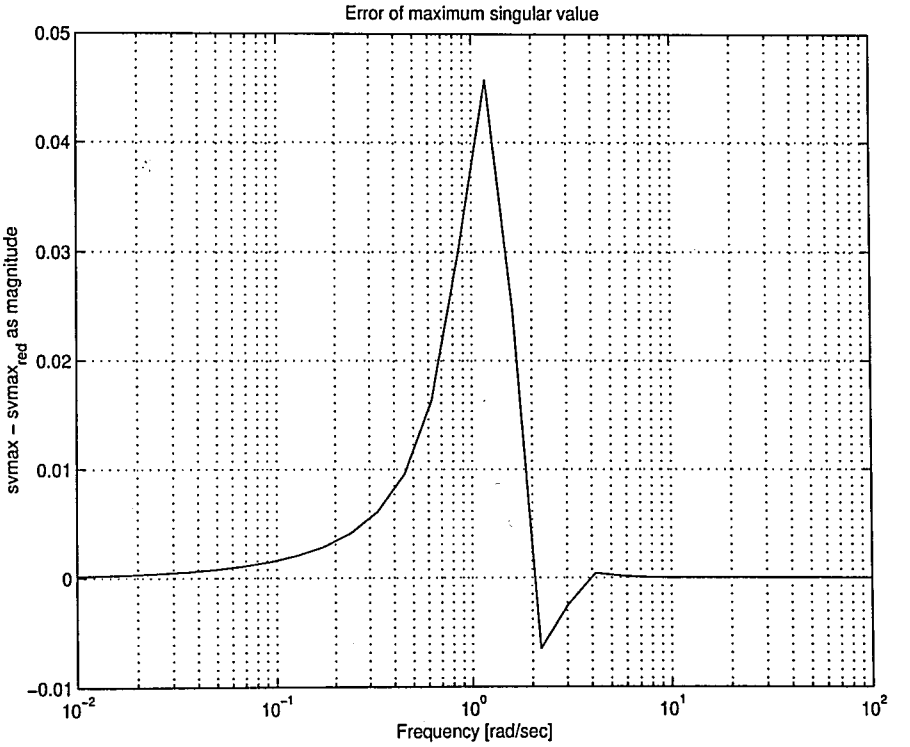

(b) Error in maximum singular value

Figure 4.17. Error responses of the MIMO system (using subsystems)

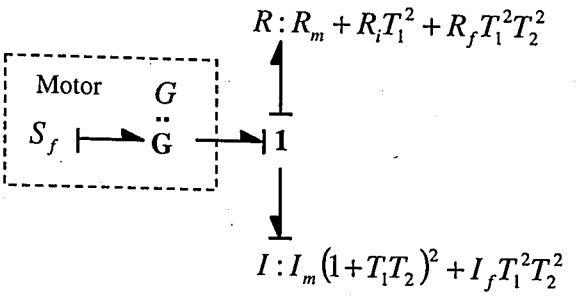

Figure 4.18. Reduced order model of the arm prosthesis system

4.5. Application of the Model Reduction Procedure to Unstable Systems

Most of the methods in literature have problems while dealing with unstable systems. For example, Hankel singular value based methods, can only deal with such problems if their stable and unstable counterparts are separated. Then it is applied to the stable part. In our case, the decomposition procedure to obtain the eigenvalues from physical parameters can still be used, and therefore an approximation to the stable and unstable parts of a system may be obtained. Obviously, afterwards, the residue information can be checked, and the reduced order model can be obtained accordingly. It should be noted that the unstable part of a system usually provides the characteristic behavior of that system and thus should not be eliminated in a reduced order model. Only the stable part should be reduced. A simple example is given for unstable systems.

Consider a $5th$ order inherently unstable system and its bond graph as shown in Figures 4.20 and 4.21 respectively. This system is unstable as the first spring, k_1, is chosen to be negative one.

Assuming that $m_1 = m_2 = m_3 = 1\ kg$, $k_1 = -2\ \frac{N}{m}$, $k_2 = 1\ \frac{N}{m}$, $b_1 = 3\ \frac{Nsec}{m}$, and $b_2 = 1\ \frac{Nsec}{m}$, it is calculated that the system has the following eigenvalues: -7.0891, 0.5914, $-0.7512 \pm 0.9310i$, and 0.

This system can be decomposed into two subsystems, namely, (m_1, m_2, b_1, k_1) that gives the eigenvalues $(-6.6056, 0.6056, 0)$ and (m_2, m_3, b_2, k_2) that gives the eigenvalues

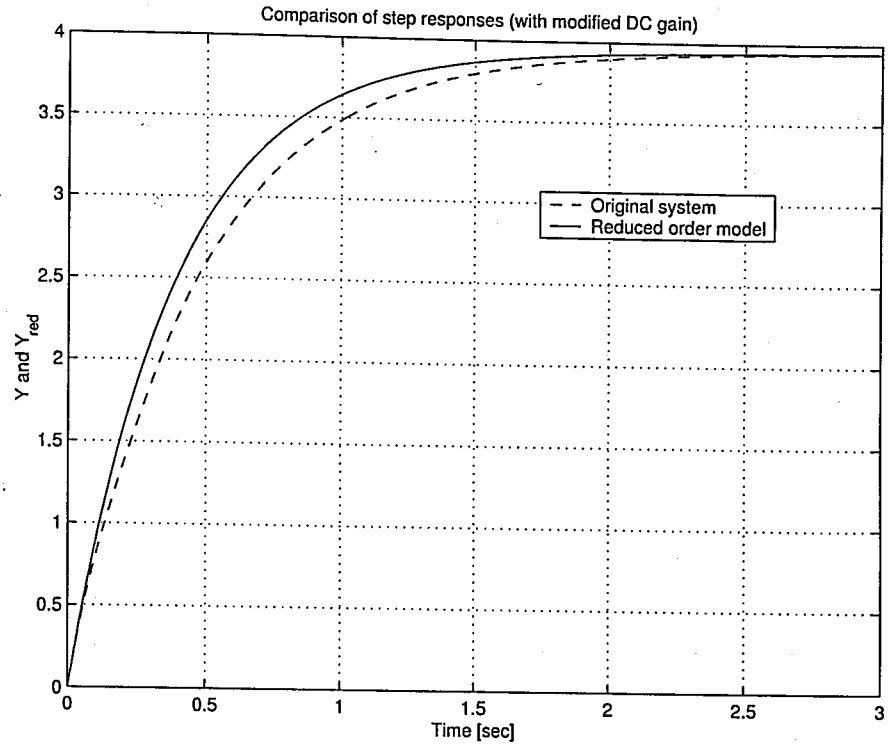

(a) Comparison of step responses

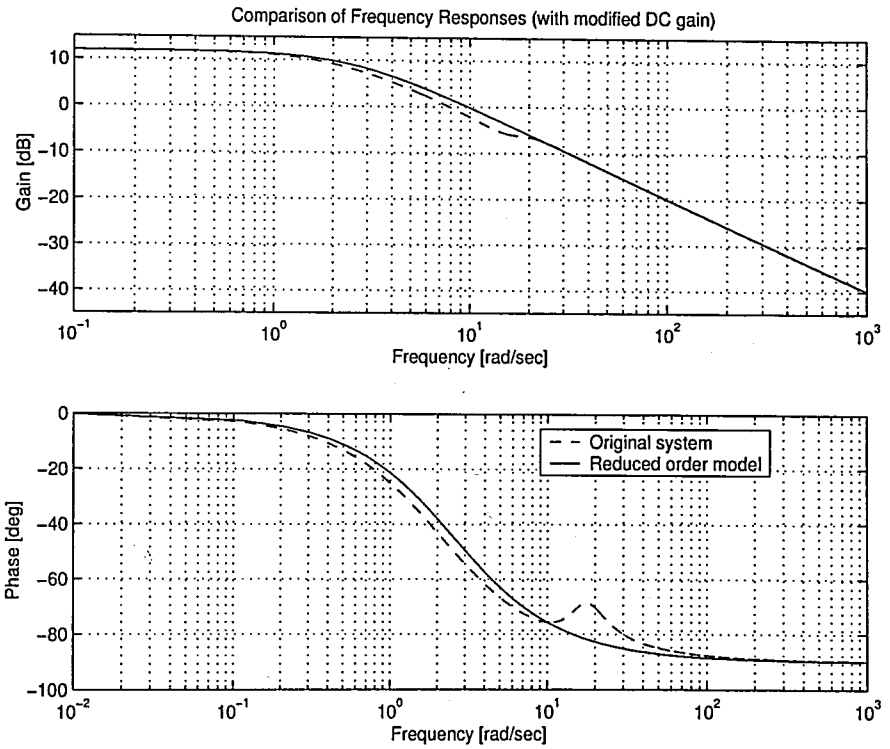

(b) Comparison of Bode plots

Figure 4.19. Comparison of responses for the arm prosthesis system

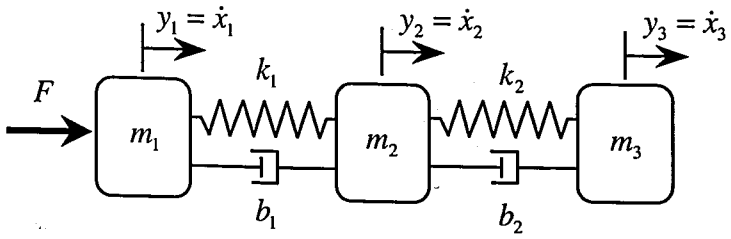

Figure 4.20. A $5th$ order unstable system

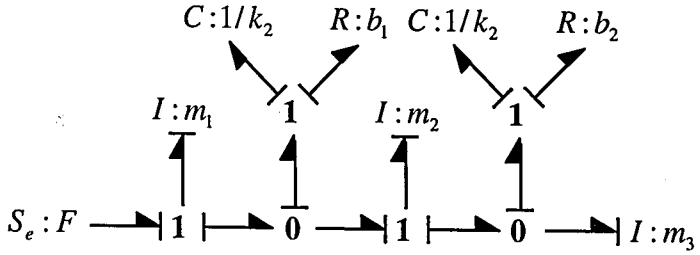

Figure 4.21. Bond graph representation of the $5th$ order unstable system

$(-1 \pm i, 0)$. The residue information indicates that the first subsystem should be retained in a possible reduced order model. This part is in fact the unstable part as suggested above.

The results of model reduction using the selected first subsystem is seen in Figure 4.22. One concludes the following: although gain plots are almost the same, there is a difference in the phase plots. But the results indicate that the reduced order model continues to portray the system behavior.

4.6. Effects of Different Inputs

In this section the effect of different inputs (especially sinusoidal) will be investigated on an example. If a specific input is applied to a system, only one of the modes of the system may be triggered. Thus, the reduced order model that needs to be selected changes depending on the triggered mode, i.e. this mode should be selected as the reduced order model.

As an example, consider the fifth order physical system of Figure 4.1. Assume

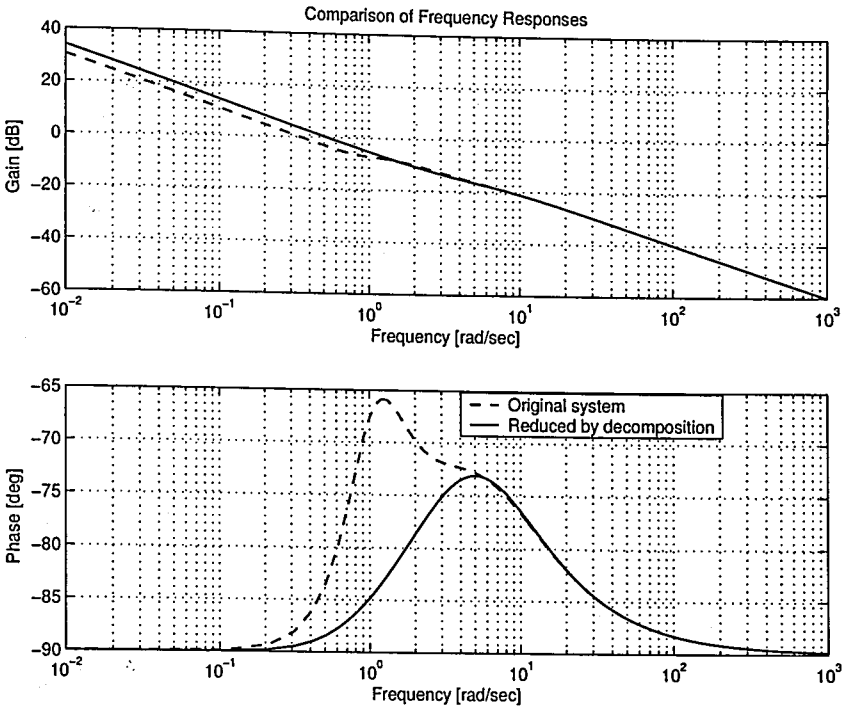

Figure 4.22. Comparison of Bode plots of full order and reduced order models obtained by the decomposition method

that the input to the system is exactly at the second mode's frequency which is $\omega = 5.45802 \ \frac{rad}{sec}$, i.e. $u(t) = \sin(5.45802t)$.

Using the same values for the component parameters, the simulation results for the original system and the selected reduced order model that consists of (m_1, m_2, k_1, k_3, b_1, b_3) for the given input is as shown in Figure 4.23. The figure indicates that the time and frequency responses are in good match and the reduced order model portrays the behavior of the full order model with its triggered second mode.

4.7. Comparison with Power and Energy Based Model Reduction

As explained previously, in the area of model reduction in the physical domain, one family of procedures are based on power criteria. The basic intuitive idea of the power criteria is that, a component associated with small power flow makes small contribution to a system's dynamic behavior. In this section by setting up a simple example, it is shown that the use of power criteria may lead to erroneous results. Further-

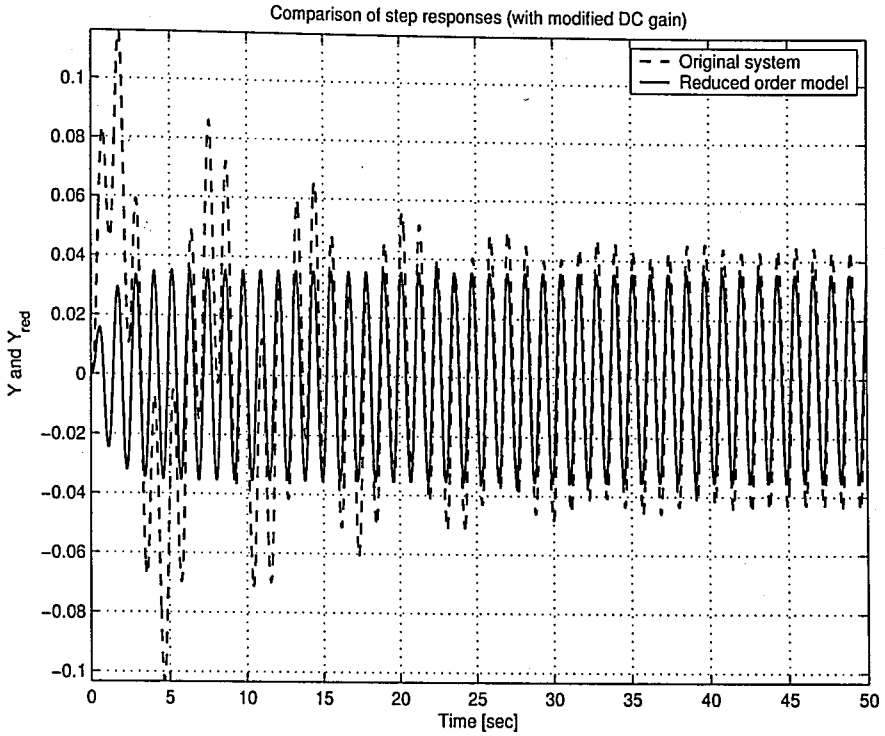

(a) Comparison of step responses

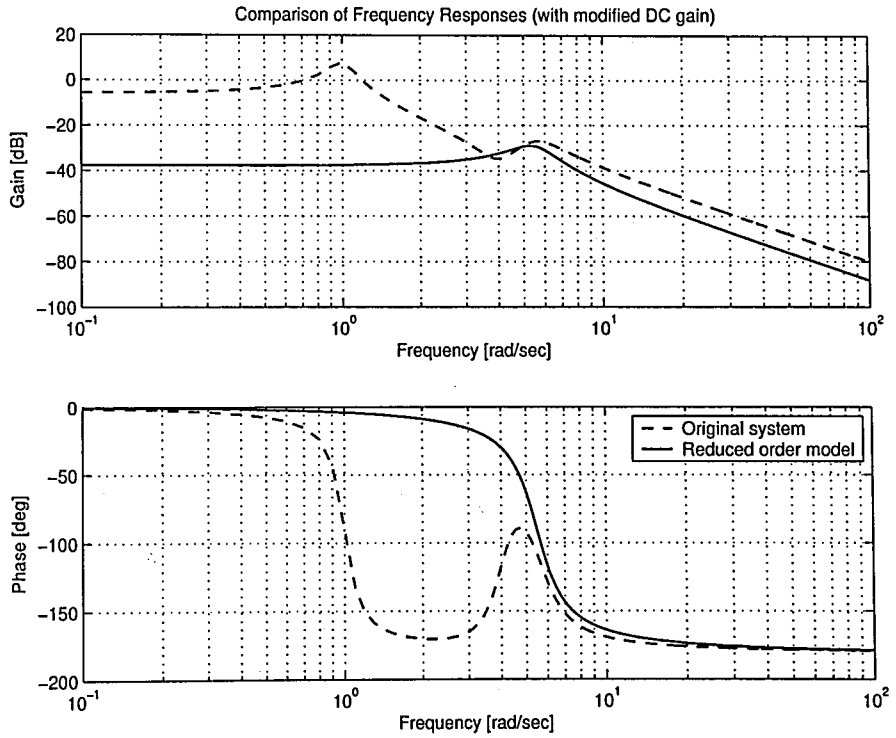

(b) Comparison of Bode plots

Figure 4.23. Comparison of responses with a specific sinusoidal input

more, the advantages of the model reduction based on the decomposition procedures presented in this thesis is indicated as appropriate.

As explained in Chapter 2, the power criteria uses various time averages of the power flow associated with a component to measure the corresponding power level. As pointed out in reference [18] the power flow of a component is in general a function of time. For example, if the current going through a resistant R is a sinusoid, $\sin(t)$, then the power flow into the resistant is $\mathcal{P} = R * i^2 = R\sin^2(t)$. It is indicated in literature [17, 18] that various time averages can be used as the measurements for the power flow level associated with a component. For this purpose two different indices have been used in the literature [17, 18, 56, 57, 58]. One of these indices is the RMS metric [18], which is the square root of the time average of the square of the power flow. Specifically, RMS metric is defined as,

$$\mathcal{P}_i = \sqrt{\frac{1}{T}\int_0^T P_i^2(t)dt}$$

where $\mathcal{P}_i(t)$ is the power associated with bond i. The other index is the activity index [17] defined as,

$$AI_i = \frac{\int_0^T |P_i(t)|dt}{\sum_{j=1}^{n}\int_0^T |P_i(t)|dt}$$

where n is the total number of bonds in a bond graph model. Activity index is basically the normalized time average of the absolute value of power flow.

Now, consider the simple electric circuit in Figure 4.24. This physical system is composed of a voltage source, a resistance, a capacitance and an inductance. Suppose that the output of the system is selected as the flow associated with the 1 junction, which is the current flowing in the circuit. Assume that $R = 0.05\ \Omega$, $L = 1\ H$ and $C = 1\ F$. Additionally, let the initial conditions be taken as zero. Then the system's

dynamic equation can be written as,

$$\frac{di^2(t)}{dt^2} + \frac{R}{L}\frac{di(t)}{dt} + \frac{1}{LC}i(t) = \frac{1}{L}\frac{d\sin(t)}{dt} \tag{4.8}$$

With the given numerical values, $i(t)$ can be solved as:

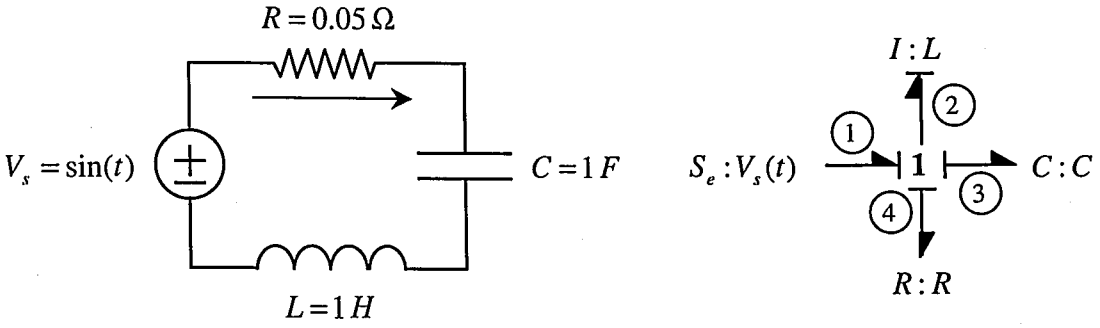

Figure 4.24. A simple electric circuit

$$i(t) = 20\sin(t) - 20.0062e^{-0.025t}\sin(0.9997t) \tag{4.9}$$

Additionally, in order to calculate the power flow associated with each component, the voltage across the inductance V_L, the capacitance V_C and the resistance V_R need to be calculated. These are given as:

$$\begin{aligned} V_L &= L\frac{di(t)}{dt} \\ V_C &= \int_{\tau=0}^{t} i(\tau)d\tau \\ V_R &= Ri(t) \end{aligned}$$

It is known that the power flow associated with each component is the multiplication of the current and the voltage associated with that component. The power responses of the components are calculated and are shown in Figure 4.25. The RMS of the power associated with the bonds 1, 2, 3, 4 are calculated as $\mathcal{P}_1 = 5.1216\,W$, $\mathcal{P}_2 = 29.6866\,W$, $\mathcal{P}_3 = 29.7308\,W$, and $\mathcal{P}_4 = 2.6454\,W$ respectively. Here, it can be observed that $\mathcal{P}_2$ and $\mathcal{P}_3$ are greater than $\mathcal{P}_1$ which is understandable as this lightly damped second order system has a resonant behavior. The system's damping coefficient is $\zeta = 0.025$.

Furthermore, the system has a natural frequency of $\omega_n = 1\,\frac{rad}{sec}$, and a damped natural frequency of $\omega_d = 0.9997\,\frac{rad}{sec}$. As the damping ratio is small, a very high resonant peak is expected. Additionally, the input frequency is very close to the damped natural frequency which drives the system very close to resonant peak. If a lightly damped system is excited close to its resonant frequency, the time average of power associated with energy storage elements can be greater than the power input to the system.

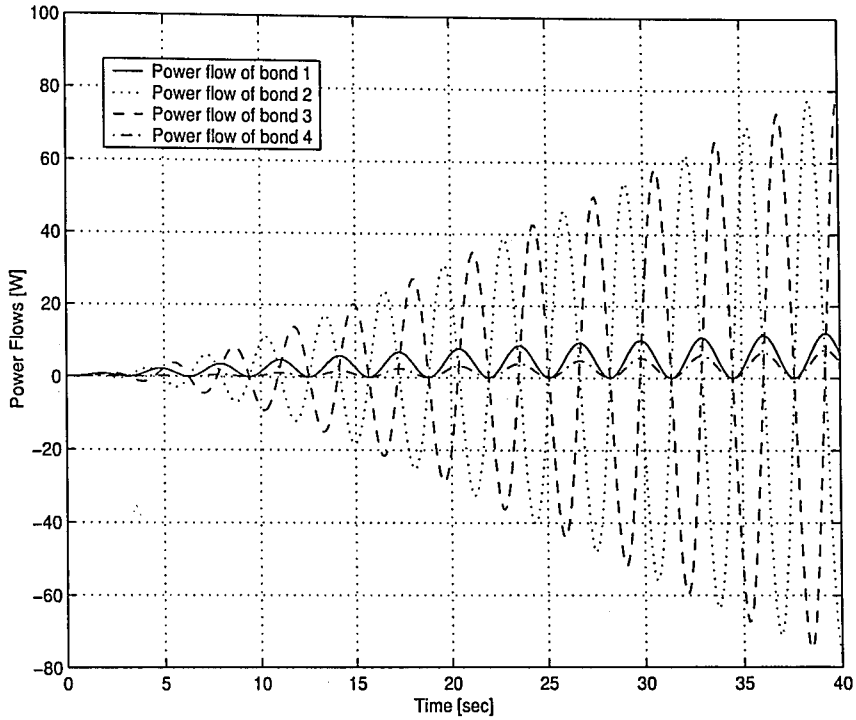

Figure 4.25. Power responses of the bonds

On the other hand, clearly, $\mathcal{P}_4$ is significantly smaller than others. Thus, according to the RMS index, bond 4 and therefore R element can be removed. In order to make a comparison, the activity indices can be calculated as $AI_1 = 0.0777$, $AI_2 = 0.4429$, $AI_3 = 0.4436$, and $AI_4 = 0.0358$. The activity index of bond 4 is again the smallest and is significantly smaller than all of the others. So the activity indices also indicate that bond 4 can be removed. Figure 4.26 shows the current (flow) of the original model and that of the reduced model. From this figure, the effect of damping on the period of the system can also be seen. The period of the original system is longer than that of the reduced model. For comparison, in Figure 4.26 at $t = 39.4\,sec$, for the original model $i(39.4\,sec) = 12.4013\,A$, and for the reduced

model $i(39.4\,sec) = 19.5173\,A$. The error of 57.3808% between these values is significant. Therefore, the R element is relevant to the flow associated with the 1 junction. The physical meaning of this result can be interpreted as follows: In the time interval $[20\,sec, 40\,sec]$, the R element dissipates about half of the power supplied by the source. Eliminating the R element significantly changes the rate of increase of the energy in the system. Therefore with the increase of time the error increases slowly but steadily. This result indicates that the R element in fact should not be removed from the system.

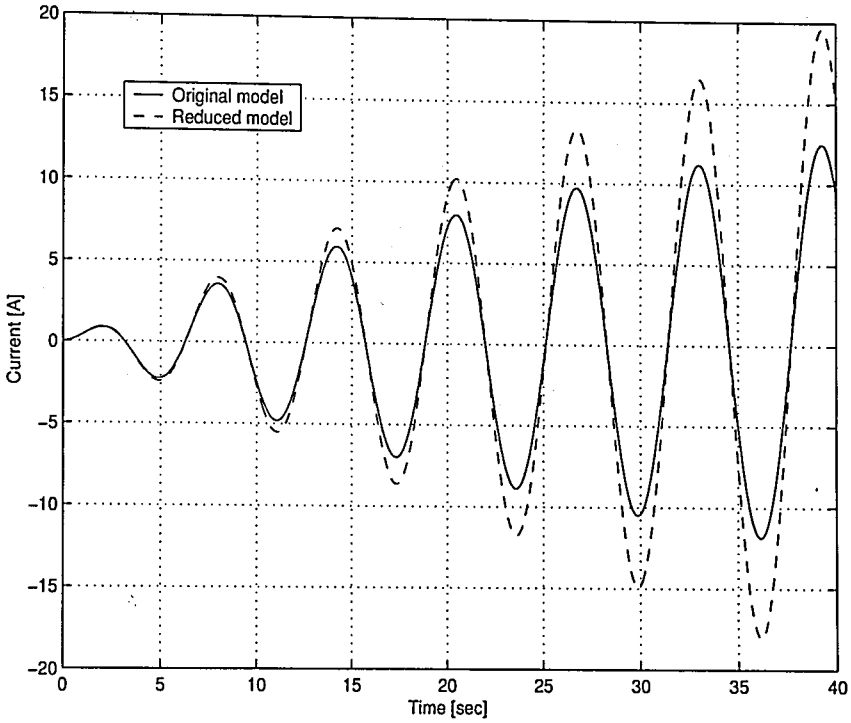

Figure 4.26. Current in the electric circuit (flow of 1 junction)

In the light of this discussion, the use of the model decomposition procedures described in this thesis is given as follows: With the given parameters, the system described above can be easily decomposed into two subsystems using the decomposition procedures, namely a damping part consisting of L and R elements, and an oscillatory part consisting of L and C elements. Notice that the removal of the R element is computed in a straightforward way by the local loop gains. Furthermore, the damping part introduces a new eigenvalue of (0.5) which only gives information on the damping factor of the system. If it is desired to find a reduced order model, it is concluded

that a suitable one cannot be found. The reason for this conclusion is that, for this system the only possible reduced order model is itself. If the oscillatory part is used and damping is eliminated (thus the R term), a large error in time response will result as indicated previously. This result also suggests that a typical second order system should not be further reduced.

4.8. Conclusion

In this chapter several examples are given to illustrate the effectiveness of the model reduction procedure described in Chapter 3. The results indicate that the model reduction procedure is indeed effective for linear dynamic systems. As discussed in Chapter 3, decomposition procedures may fail to identify relevant components when the system has uniform parameters or when the loop gains can not be distinguished. In order to overcome these problems two different procedures will be introduced in the next chapter.

5. EIGENVALUE SENSITIVITY AND EFFECT MATRIX

As discussed throughout this thesis, in industry and academia, the identification of subsystems and / or components that is related to a given eigenvalue of the overall system is a challenging and important topic. This chapter proposes a set of theorems and definitions that lead to an efficient procedure for this purpose. The basic procedure is based upon the calculation of sensitivity of eigenvalues. A so called "effect" matrix is produced that indicates the relative importance of physical parameters on a selected eigenvalue. In addition to the relative importance, the effect matrix is used for an efficient physical model reduction procedure. Furthermore, reasons of different dynamic behavior of a system can be explained. Within the chapter, the improvement of the physical model reduction method based on decomposition procedures will also be given.

5.1. Introduction

Sensitivity of a dynamic system to its physical parameters is often of interest. In this context, eigenvalue and eigenvector derivatives have been useful for determining the sensitivity of dynamic response to system parameter variations. For example, knowledge of the eigenvector derivatives with respect to physical parameters can be used to optimize a structural design or minimize its sensitivity to parameters. Such information can be used regularly for structural optimization, and for the improvement of the agreement between analytical and experimental results [68, 69]. Furthermore, eigen derivatives can be directly applied to system identification and robust performance tests for structural control systems [68, 69]. On the other hand, the eigenvalue sensitivity with respect to a physical parameter gives an estimate of the eigenvalue shift when such parameter is changed.

Several methods have been proposed to analyze the connection between a system variable and its modes [68, 69, 70]. The participation factor approach has been extensively used for the analysis of power systems [70, 71]. Dynamic systems with large number of state variables, such as power systems, are often too complex to be ana-

lyzed. The physical knowledge of the system might be utilized to simplify the model: knowing that the system presents an oscillatory behavior, the interest might be focused on a particular system eigenvalue (mode), by looking for the physical state variables most involved in the oscillation. In such cases, the participation factors might be useful in exploring the state variables that are relevant in the evolution of a particular eigenvalue [72].

Since the participation factors can be used to detect the states that are most involved in an eigenvalue, it is clear that once the eigenvalues of interest are identified, participation factors might help to obtain a reduced order model which still conserves the most relevant dynamics of the system. In particular, the most important problem is the identification of subsystems / components that affect a given eigenvalue.

In this chapter, a solution to the problem of sensitivity of a physical system with respect to its parameters is provided. For this purpose, in addition to a general analysis of participation factors and its relation to residues and eigenvalues, the use of eigenvalue sensitivity using special state-space descriptions has been investigated. The use of system matrices with certain structures lead to clearer and simpler results. Analyzing the procedures for obtaining system matrices using bond graphs leads to a very efficient solution. Thus in the following sections, the state-space representation discussed above will be briefly summarized. Then, the calculation of eigenvalue sensitivities using eigenvectors and their relationship to participation factors will be analyzed. Based on this analysis an "effect" matrix is introduced that indicates the relative importance of physical parameters on a selected eigenvalue. The effect matrices given in this chapter not only identify the irrelevant components but also give a relative measure of their contribution to the eigenvalue.

5.2. Structured Representation of LTI Systems Using Bond Graphs

A linear physical system can be characterized with matrices that identify the components and that define the structure of a system [73, 74]. The parameters of the components can be described by two matrices, one for independent energy stor-

age elements and one for dissipation elements. The energy storage elements can be represented by the matrix $\mathbf{S}$, defined as

$$\mathbf{z} = \mathbf{S}\mathbf{x} \tag{5.1}$$

where $\mathbf{x}$ is the generalized momentum / displacement vector and $\mathbf{z}$ is the corresponding flow / effort vector. In these vectors, x_i is the generalized momentum / displacement associated with the i'th independent energy storage element (state) and z_i is the flow / effort as the causal output of that element. For an LTI system with all of the independent energy storage elements of a total number of n are one port, $\mathbf{S}$ is a diagonal matrix of the form $\text{diag}[s_1, s_2, \ldots, s_n]$, with s_i's as the parameters of the energy storage elements. From a computation point of view, if the i'th independent energy storage element is a capacitance or an inertance, then $s_i = \frac{1}{C_i}$ or $s_i = \frac{1}{I_i}$, respectively.

On the other hand, the dissipation elements can be represented by the matrix $\mathbf{L}$, which contains the parameter values as follows: $\mathbf{d}_{out} = \mathbf{L}\mathbf{d}_{in}$, where d_{in_j} and d_{out_j} stand for the causal input and causal output of the j'th dissipation element, respectively. Again, for an LTI system with m one port dissipation elements, $\mathbf{L}$ is diagonal and of the form $\text{diag}[l_1, l_2, \ldots, l_m]$. When the j'th dissipation component has a flow or an effort as the causal input and an effort or a flow as the causal output, then $l_j = R_j$ or $l_j = \frac{1}{R_j}$, respectively.

Then, the structure of a system is described by [74]:

$$\dot{\mathbf{x}} = \mathbf{J}_{SS}\mathbf{z} + \mathbf{J}_{SL}\mathbf{d}_{out} + \mathbf{J}_{SU}\mathbf{u} \tag{5.2}$$

$$\mathbf{d}_{in} = \mathbf{J}_{LS}\mathbf{z} + \mathbf{J}_{LL}\mathbf{d}_{out} + \mathbf{J}_{LU}\mathbf{u} \tag{5.3}$$

where, $\mathbf{J}_{ij}$ represents the connectivity matrix between the outputs of j elements to inputs of i elements. In this representation L, S and U refers to dissipation, energy storage and input variables, respectively.

As a result, the system's state space equation can be rearranged as,

$$\dot{\mathbf{x}} = \mathbf{A}\mathbf{x} + \mathbf{B}\mathbf{u} \tag{5.4}$$

where

$$\mathbf{A} = \left[\mathbf{J}_{SS} + \mathbf{J}_{SL}\mathbf{L}(\mathbf{I} - \mathbf{J}_{LL}\mathbf{L})^{-1}\mathbf{J}_{LS}\right]\mathbf{S} \equiv \mathbf{J}\mathbf{S} \tag{5.5}$$

$$\mathbf{B} = \mathbf{J}_{SU} + \mathbf{J}_{SL}\mathbf{L}(\mathbf{I} - \mathbf{J}_{LL}\mathbf{L})^{-1}\mathbf{J}_{LU} \tag{5.6}$$

5.3. Calculation of Eigenvalue Sensitivities

Consider the LTI continuous time system

$$\dot{\mathbf{x}} = \mathbf{A}\mathbf{x} \tag{5.7}$$

where $\mathbf{x} \in \mathcal{R}^n$ and $\mathbf{A} \in \mathcal{R}^{n\times n}$.

Using modal decomposition matrix $\mathbf{A}$ can be written as:

$$\begin{aligned}\mathbf{A} &= \mathbf{U}\Lambda\mathbf{V} \\ &= \begin{bmatrix} \mathbf{u}_1 & \mathbf{u}_2 & \cdots & \mathbf{u}_n \end{bmatrix} \begin{bmatrix} \lambda_1 & 0 & \cdots & 0 \\ 0 & \lambda_2 & \cdots & 0 \\ 0 & 0 & \ddots & 0 \\ 0 & 0 & \cdots & \lambda_n \end{bmatrix} \begin{bmatrix} \mathbf{v}_1^T \\ \mathbf{v}_2^T \\ \vdots \\ \mathbf{v}_n^T \end{bmatrix}\end{aligned} \tag{5.8}$$

where $\mathbf{U}$ and $\mathbf{V}$ are the right and left eigenvector matrices, and Λ is a diagonal eigenvalue matrix. It should be noted that the eigenvectors $\mathbf{u}_i$ and $\mathbf{v}_i$ can always be chosen so that $\mathbf{u}_i^T\mathbf{v}_i = 1$, or similarly in matrix form, $\mathbf{UV} = \mathbf{VU} = \mathbf{I}$. Furthermore, in this representation, the $\mathbf{A}$ matrix is assumed to have only distinct eigenvalues. This assumption is used throughout this chapter.

Using the modal decomposition with a given initial condition vector $\mathbf{x}(0)$, the solution of Equation (5.7) is given as:

$$\mathbf{x}(t) = \sum_{i=1}^{n} e^{\lambda_i t} \mathbf{u}_i \mathbf{v}_i^T \mathbf{x}(0) \tag{5.9}$$

From this equation, one can write the kth state as follows:

$$\begin{aligned} \mathbf{x}^k(t) &= \sum_{i=1}^{n} e^{\lambda_i t} \mathbf{u}_i^k \mathbf{v}_i^T \mathbf{x}(0) \\ &= \sum_{i=1}^{n} e^{\lambda_i t} \mathbf{u}_i^k \left[\mathbf{v}_i^k \mathbf{x}^k(0) + \sum_{j=1, j\neq i}^{n} \mathbf{v}_i^j \mathbf{x}^j(0) \right] \\ &= \sum_{i=1}^{n} e^{\lambda_i t} p_{ki} \mathbf{x}^k(0) + \sum_{i=1}^{n} e^{\lambda_i t} \left[\sum_{j=1, j\neq k}^{n} P_{kij} \mathbf{x}^j(0) \right] \end{aligned} \tag{5.10}$$

where

$$\begin{aligned} p_{ki} &\triangleq \mathbf{u}_i^k \mathbf{v}_i^k \quad \text{participation factor} \\ P_{kij} &\triangleq \mathbf{u}_i^k \mathbf{v}_i^j \quad \text{generalized participation factor} \end{aligned} \tag{5.11}$$

The concept of participation factor was developed in [71] to measure the degree of participation of a state variable in a mode. Therefore, participation factor p_{ki} can be interpreted as the weight of the participation of i-th mode in the k-th state component. Simply, the participation factors can be seen as right eigenvectors weighted by left eigenvectors [71].

Using the participation values, a participation matrix can be formed as [71]:

$$\mathbf{H} = \begin{bmatrix} p_{11} & p_{12} & \cdots & p_{1n} \\ p_{21} & p_{22} & \cdots & p_{2n} \\ \vdots & \vdots & \vdots & \vdots \\ p_{n1} & p_{n2} & \cdots & p_{nn} \end{bmatrix} \tag{5.12}$$

For matrix $\mathbf{H}$, and for generalized participation values, the following properties

can be identified [72]:

i. $\sum_{i=1}^{n} p_{ki} = 1.$

ii. $\sum_{k=1}^{n} p_{ki} = 1.$

iii. $\sum_{i=1}^{n} P_{kij} = 0.$

In addition to the above basic properties, the following theorems can be stated and proved:

Theorem 1 *The generalized participation values are considered as the sensitivities of the eigenvalues of the matrix* **A***:*

$$P_{kij} = \frac{\partial \lambda_i}{\partial a_{jk}} \tag{5.13}$$

where a_{jk} represents the jk-th element of matrix **A** *[72].*

Proof:

$$\mathbf{v}_i^T \mathbf{A} \mathbf{u}_i = \lambda_i \mathbf{v}_i^T \mathbf{u}_i = \lambda_i$$

Then,

$$\begin{aligned}
\frac{\partial \lambda_i}{\partial q} &= \frac{\partial (\mathbf{v}_i^T \mathbf{A} \mathbf{u}_i)}{\partial q} \\
&= \frac{\partial \mathbf{v}_i^T}{\partial q} \underbrace{\mathbf{A}\mathbf{u}_i}_{\lambda_i \mathbf{u}_i} + \mathbf{v}_i^T \frac{\partial (\mathbf{A}\mathbf{u}_i)}{\partial q} \\
&= \lambda_i \frac{\partial \mathbf{v}_i^T}{\partial q} \mathbf{u}_i + \mathbf{v}_i^T \left(\frac{\partial \mathbf{A}}{\partial q} \mathbf{u}_i + \mathbf{A} \frac{\partial \mathbf{u}_i}{\partial q} \right) \\
&= \lambda_i \frac{\partial \mathbf{v}_i^T}{\partial q} \mathbf{u}_i + \mathbf{v}_i^T \frac{\partial \mathbf{A}}{\partial q} \mathbf{u}_i + \underbrace{\mathbf{v}_i^T \mathbf{A}}_{\lambda_i \mathbf{v}_i^T} \frac{\partial \mathbf{u}_i}{\partial q}
\end{aligned}$$

$$
\begin{aligned}
&= \mathbf{v}_i^T \frac{\partial \mathbf{A}}{\partial q}\mathbf{u}_i + \lambda_i \frac{\partial \mathbf{v}_i^T}{\partial q}\mathbf{u}_i + \lambda_i \mathbf{v}_i^T \frac{\partial \mathbf{u}_i}{\partial q} \\
&= \mathbf{v}_i^T \frac{\partial \mathbf{A}}{\partial q}\mathbf{u}_i + \underbrace{\lambda_i \frac{\partial (\mathbf{v}_i^T \mathbf{u}_i)}{\partial q}}_{= 0 \text{ as } \mathbf{v}_i^T \mathbf{u}_i = 1} \\
&= \mathbf{v}_i^T \frac{\partial \mathbf{A}}{\partial q}\mathbf{u}_i
\end{aligned}
$$

If the parameter q is the element a_{jk} of the matrix $\mathbf{A}$, then $\frac{\partial \mathbf{A}}{\partial a_{jk}}$ is a matrix whose elements are all zero and the element in j-th row and k-th column is one. Thus, one can write,

$$\frac{\partial \mathbf{A}}{\partial a_{jk}} = \mathbf{e}_j \mathbf{e}_k^T$$

where $\mathbf{e}_j$ and $\mathbf{e}_k$ are the j-th and k-th column of an identity matrix $\mathbf{I}_{n \times n}$, respectively. As a result,

$$\frac{\partial \lambda_i}{\partial a_{jk}} = \mathbf{v}_i^T \mathbf{e}_j \mathbf{e}_k^T \mathbf{u}_i = \mathbf{v}_i^j \mathbf{u}_i^k \equiv P_{kij}$$

□ End of proof.

It should be noted that this proof directly leads to the result that participation factors are the sensitivities of the diagonal terms of $\mathbf{A}$, i.e.:

$$p_{ki} = \frac{\partial \lambda_i}{\partial a_{kk}}$$

From the descriptions above the following theorem can also be deduced:

Theorem 2 *The entries of the system matrix* $\mathbf{A}$ *can be expressed as a linear combination of the eigenvalues with the coefficients being the participation values [72].*

Proof:

The $\mathbf{A}$ matrix can be written as:

$$\mathbf{A} = \sum_{i=1}^{n} \lambda_i \mathbf{u}_i \mathbf{v}_i^T$$

utilizing the dyadic form. Then,

$$\begin{aligned} a_{kj} &= \mathbf{e}_k^T \mathbf{A} \mathbf{e}_j \\ &= \sum_{i=1}^{n} \lambda_i \underbrace{\mathbf{e}_k^T \mathbf{u}_i}_{\mathbf{u}_i^k} \overbrace{\mathbf{v}_i^T \mathbf{e}_j}^{\mathbf{v}_i^j} \\ &= \sum_{i=1}^{n} \lambda_i P_{kij} \end{aligned}$$

Specifically, for the diagonal elements,

$$a_{kk} = \sum_{i=1}^{n} \lambda_i p_{ki}$$

is obtained. □ End of proof.

Furthermore, the following lemma can be written.

Lemma 1 *The following relation between the participation values (P_{kij}) and partial fraction expansion residues (R_i) holds:*

$$P_{kij} \triangleq \mathbf{e}_k^T R_i \mathbf{e}_j$$

Proof:

As one can write,

$$(s\mathbf{I}-\mathbf{A})^{-1}=\sum_{i=1}^{n}\frac{R_i}{s-\lambda_i}$$

and

$$\begin{aligned} e^{\mathbf{A}t} &= e^{\mathbf{U}\Lambda\mathbf{V}t}=\mathbf{U}e^{\Lambda t}\mathbf{V} \\ &= \sum_{i=1}^{n} e^{\lambda_i t}\mathbf{u}_i\mathbf{v}_i^T \quad \Rightarrow \quad R_i=\mathbf{u}_i\mathbf{v}_i^T \end{aligned}$$

then the participation values can be written as:

$$\begin{aligned} P_{kij} &\triangleq \mathbf{u}_i^k\mathbf{v}_i^j \\ &= \mathbf{e}_k^T\underbrace{\mathbf{u}_i\mathbf{v}_i^T}_{R_i}\mathbf{e}_j \\ \Rightarrow P_{kij} &\triangleq \mathbf{e}_k^T R_i\mathbf{e}_j \end{aligned}$$

□ End of proof.

The above definitions and theorems lead to a better understanding of the relationship between states and physical parameters.

5.4. Effect Matrices

In the previous sections the following state-space representation has been derived:

$$\dot{\mathbf{x}}=\mathbf{A}\mathbf{x} \tag{5.14}$$

where

$$\mathbf{A}=(\mathbf{J}_{SS}+\mathbf{J}_{SL}\mathbf{L}(\mathbf{I}-\mathbf{J}_{LL}\mathbf{L})^{-1}\mathbf{J}_{LS})\mathbf{S}\equiv\mathbf{J}\mathbf{S} \tag{5.15}$$

Using this special form of the state-space equations, two equations based on eigenvalue sensitivity can be formed.

Lemma 2 *The following relation is valid for the partial derivative of an eigenvalue with respect to an energy storage element when the structural state-space equation is used:*

$$\frac{\partial \lambda_i}{\partial s_j} = \mathbf{v}_i^T (\mathbf{J} t_j \mathbf{e}_j \mathbf{e}_j^T) \mathbf{u}_i \tag{5.16}$$

where t_j is a multiplication factor.

Proof:

$$\begin{aligned}
\frac{\partial \lambda_i}{\partial q} &= \mathbf{v}_i^T \frac{\partial \mathbf{A}}{\partial q} \mathbf{u}_i \\
\frac{\partial \lambda_i}{\partial s_j} &= \mathbf{v}_i^T \frac{\partial \mathbf{A}}{\partial s_j} \mathbf{u}_i \\
&= \mathbf{v}_i^T \frac{\partial (\mathbf{J}_{SS} + \mathbf{J}_{SL}\mathbf{L}(\mathbf{I} - \mathbf{J}_{LL}\mathbf{L})^{-1}\mathbf{J}_{LS})\mathbf{S}}{\partial s_j} \mathbf{u}_i \quad \text{or simply} \\
\frac{\partial \lambda_i}{\partial s_j} &= \mathbf{v}_i^T \frac{\partial \mathbf{J}\mathbf{S}}{\partial s_j} \mathbf{u}_i
\end{aligned}$$

as $\dfrac{\partial \mathbf{J}}{\partial s_j} = 0$ i.e., is constant with respect to s_j,

$$\begin{aligned}
\frac{\partial \lambda_i}{\partial s_j} &= \mathbf{v}_i^T \mathbf{J} \frac{\partial \mathbf{S}}{\partial s_j} \mathbf{u}_i \quad \text{and} \\
\frac{\partial \lambda_i}{\partial s_j} &= \mathbf{v}_i^T \mathbf{J} t_j \mathbf{e}_j \mathbf{e}_j^T \mathbf{u}_i
\end{aligned}$$

where s stands for energy storage elements as defined before.

□ End of proof.

It should be noted that the partial derivative is taken as $\mathbf{e}_j \mathbf{e}_j^T$ as the matrix $\mathbf{S}$ is diagonal. It is apparent that the multiplication factor t_j can be calculated in

a straightforward way. The multiplication factor depends on the form of the energy storage element as explained in Section 5.2. Table 5.1 gives a list of these multiplication factors.

Similarly, a second equation is formed as follows:

Lemma 3 *The following relation is valid for the partial derivative of an eigenvalue with respect to an energy dissipation element when the structural state-space equation is used:*

$$\frac{\partial \lambda_i}{\partial l_j} = \mathbf{v}_i^T (\mathbf{J}_{SL} z_j \mathbf{e}_j \mathbf{e}_j^T \mathbf{J}_{LS} \mathbf{S}) \mathbf{u}_i \tag{5.17}$$

where z_j is again a multiplication factor.

Proof:

$$\begin{aligned}
\frac{\partial \lambda_i}{\partial q} &= \mathbf{v}_i^T \frac{\partial \mathbf{A}}{\partial q} \mathbf{u}_i \\
\frac{\partial \lambda_i}{\partial l_j} &= \mathbf{v}_i^T \frac{\partial \mathbf{A}}{\partial l_j} \mathbf{u}_i \\
&= \mathbf{v}_i^T \frac{\partial (\mathbf{J}_{SS} + \mathbf{J}_{SL}\mathbf{L}(\mathbf{I} - \mathbf{J}_{LL}\mathbf{L})^{-1}\mathbf{J}_{LS})\mathbf{S}}{\partial l_j} \mathbf{u}_i \\
\frac{\partial \lambda_i}{\partial l_j} &= \mathbf{v}_i^T \left(\mathbf{J}_{SL} \frac{\partial \mathbf{L}}{\partial l_j} (\mathbf{I} - \mathbf{J}_{LL}\mathbf{L})^{-1} \mathbf{J}_{LS}\mathbf{S} + \mathbf{J}_{SL}\mathbf{L}(\mathbf{I} - \mathbf{J}_{LL}\mathbf{L})^{-2}\mathbf{J}_{LL}\mathbf{J}_{LS}\mathbf{S} \right) \mathbf{u}_i
\end{aligned}$$

if $\mathbf{J}_{LL} = 0$ i.e., no causal connection between dissipation elements,

$$\begin{aligned}
\frac{\partial \lambda_i}{\partial l_j} &= \mathbf{v}_i^T \mathbf{J}_{SL} \frac{\partial \mathbf{L}}{\partial l_j} \mathbf{J}_{LS} \mathbf{S} \mathbf{u}_i \quad \text{and} \\
\frac{\partial \lambda_i}{\partial l_j} &= \mathbf{v}_i^T \mathbf{J}_{SL} z_j \mathbf{e}_j \mathbf{e}_j^T \mathbf{J}_{LS} \mathbf{S} \mathbf{u}_i
\end{aligned}$$

where l stands for energy dissipation elements as defined before.

□ End of proof.

Table 5.1. A list of multiplication factors for effect matrices

Domain of interest	R element	$z_j = \frac{\partial R}{\partial l}$	I element	$t_j = \frac{\partial I}{\partial s}$	C element	$t_j = \frac{\partial C}{\partial s}$
Mechanical translation	b	1	$\frac{1}{m}$	$-\frac{1}{m^2}$	k	1
Mechanical rotation	c	1	$\frac{1}{J}$	$-\frac{1}{J^2}$	k	1
Hydraulic	R	1	$\frac{1}{I}$	$-\frac{1}{I^2}$	$\frac{1}{C}$	$-\frac{1}{C^2}$
Electrical	R	1	$\frac{1}{L}$	$-\frac{1}{L^2}$	$\frac{1}{C}$	$-\frac{1}{C^2}$

Here, for simplicity, it is assumed that $\mathbf{J}_{LL} \equiv 0$, i.e. none of the dissipation elements are directly casually related. This is not a critical assumption as this is a common case in structures. With this assumption $\mathbf{A}$ becomes as $\mathbf{A} = (\mathbf{J}_{SS} + \mathbf{J}_{SL}\mathbf{L}\mathbf{J}_{LS})\,\mathbf{S}$. Similar to the energy storage case the partial derivative on the right hand side of this equation is simply $\mathbf{e}_j\mathbf{e}_j^T$ since the matrix $\mathbf{L}$ is diagonal. Once again, a multiplication factor, z_j may be generated depending on the form of the dissipation element, see Table 5.1.

Using the eigenvalue sensitivities we can form and define two "effect" matrices, namely, one for energy storage, $\mathbf{E}_{IC}$, and one for energy dissipation elements, $\mathbf{E}_R$. The following six step procedure can be employed to form these matrices that will portray the relative contribution of physical elements on a selected eigenvalue:

1. After forming the bond graph of the system, calculate the system matrices $\mathbf{S}$, $\mathbf{J}_{SS}$, $\mathbf{L}$, $\mathbf{J}_{SL}$, $\mathbf{J}_{LS}$, $\mathbf{J}_{LL}$ and $\mathbf{A}$.
2. Form the state matrix of the system as $\mathbf{A} = \mathbf{JS}$ where $\mathbf{J}$ is defined as Equation (5.15).
3. Calculate the left and right eigenvector matrices of the state matrix $\mathbf{A}$, i.e. $\mathbf{V}$ and $\mathbf{U}$ matrices respectively.

4. For each eigenvalue calculate the following physical parameter sensitivities,

$$\begin{aligned}\frac{\partial \lambda_i}{\partial s_j} &= \mathbf{v}_i^T \mathbf{J} t_j \mathbf{e}_j \mathbf{e}_j^T \mathbf{u}_i \\ \frac{\partial \lambda_i}{\partial l_j} &= \mathbf{v}_i^T \left(\mathbf{J}_{SL} \frac{\partial \mathbf{L}}{\partial l_j} (\mathbf{I} - \mathbf{J}_{LL}\mathbf{L})^{-1} \mathbf{J}_{LS}\mathbf{S} + \mathbf{J}_{SL}\mathbf{L}(\mathbf{I} - \mathbf{J}_{LL}\mathbf{L})^{-2} \mathbf{J}_{LL}\mathbf{J}_{LS}\mathbf{S} \right) \mathbf{u}_i\end{aligned}$$

where $i = 1, \ldots, n$. Additionally $j = 1, \ldots, r$ for energy storage elements, and $j = 1, \ldots, m$ for dissipation elements.

5. Take the absolute value of the results, i.e. calculate $\left|\frac{\partial \lambda_i}{\partial s_j}\right|$ and $\left|\frac{\partial \lambda_i}{\partial l_j}\right|$.

6. Form the $\mathbf{E}_{IC}$ and $\mathbf{E}_R$ matrices using the eigenvalue sensitivity values such that each row corresponds to one eigenvalue, and each column corresponds to one energy storage or energy dissipation element, respectively, i.e.

$$\mathbf{E}_{IC} = \begin{bmatrix} \left|\frac{\partial \lambda_1}{\partial s_1}\right| & \left|\frac{\partial \lambda_1}{\partial s_2}\right| & \cdots & \left|\frac{\partial \lambda_1}{\partial s_r}\right| \\ \left|\frac{\partial \lambda_2}{\partial s_1}\right| & \left|\frac{\partial \lambda_2}{\partial s_2}\right| & \cdots & \left|\frac{\partial \lambda_2}{\partial s_r}\right| \\ \vdots & \vdots & \vdots & \vdots \\ \left|\frac{\partial \lambda_n}{\partial s_1}\right| & \left|\frac{\partial \lambda_n}{\partial s_2}\right| & \cdots & \left|\frac{\partial \lambda_n}{\partial s_r}\right| \end{bmatrix} \quad \text{and} \quad \mathbf{E}_R = \begin{bmatrix} \left|\frac{\partial \lambda_1}{\partial l_1}\right| & \left|\frac{\partial \lambda_1}{\partial l_2}\right| & \cdots & \left|\frac{\partial \lambda_1}{\partial l_m}\right| \\ \left|\frac{\partial \lambda_2}{\partial l_1}\right| & \left|\frac{\partial \lambda_2}{\partial l_2}\right| & \cdots & \left|\frac{\partial \lambda_2}{\partial l_m}\right| \\ \vdots & \vdots & \vdots & \vdots \\ \left|\frac{\partial \lambda_n}{\partial l_1}\right| & \left|\frac{\partial \lambda_n}{\partial l_2}\right| & \cdots & \left|\frac{\partial \lambda_n}{\partial l_m}\right| \end{bmatrix}$$

It is important to note that the introduction of the effect matrix, $\mathbf{E}_{IC}$ constitutes the superset of a method developed in [73]. In [73] a procedure was outlined for the identification of components that are irrelevant to a given eigenvalue, in which both eigenvectors of λ_i needs to be looked at separately. On contrast, the effect matrices given in this chapter not only identify the irrelevant components but also give a relative measure of their contribution to the selected eigenvalue. In the next section a sub-procedure for physical model reduction method based on decomposition procedures will be given. This sub-procedure uses the idea of [73], also see [75].

This section concludes the introduction of effect matrices. In the next section one of the applications of these matrices, namely physical based model reduction procedures will be explained.

5.4.1. Physical Model Reduction

For complex dynamic systems, it is often useful to find a simplified model for purposes such as controller design, parameter optimization, design assessment under uncertainty, and to get better insight into the system behavior. In recent years, physical based model reduction procedures have been developed as explained previously. For example, in chapter 3, a physical based model reduction procedure is developed and is assessed in chapter 4. The method leads to an appropriate reduced order model while retaining a physical relevance to the full order model. The proposed methodology in chapter 3 exploits the concept of decomposition of physical systems suitable for the identification of dominant subsystems. Although this procedure is efficient, when a system has uniform parameters or has numerically identical loop gains, it may fail to identify all of the modes of the system. In such cases the following three step sub-procedure improves the results:

1. First, the component that is irrelevant to a given mode is identified [73]. (This given mode is the mode that the decomposition procedure identifies as a candidate for a subsystem.)
2. Then the causal paths with this component and the rest of the system is examined on the bond graph.
3. The irrelevant component and the components that have a causal relation to it are placed in a separate subsystem.

Once the subsystems are identified the rest of the physical domain model reduction technique can be applied without any change, i.e. the residue information is used to select the physical reduced order model.

Although the above improved procedure is very effective, one needs to observe exact "zero" components in the eigenvectors. Alternatively, the effect matrices introduced in this chapter can be utilized to obtain a more efficient procedure. The use of effect matrices adds additional flexibility to the step of obtaining subsystems, i.e. depending on the relationship using the bond graph causality assignment, the physical

parameters that do not affect an eigenvalue of interest can be removed. Furthermore, the physical elements can be put in subsystems that define their specific behavior.

The physical domain model reduction procedure based on effect matrices is performed using the following five steps:

1. Calculate the $\mathbf{E}_{IC}$ and $\mathbf{E}_R$ matrices.
2. Calculate the residues of the system using $R_i = \mathbf{u}_i \mathbf{v}_i^T$ and indicate the eigenvalues that are more important, i.e. have the most contribution to the response and thus will be retained in a reduced order model.
3. Identify relevant or most effective energy storage elements for the selected eigenvalue in Step 2.
4. Identify the energy dissipation elements whose inputs are linear combinations of the outputs of the energy storage elements identified in Step 3.
5. Collect the elements identified in Steps 3 and 4. These elements constitute subsystem that generates the selected behavior and thus provide the reduced order model for the given system.

The identification of the energy dissipation elements of Step 4 is completed as follows:

- For each of the dissipation elements, follow the causal path initiated at its output, until all branches of the causal path reach an energy storage element.
- The input to the dissipation element is a linear combination of the identified energy storage elements, if every energy storage element reached by the branches of the causal path is the energy storage element identified in Step 3.

In the physical model reduction procedure the relevancy of energy dissipation elements to eigenvalues is determined in Step 4. The proof of this statement is accomplished by adopting a theorem given in [73]:

Theorem 3 *A dissipation element has the greatest contribution on the i'th eigenvalue λ_i, if its causal input is a linear combination of the outputs of the energy storage*

elements that have the highest contribution on λ_i.

Proof:

Assume that a dissipation element R_j with the parameter l_j is given. As

$$\dot{\mathbf{x}} = \mathbf{J}_{SS}\mathbf{z} + \mathbf{J}_{SL}\mathbf{d}_{out} + \mathbf{J}_{SU}\mathbf{u}$$

the parameter of the dissipation element enters the state matrix $\mathbf{A}$ via the output of the element $\mathbf{d}_{out}$. If the causal input of R_j is a linear combination of the energy storage elements, one has,

$$\mathbf{d}_{out_j} = l_j \cdot \sum_{k=r+1}^{n} \alpha_k s_k \mathbf{x}_k \tag{5.18}$$

where α_k are real numbers. Now suppose λ_i changes when l_j is set to be βl_j where β is a real number not equal to unity, i.e. $\beta \neq 1$. This means that λ_i changes when

$$\begin{aligned} \mathbf{d}_{out_j} &= (\beta l_j) \cdot \textstyle\sum_{k=r+1}^{n} \alpha_k s_k \mathbf{x}_k \\ &= l_j \cdot \textstyle\sum_{k=r+1}^{n} \alpha_k (\beta s_k) \mathbf{x}_k \end{aligned} \tag{5.19}$$

This means that changing l_j to βl_j while keeping all s_k constant is equivalent to changing all s_k's ($k \in [r+1, n]$) to βs_k while keeping l_j constant. Thus, if λ_i changes when l_j changes, it must be true that λ_i changes when s_k's change. Therefore it can be concluded that:

- The dissipation elements that have larger numerical values in effect matrix $\mathbf{E}_R$ and have causal connection to the energy storage elements with larger numerical values in effect matrix $\mathbf{E}_{IC}$ contribute more to λ_i.
- The dissipation elements that have zero values in effect matrix $\mathbf{E}_R$ and has causal connection to the energy storage elements with zero values in effect matrix $\mathbf{E}_{IC}$ are irrelevant to λ_i [73].

□ End of proof.

5.5. Implementation Examples

In this section three examples will be given: The first two examples are given to illustrate the construction of effect matrices for obtaining the relationship between eigenvalues and physical parameters, and the last one shows the use of the procedure for model reduction. The first example is a mass-spring-damper system. The second example is a standard bond graph example that can easily be found in electrical or mechanical systems, but it gives repeated eigenvalues. The example chosen for the repeated eigenvalue case is taken and adopted from [73], whereas the example for the model reduction sub-procedure is taken and adopted from chapter 4.

5.5.1. A Mass-Spring-Damper System

In this section, the eigenvalue sensitivity method will be applied to a mass-spring-damper system shown in Figure 5.1. The bond graph representation of this system is seen in Figure 5.2. This system is of order six, but with the states chosen in bond graph representation it possesses three excess states. The numerical values of the physical parameters are given as: $m_1 = m_2 = m_3 = 1\,kg$, $k_1 = 4\,N/m$, $k_2 = k_3 = k_4 = 1\,N/m$, $k_5 = 2.5\,N/m$, $k_6 = 5\,N/m$, and $b_1 = 1.5\,N\,sec/m$, $b_2 = b_3 = 0.5\,N\,sec/m$, $b_4 = 1\,N\,sec/m$, $b_5 = 0.4\,N\,sec/m$, $b_6 = 0.2\,N\,sec/m$.

For this system, the following matrices can be constructed:

$$\mathbf{S} = \begin{bmatrix} \frac{1}{m_1} & 0 & 0 & 0 & 0 & 0 & 0 & 0 & 0 \\ 0 & \frac{1}{m_2} & 0 & 0 & 0 & 0 & 0 & 0 & 0 \\ 0 & 0 & \frac{1}{m_3} & 0 & 0 & 0 & 0 & 0 & 0 \\ 0 & 0 & 0 & k_1 & 0 & 0 & 0 & 0 & 0 \\ 0 & 0 & 0 & 0 & k_2 & 0 & 0 & 0 & 0 \\ 0 & 0 & 0 & 0 & 0 & k_3 & 0 & 0 & 0 \\ 0 & 0 & 0 & 0 & 0 & 0 & k_4 & 0 & 0 \\ 0 & 0 & 0 & 0 & 0 & 0 & 0 & k_5 & 0 \\ 0 & 0 & 0 & 0 & 0 & 0 & 0 & 0 & k_6 \end{bmatrix} \tag{5.20}$$

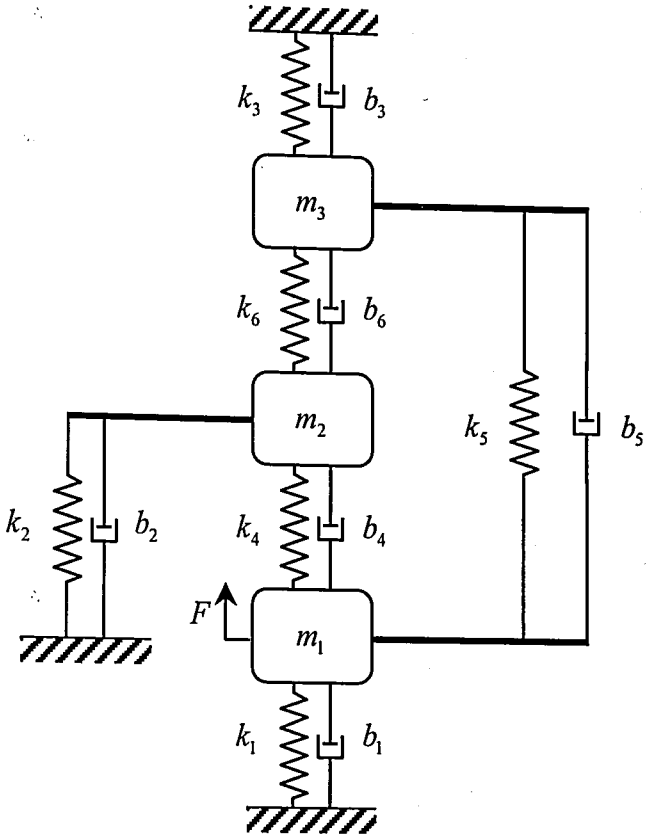

Figure 5.1. A mass-spring-damper system

$$\mathbf{J}_{SS} = \begin{bmatrix} 0 & 0 & 0 & -1 & 0 & 0 & -1 & -1 & 0 \\ 0 & 0 & 0 & 0 & -1 & 0 & 1 & 0 & -1 \\ 0 & 0 & 0 & 0 & 0 & -1 & 0 & 1 & 1 \\ 1 & 0 & 0 & 0 & 0 & 0 & 0 & 0 & 0 \\ 0 & 1 & 0 & 0 & 0 & 0 & 0 & 0 & 0 \\ 0 & 0 & 1 & 0 & 0 & 0 & 0 & 0 & 0 \\ 1 & -1 & 0 & 0 & 0 & 0 & 0 & 0 & 0 \\ 1 & 0 & -1 & 0 & 0 & 0 & 0 & 0 & 0 \\ 0 & 1 & -1 & 0 & 0 & 0 & 0 & 0 & 0 \end{bmatrix} \tag{5.21}$$

$$\mathbf{L} = \text{diag}\begin{bmatrix} b_1 & b_2 & b_3 & b_4 & b_5 & b_6 \end{bmatrix} \qquad \mathbf{J}_{LL} = \mathbf{0}_{6\times 6} \tag{5.22}$$

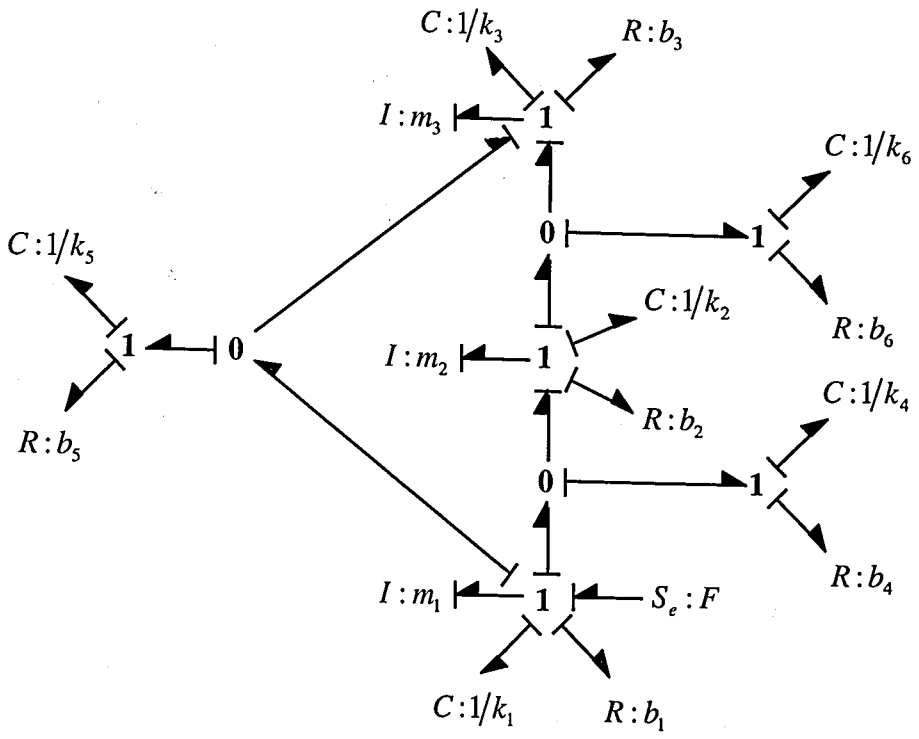

Figure 5.2. Bond graph representation of the mass-spring-damper system

$$\mathbf{J}_{SL} = \begin{bmatrix} -1 & 0 & 0 & -1 & -1 & 0 \\ 0 & -1 & 0 & 1 & 0 & -1 \\ 0 & 0 & -1 & 0 & 1 & 1 \\ 0 & 0 & 0 & 0 & 0 & 0 \\ 0 & 0 & 0 & 0 & 0 & 0 \\ 0 & 0 & 0 & 0 & 0 & 0 \\ 0 & 0 & 0 & 0 & 0 & 0 \\ 0 & 0 & 0 & 0 & 0 & 0 \\ 0 & 0 & 0 & 0 & 0 & 0 \end{bmatrix} \tag{5.23}$$

$$\mathbf{J}_{LS} = \begin{bmatrix} 1 & 0 & 0 & 0 & 0 & 0 & 0 & 0 & 0 \\ 0 & 1 & 0 & 0 & 0 & 0 & 0 & 0 & 0 \\ 0 & 0 & 1 & 0 & 0 & 0 & 0 & 0 & 0 \\ 1 & -1 & 0 & 0 & 0 & 0 & 0 & 0 & 0 \\ 1 & 0 & -1 & 0 & 0 & 0 & 0 & 0 & 0 \\ 0 & 1 & -1 & 0 & 0 & 0 & 0 & 0 & 0 \end{bmatrix} \tag{5.24}$$

With these matrices the dynamic **A** matrix of the system is obtained as:

$$\mathbf{A} = \begin{bmatrix} -\frac{(b_1+b_4+b_5)}{m_1} & \frac{b_4}{m_2} & \frac{b_5}{m_3} & -k_1 & 0 & 0 & -k_4 & -k_5 & 0 \\ \frac{b_4}{m_1} & -\frac{(b_2+b_4+b_6)}{m_2} & \frac{b_6}{m_3} & 0 & -k_2 & 0 & k_4 & 0 & -k_6 \\ \frac{b_5}{m_1} & \frac{b_6}{m_2} & -\frac{(b_3+b_5+b_6)}{m_3} & 0 & 0 & -k_3 & 0 & k_5 & k_6 \\ \frac{1}{m_1} & 0 & 0 & 0 & 0 & 0 & 0 & 0 & 0 \\ 0 & \frac{1}{m_2} & 0 & 0 & 0 & 0 & 0 & 0 & 0 \\ 0 & 0 & \frac{1}{m_3} & 0 & 0 & 0 & 0 & 0 & 0 \\ \frac{1}{m_1} & -\frac{1}{m_2} & 0 & 0 & 0 & 0 & 0 & 0 & 0 \\ \frac{1}{m_1} & 0 & -\frac{1}{m_3} & 0 & 0 & 0 & 0 & 0 & 0 \\ 0 & \frac{1}{m_2} & -\frac{1}{m_3} & 0 & 0 & 0 & 0 & 0 & 0 \end{bmatrix} \tag{5.25}$$

The eigenvalues of matrix **A** are calculated to be:

$$\begin{aligned} \lambda_{1,2} &= -0.7292 \pm 3.5448i \\ \lambda_{3,4} &= -1.7433 \pm 2.2674i \\ \lambda_{5,6} &= -0.3774 \pm 1.2456i \end{aligned}$$

Additionally, with the calculation of eigenvectors, the effect matrices are formed as:

$$\mathbf{E}_{IC} = \begin{bmatrix} 0.1005 & \mathbf{0.6548} & \mathbf{1.0945} & 0.0077 & 0.0500 & 0.0836 & 0.0185 & 0.1416 & \mathbf{0.2626} \\ 0.1005 & \mathbf{0.6548} & \mathbf{1.0945} & 0.0077 & 0.0500 & 0.0836 & 0.0185 & 0.1416 & \mathbf{0.2626} \\ 1.3926 & 0.4001 & 0.0176 & 0.1702 & 0.0489 & 0.0022 & 0.4009 & 0.2091 & 0.0309 \\ 1.3926 & 0.4001 & 0.0176 & 0.1702 & 0.0489 & 0.0022 & 0.4009 & 0.2091 & 0.0309 \\ 0.1064 & 0.3048 & 0.2720 & 0.0628 & 0.1799 & 0.1606 & 0.0308 & 0.0227 & 0.0008 \\ 0.1064 & 0.3048 & 0.2720 & 0.0628 & 0.1799 & 0.1606 & 0.0308 & 0.0227 & 0.0008 \end{bmatrix} \tag{5.26}$$

and

$$\mathbf{E}_R = \begin{bmatrix} 0.0278 & 0.1809 & 0.3024 & 0.0671 & 0.5125 & \mathbf{0.9504} \\ 0.0278 & 0.1809 & 0.3024 & 0.0671 & 0.5125 & \mathbf{0.9504} \\ 0.4869 & 0.1399 & 0.0062 & 1.1466 & 0.5980 & 0.0885 \\ 0.4869 & 0.1399 & 0.0062 & 1.1466 & 0.5980 & 0.0885 \\ 0.0818 & 0.2342 & 0.2090 & 0.0400 & 0.0295 & 0.0010 \\ 0.0818 & 0.2342 & 0.2090 & 0.0400 & 0.0295 & 0.0010 \end{bmatrix} \tag{5.27}$$

Here, in matrix $\mathbf{E}_{IC}$ each column corresponds to one energy storage element, in the same order as that of matrix $\mathbf{S}$, and each row corresponds to one eigenvalue. For example the values $\mathbf{E}_{IC_{31}}$ and $\mathbf{E}_{IC_{41}}$ of 1.3926 give the relative weights of m_1 on eigenvalues $\lambda_{3,4} = -1.7433 \pm 2.2674i$. Similarly, in matrix $\mathbf{E}_R$ each column corresponds to one energy dissipation element in the same order of matrix $\mathbf{L}$, and each row corresponds to one eigenvalue. From the effect matrices, one can observe that the parameters m_2, m_3, k_6 and b_6 (shown in bold case) have the most effect on $\lambda_{1,2}$ values. This result indicates that these physical parameters influence that eigenvalue. As these parameters are directly casually related in the bond graph, they can be put in a subsystem that portrays the behavior of the first complex-conjugate eigenvalue. This result is important, as it directly helps in identifying the relevant parameters for a selected eigenvalue, and also allows the user to select the parameters to obtain a predefined eigenvalue.

5.5.2. A Simple Example with Repeated Roots

Consider the system given by the bond graph in Figure 5.3, [73]. All parameter values except α are shown on the figure. For this example $\alpha = 1$ is chosen.

For this system, using the same approach as in the first example the following

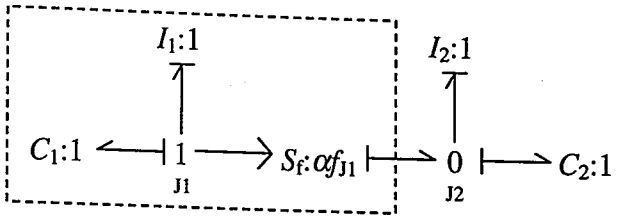

Figure 5.3. A simple system

system matrices can be constructed:

$$\mathbf{S} = \begin{bmatrix} \frac{1}{I_1} & 0 & 0 & 0 \\ 0 & \frac{1}{C_1} & 0 & 0 \\ 0 & 0 & \frac{1}{I_2} & 0 \\ 0 & 0 & 0 & \frac{1}{C_2} \end{bmatrix} \quad \mathbf{J} = \begin{bmatrix} 0 & -1 & 0 & 0 \\ 1 & 0 & 0 & 0 \\ 0 & 0 & 0 & 1 \\ 1 & 0 & -1 & 0 \end{bmatrix} \tag{5.28}$$

With these two matrices the dynamic **A** matrix of the system is obtained as:

$$\mathbf{A} = \mathbf{JS} = \begin{bmatrix} 0 & -\frac{1}{C_1} & 0 & 0 \\ \frac{1}{I_1} & 0 & 0 & 0 \\ 0 & 0 & 0 & \frac{1}{C_2} \\ \frac{1}{I_1} & 0 & -\frac{1}{I_2} & 0 \end{bmatrix} \tag{5.29}$$

This system produces the symbolic eigenvalues as: $\pm\sqrt{\frac{1}{I_1C_1}}i$, and $\pm\sqrt{\frac{1}{I_2C_2}}i$. With the chosen parameter values the numerical eigenvalues are calculated as: $\pm i$, $\pm i$, which indicates that there are two repeated roots. Thus, generalized eigenvectors have to be calculated. As a result, the right and left eigenvector matrices for this **A** matrix are computed as:

$$\mathbf{U} = \begin{bmatrix} \mathbf{u}_1 & \mathbf{u}_2 & \mathbf{u}_3 & \mathbf{u}_4 \end{bmatrix} \tag{5.30}$$

$$\mathbf{V} = \begin{bmatrix} \mathbf{v}_1 & \mathbf{v}_2 & \mathbf{v}_3 & \mathbf{v}_4 \end{bmatrix} \tag{5.31}$$

where

$$\mathbf{u}_1 = \begin{bmatrix} 0 \\ 0 \\ -0.2500i \\ 0.2500 \end{bmatrix}, \mathbf{u}_2 = \begin{bmatrix} 0.5000 \\ -0.5000i \\ 0 \\ -0.2500i \end{bmatrix}$$

$$\mathbf{u}_3 = \begin{bmatrix} 0 \\ 0 \\ 0.2500i \\ 0.2500 \end{bmatrix}, \mathbf{u}_4 = \begin{bmatrix} 0.5000 \\ 0.5000i \\ 0 \\ 0.2500i \end{bmatrix}$$

and

$$\mathbf{v}_1 = \begin{bmatrix} 0 \\ -1.0000 \\ -2.0000i \\ 2.0000 \end{bmatrix}, \mathbf{v}_2 = \begin{bmatrix} 1.0000 \\ -1.0000i \\ 0 \\ 0 \end{bmatrix}$$

$$\mathbf{v}_3 = \begin{bmatrix} 0 \\ 1.0000 \\ 2.0000i \\ 2.0000 \end{bmatrix}, \mathbf{v}_4 = \begin{bmatrix} 1.0000 \\ 1.0000i \\ 0 \\ 0 \end{bmatrix}$$

As this system has repeated eigenvalues the eigenvectors are the generalized eigenvectors. But as explained before, this does not alter the given derivations. Since there are no dissipation elements in this system, $\mathbf{E}_R = \mathbf{0}$, and $\mathbf{E}_{IC}$ is calculated to be:

$$\mathbf{E}_{IC} = \begin{bmatrix} 0 & 0 & 0.5000 & 0.5000 \\ 0.5000 & 0.5000 & 0 & 0 \\ 0 & 0 & 0.5000 & 0.5000 \\ 0.5000 & 0.5000 & 0 & 0 \end{bmatrix} \tag{5.32}$$

For this system the eigenvalues are in order of $i, i, -i, -i$. The effect matrix indicates that all the elements have the same effect on eigenvalues. It can be observed that these results are expected. It can also be observed that only $I_1 - C_1$ affect one set of eigenvalues, and $I_2 - C_2$ affect the other. This is consistent with the symbolic calculation.

5.5.3. A SISO Physical Example

In this subsection, the use of the sub-procedure for model reduction for a single-input single-output (SISO) physical system is presented.

Consider the system shown in Figure 5.4. The bond graph representation of this system is displayed in Figure 5.5.

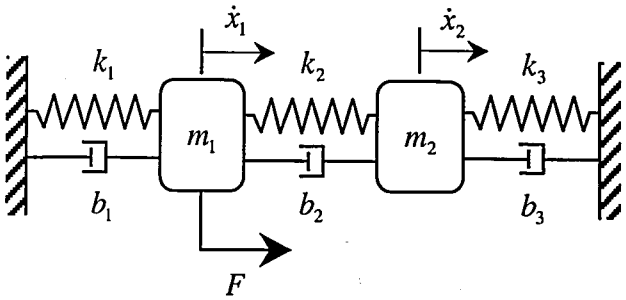

Figure 5.4. A SISO physical system

Let's assume that the system has uniform parameters, i.e. $m_1 = m_2 = 1\,kg$, $k_1 = k_2 = k_3 = 2\,N/m$, $b_1 = b_2 = b_3 = 1\,N\,sec/m$. For this set of parameters the physical model reduction method described in Chapter 3, Section 3.7 is not efficient.

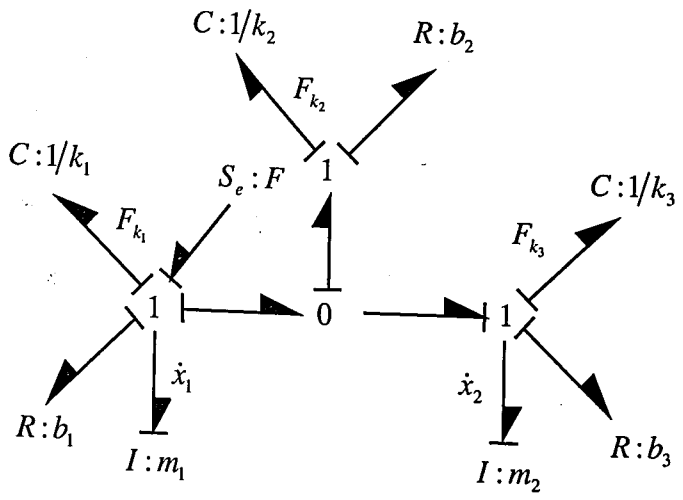

Figure 5.5. Bond graph representation of the SISO physical system

This is because the local damping ratios and loop gains are numerically exactly the same, and the sum of loop gains are approximately the same. Thus, for model reduction the sub-procedure explained in this chapter will be applied.

For this system, the following system matrices can be constructed:

$$\mathbf{S} = \begin{bmatrix} \frac{1}{m_1} & 0 & 0 & 0 & 0 \\ 0 & \frac{1}{m_2} & 0 & 0 & 0 \\ 0 & 0 & k_1 & 0 & 0 \\ 0 & 0 & 0 & k_2 & 0 \\ 0 & 0 & 0 & 0 & k_3 \end{bmatrix} \tag{5.33}$$

$$\mathbf{J}_{SS} = \begin{bmatrix} 0 & 0 & -1 & -1 & 0 \\ 0 & 0 & 0 & 1 & -1 \\ 1 & 0 & 0 & 0 & 0 \\ 1 & -1 & 0 & 0 & 0 \\ 0 & 1 & 0 & 0 & 0 \end{bmatrix} \tag{5.34}$$

$$\mathbf{L} = \begin{bmatrix} b_1 & 0 & 0 \\ 0 & b_2 & 0 \\ 0 & 0 & b_3 \end{bmatrix} \quad \mathbf{J}_{LL} = \begin{bmatrix} 0 & 0 & 0 \\ 0 & 0 & 0 \\ 0 & 0 & 0 \end{bmatrix} \tag{5.35}$$

$$\mathbf{J}_{SL} = \begin{bmatrix} -1 & -1 & 0 \\ 0 & 1 & -1 \\ 0 & 0 & 0 \\ 0 & 0 & 0 \\ 0 & 0 & 0 \end{bmatrix} \quad \mathbf{J}_{LS} = \begin{bmatrix} 1 & 0 & 0 & 0 & 0 \\ 1 & -1 & 0 & 0 & 0 \\ 0 & 1 & 0 & 0 & 0 \end{bmatrix} \tag{5.36}$$

With these matrices the dynamic **A** matrix of the system is obtained as:

$$\mathbf{A} = \begin{bmatrix} -\frac{b_1+b_2}{m_1} & \frac{b_2}{m_2} & -k_1 & -k_2 & 0 \\ \frac{b_2}{m_1} & -\frac{b_2+b_3}{m_2} & 0 & k_2 & -k_3 \\ \frac{1}{m_1} & 0 & 0 & 0 & 0 \\ \frac{1}{m_1} & -\frac{1}{m_2} & 0 & 0 & 0 \\ 0 & \frac{1}{m_2} & 0 & 0 & 0 \end{bmatrix} \tag{5.37}$$

The eigenvalues, and the right and left eigenvector matrices of matrix **A** are computed as:

$$\begin{aligned} \lambda_{1,2} &= -1.5000 \pm 1.9365i \\ \lambda_{3,4} &= -0.5000 \pm 1.3229i \\ \lambda_5 &= 0 \end{aligned}$$

$$\mathbf{U} = \begin{bmatrix} \mathbf{u}_1 & \mathbf{u}_2 & \mathbf{u}_3 & \mathbf{u}_4 & \mathbf{u}_5 \end{bmatrix} \tag{5.38}$$

$$\mathbf{V} = \begin{bmatrix} \mathbf{v}_1 & \mathbf{v}_2 & \mathbf{v}_3 & \mathbf{v}_4 & \mathbf{v}_5 \end{bmatrix} \tag{5.39}$$

where

$$\mathbf{u}_1 = \begin{bmatrix} -0.4193 + 0.3969i \\ 0.4193 - 0.3969i \\ 0.2329 + 0.0361i \\ 0.4658 + 0.0722i \\ -0.2329 - 0.0361i \end{bmatrix}, \mathbf{u}_2 = \begin{bmatrix} -0.4193 - 0.3969i \\ 0.4193 + 0.3969i \\ 0.2329 - 0.0361i \\ 0.4658 - 0.0722i \\ -0.2329 + 0.0361i \end{bmatrix}$$

$$\mathbf{u}_3 = \begin{bmatrix} 0.3906 + 0.4252i \\ 0.3906 + 0.4252i \\ 0.1836 - 0.3646i \\ 0 \\ 0.1836 - 0.3646i \end{bmatrix}, \mathbf{u}_4 = \begin{bmatrix} 0.3906 - 0.4252i \\ 0.3906 - 0.4252i \\ 0.1836 + 0.3646i \\ 0 \\ 0.1836 + 0.3646i \end{bmatrix}, \mathbf{u}_5 = \begin{bmatrix} 0 \\ 0 \\ -0.5774 \\ 0.5774 \\ 0.5774 \end{bmatrix}$$

and

$$\mathbf{v}_1 = \begin{bmatrix} -0.0838 + 0.5413i \\ 0.0838 - 0.5413i \\ 0.3075 + 0.3248i \\ 0.6149 + 0.6495i \\ -0.3075 - 0.3248i \end{bmatrix}, \mathbf{v}_2 = \begin{bmatrix} -0.0838 - 0.5413i \\ 0.0838 + 0.5413i \\ 0.3075 - 0.3248i \\ 0.6149 - 0.6495i \\ -0.3075 + 0.3248i \end{bmatrix}$$

$$\mathbf{v}_3 = \begin{bmatrix} 0.4135 + 0.2082i \\ 0.4135 + 0.2082i \\ 0.4821 - 0.4429i \\ 0 \\ 0.4821 - 0.4429i \end{bmatrix}, \mathbf{v}_4 = \begin{bmatrix} 0.4135 - 0.2082i \\ 0.4135 - 0.2082i \\ 0.4821 + 0.4429i \\ 0 \\ 0.4821 + 0.4429i \end{bmatrix}, \mathbf{v}_5 = \begin{bmatrix} 0 \\ 0 \\ -0.5774 \\ 0.5774 \\ 0.5774 \end{bmatrix}$$

Additionally, the effect matrices are calculated as:

$$\mathbf{E}_{IC} = \begin{bmatrix} 0.7746 & 0.7746 & 0.1291 & 0.5164 & 0.1291 \\ 0.7746 & 0.7746 & 0.1291 & 0.5164 & 0.1291 \\ 0.3780 & 0.3780 & 0.1890 & \mathbf{0.0000} & 0.1890 \\ 0.3780 & 0.3780 & 0.1890 & \mathbf{0.0000} & 0.1890 \\ 0.0000 & 0.0000 & 0.0000 & 0.0000 & 0.0000 \end{bmatrix} \tag{5.40}$$

and

$$\mathbf{E}_{R} = \begin{bmatrix} 0.3162 & 1.2649 & 0.3162 \\ 0.3162 & 1.2649 & 0.3162 \\ 0.2673 & \mathbf{0.0000} & 0.2673 \\ 0.2673 & \mathbf{0.0000} & 0.2673 \\ 0.0000 & 0.0000 & 0.0000 \end{bmatrix} \tag{5.41}$$

Upon examination of the effect matrices, one can immediately see that the physical parameters k_2 and b_2 has no influence on $\lambda_{3,4} = -0.5000 \pm 1.3229i$ as their values are exactly zero. These values are shown in bold case in the matrices. The application of the sub-procedure outlined in Section 5.4.1 produces the two subsystems of Figure 5.6. It is also noted that the effect matrices indicate the symmetry of the system.

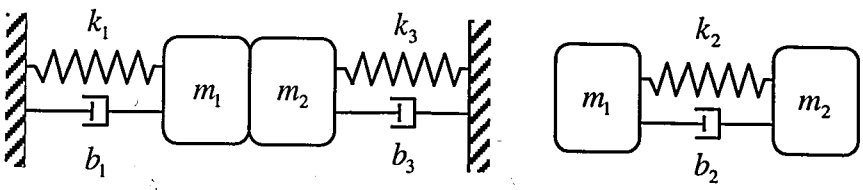

(a) Subsystem 1 (b) Subsystem 2

Figure 5.6. Subsystems of the SISO physical system

From this point, if the physical domain model reduction given in Section 3.7 is worked out as usual, the simulated results are as shown in Figure 5.7. In this type of physical model reduction procedures there can be a DC gain discrepancy between the

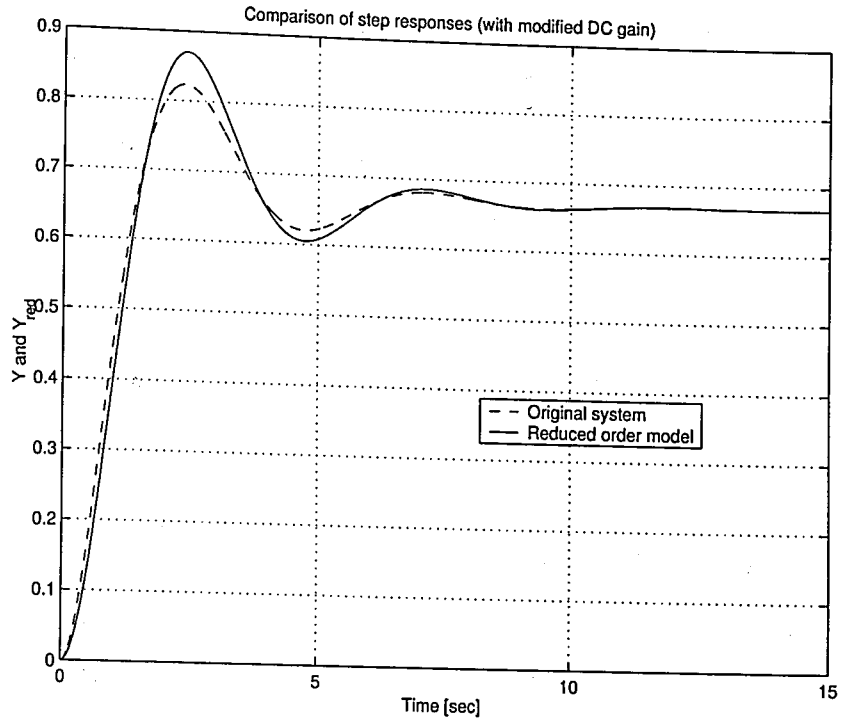

(a) Comparison of step responses

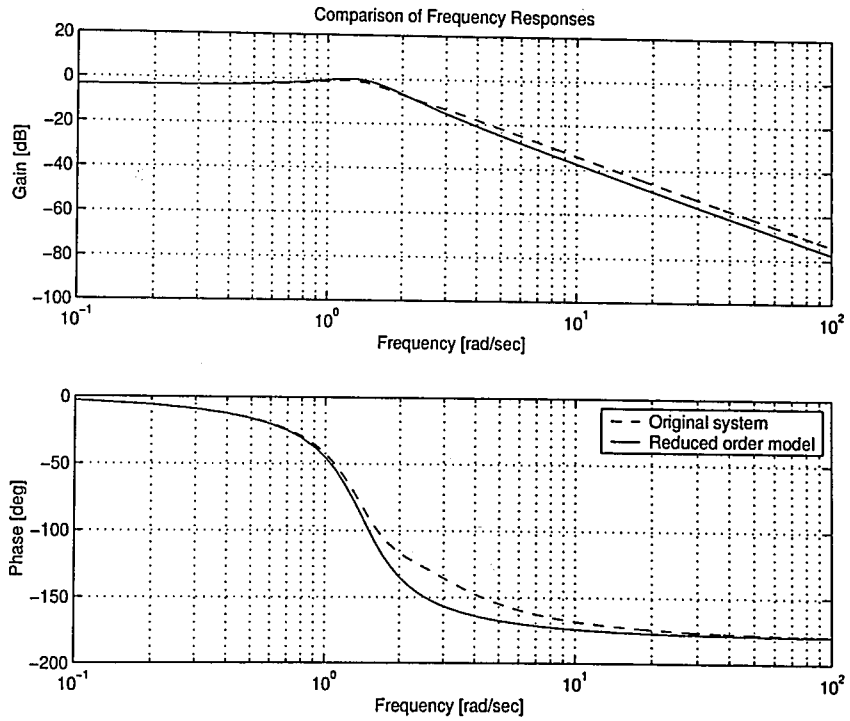

(b) Comparison of Bode plots

Figure 5.7. Comparison of full order and reduced order model with uniform parameters

reduced and the full order models that can be corrected easily. The DC gain difference may occur in cases where some parameters are eliminated without compensating their effects on the system as described previously. As it can be seen from these figures, the results are acceptable and the reduced order model provides a good approximation with this modification of gain.

5.6. Conclusions

In this chapter, a set of theorems and definitions that lead to an efficient procedure for the identification of subsystems and / or components that determine a given eigenvalue of the overall system is proposed. In the procedure, a special type of state-space description obtained from bond graphs is utilized. After the calculation of eigenvectors and the defined effect matrices, the relative importance of physical parameters in a selected eigenvalue is readily obtained. Furthermore two physical based model reduction procedures are explained: a sub-procedure is given to improve the decomposition based physical model reduction method, and one new procedure is given that utilizes the effect matrices. Three examples are given to illustrate the results.

6. DISCUSSION, CONCLUSIONS AND RECOMMENDATIONS FOR FUTURE WORK

Establishing relations between the physical components of a system and its dynamic behavior is an interesting and important topic. With the understanding of such a relation, desirable dynamic behavior of a system can be achieved by appropriate choices of its parameters and structures. Additionally, simplified models of the systems having several advantages including the reduction of computational complexity and improved understanding of the original system structure can be obtained. Thus, this thesis is concerned with obtaining physical based low order approximations of linear physical systems. For this purpose several methodologies are presented in order to provide useful information about the physical systems and appropriate physical reduced order models.

The thesis has presented a fundamental framework for a systematic model reduction in the physical domain. For this purpose, the relationship between the components of the system in bond graph representation is explored. Based on this exploration, existing decomposition procedures are utilized to identify different behavior of dynamic systems. In addition, past researches on physical domain model reduction methods are reconsidered. Advantages and restrictions of some of the past work are reviewed and new concepts are proposed. For example, a relation between partial fraction expansion residues and Hankel singular values is presented. This relationship indicates that the presented physical domain model reduction procedure based on partial fraction expansion residues and balanced truncation methods are in fact very close to each other, as residues and HSVs provide similar results. This leads to the explanation of the eigenvalues obtained from balanced truncation type of approaches.

The approaches in this thesis can be applied to both SISO and MIMO systems. Furthermore, as an approximate eigenvalue distribution is obtained by using the exiting decomposition procedures, a suitable reduced order model for specific inputs (with

specific frequency content) can be selected in a straightforward way. This reduces the computational effort that occurs in purely numerical techniques. In numerical techniques such as the balanced truncation type of approaches, the reduced order model needs to be calculated from the beginning for different inputs. On the contrary, the decomposition procedures explained in this thesis enable the user to directly select the appropriate reduced order model by looking at the partial fraction expansion residue information and the corresponding subsystems.

One of the proposed methodologies exploits the idea of decomposition of physical systems suitable for the identification of dominant subsystems. Most of the previous model reduction techniques use numerical approaches and the resulting reduced order model does not have a physical relevance to the original system. Physical based model reduction methods making use of the bond graphs and power and energy level information eliminate *elements* that are considered unnecessary without indicating which *subsystems* to remove in *a systemic perspective view.* In contrast, the proposed model reduction procedures are directly implemented on the model providing a better perception of the physical model reduction and a better design point of view. In addition to this feature, the simple and the extended decomposition procedures in the literature that are used to identify, i) fast-slow dynamics, ii) high-low frequency oscillation modes and, iii) heavily-lightly damped dynamic subsystems are utilized to obtain a systematic physical model reduction procedure. The additional use of type (ii) and type (iii) dynamic subsystems *in conjunction with the residues and eigenvalues information* for model reduction constitutes the main contribution of this first approach. The relevant physical subsystems are retained by assessing the magnitude of the residues of the full model.

Although this approach of physical model reduction is efficient, when a system has uniform parameters or has numerically same loop gains, it may fail to identify all of the eigenvalues (modes) of the system. For such cases a sub-procedure that utilizes a previous work on identifying irrelevant components for a given eigenvalue is presented. The sub-procedure relies on the computation of exact 'zero' components in the eigenvectors which is considered as the shortcoming of the approach. This shortcoming of

the procedure led to a detailed research on the computation of eigenvalues and eigenvectors from state-space equations and their relationship to eigenvalue sensitivity. This analysis provided the background for a second methodology of physical domain model reduction.

Thus, as a second methodology, the identification of subsystems and / or components that determine a given eigenvalue of the overall system has been explored and the effect matrix method has been produced. In the thesis a set of theorems and definitions are given that lead to an efficient procedure for this aim. In this procedure, a specific bond graph state-space representation of dynamic systems is utilized as it led to better understanding of the system structure. In fact, the use of this special form of state-space representation that is obtained directly from bond graphs enabled the identification of relative importance of components to a selected eigenvalue. This is accomplished by the calculation of eigenvectors and then constructing two 'effect' matrices, namely one for energy storage elements and one for energy dissipation elements. Furthermore, an efficient physical domain model reduction procedure is given that utilizes these effect matrices.

Several examples have been presented which include real engineering systems, such as the multi-energy domain arm-prosthesis system. Through the presented examples the advantages of using the physical domain model reduction procedures are explained. Additionally, their usefulness in identifying the subsystems and then helping the control engineer to modify the system dynamics to eliminate undesirable behavior is presented.

For future research one of the areas is the nonlinear systems. For this purpose, existing analogies between nonlinear components relating total system variables and linearized models relating incremental system variables can be explored. As bond graphs can also be used to model nonlinear systems, physically reduced nonlinear systems may be obtained. Thus, different set of procedures for the decomposition of nonlinear systems may be constructed following the framework of this thesis.

As a second research topic, the robust performance analysis of physically reduced uncertain systems may be studied. The coefficients of physically based models are often only known within certain bounds. Such parameter uncertainty complicates the control design problem. As eliminating all uncertainty is not a realistic option, formulating the model in such a way that its behavior over key frequency ranges can be determined, becomes important. Beginning with the work of Kharitonov, a large body of theory concerning interval polynomials has been developed. With a model expressed in the form of a ratio of interval polynomials, robust controllers can be designed and system performance information such as the bounds of Nyquist plots and bounds of Bode plots can be readily obtained. Although this is the case, there is little work that has been done for the analysis of reduced order uncertain models. Thus by somehow combining the decomposition procedures and/or the effect matrices introduced in this thesis with the interval plant models of the physically reduced uncertain systems, this problem may be addressed.

APPENDIX A: KRONECKER ALGEBRA IN SYSTEM THEORY

In this appendix the $n \times n$ unit matrix is denoted as $\mathbf{I}_n$. The kth row of a matrix such as $\mathbf{A}$ will be denoted $\mathbf{A}_{k.}$, and the kth column will be denoted as $\mathbf{A}_{.k}$. The ik element of $\mathbf{A}$ will be denoted as a_{ik}.

The Kronecker product of $\mathbf{A}$ $(p \times q)$ and $\mathbf{B}$ $(m \times n)$ is denoted $\mathbf{A} \otimes \mathbf{B}$ is a $pm \times qn$ matrix defined by

$$\mathbf{A} \otimes \mathbf{B} \triangleq \begin{bmatrix} a_{11}\mathbf{B} & a_{12}\mathbf{B} & \cdots & a_{1q}\mathbf{B} \\ a_{21}\mathbf{B} & & & \\ \vdots & & & \\ a_{p1}\mathbf{B} & & & a_{pq}\mathbf{B} \end{bmatrix} \tag{A.1}$$

Additionally, the Kronecker sum [27] of $\mathbf{N}$ $(n \times n)$ and $\mathbf{M}$ $(m \times m)$ is defined by

$$\mathbf{N} \oplus \mathbf{M} = \mathbf{N} \otimes \mathbf{I}_m + \mathbf{I}_n \otimes \mathbf{M} \tag{A.2}$$

An important vector valued function of a matrix was defined by Neudecker [76] as

$$\underset{(pq \times 1)}{\text{vec}(\mathbf{A})} \triangleq \begin{bmatrix} \mathbf{A}_{.1} \\ \mathbf{A}_{.2} \\ \vdots \\ \mathbf{A}_{.q} \end{bmatrix} \tag{A.3}$$

Table A.1 gives some important theorems on the algebra of Kronecker products. The dimensions of matrices and vectors used in this table is as follows:

$\mathbf{A}(p \times q)$	$\mathbf{B}(s \times t)$	$\mathbf{C}(r \times l)$	$\mathbf{D}(q \times s)$	$\mathbf{G}(t \times u)$
$\mathbf{H}(p \times q)$	$\mathbf{M}(m \times m)$	$\mathbf{N}(n \times n)$	$\mathbf{R}(s \times t)$	$\mathbf{W}(s \times p)$
$\mathbf{z}(z \times 1)$				

Table A.1. Some theorems on algebra of Kronecker products

Theorems	References
$(\mathbf{A} \otimes \mathbf{B}) \otimes \mathbf{C} = \mathbf{A} \otimes (\mathbf{B} \otimes \mathbf{C})$	[27]
$(\mathbf{A} + \mathbf{H}) \otimes (\mathbf{B} + \mathbf{R}) = \mathbf{A} \otimes \mathbf{B} + \mathbf{A} \otimes \mathbf{R} + \mathbf{H} \otimes \mathbf{B} + \mathbf{H} \otimes \mathbf{R}$	[27]
$(\mathbf{A} \otimes \mathbf{B})^T = \mathbf{A}^T \otimes \mathbf{B}^T$	[27]
$(\mathbf{A} \otimes \mathbf{B})(\mathbf{D} \otimes \mathbf{G}) = \mathbf{AD} \otimes \mathbf{BG}$	[27]
$(\mathbf{N} \otimes \mathbf{M})^{-1} = \mathbf{N}^{-1} \otimes \mathbf{M}^{-1}$	[27]
$\det(\mathbf{N} \otimes \mathbf{M}) = (\det(\mathbf{N}))^m (\det(\mathbf{M}))^n$	[27]
$\text{trace}(\mathbf{N} \otimes \mathbf{M}) = \text{trace}(\mathbf{N})\text{trace}(\mathbf{M})$	[27]
$(\mathbf{I}_m \otimes \mathbf{N})(\mathbf{M} \otimes \mathbf{I}_n) = (\mathbf{M} \otimes \mathbf{I}_n)(\mathbf{I}_m \otimes \mathbf{N})$	[76]
$\exp(\mathbf{N} \otimes \mathbf{M}) = \exp(\mathbf{N}) \otimes \exp(\mathbf{M})$	[76]
$\text{vec}(\mathbf{ADB}) = (\mathbf{B}^T \otimes \mathbf{A})\text{vec}(\mathbf{D})$	[77]
$\mathbf{N} \otimes \mathbf{M}$ is positive definite if $\mathbf{N}$, $\mathbf{M}$ are symmetric and sign definite of the same sign. $\mathbf{N} \otimes \mathbf{M}$ is negative definite if $\mathbf{N}$, $\mathbf{M}$ are sign definite of opposite sign.	
$\mathbf{N}$ and $\mathbf{M}$ are symmetric and sign definite of the same sign then $\mathbf{N} \otimes \mathbf{M}$ is also sign definite of that sign.	
$(\mathbf{I}_p \otimes \mathbf{z})\mathbf{A} = \mathbf{A} \otimes \mathbf{z}$	
$\mathbf{A}(\mathbf{I}_q \otimes \mathbf{z}^T) = \mathbf{A} \otimes \mathbf{z}^T$	
$\text{vec}(\mathbf{A} + \mathbf{H}) = \text{vec}(\mathbf{A}) + \text{vec}(\mathbf{H})$	
$\mathbf{A}^{k+1} = \mathbf{A} \otimes \mathbf{A}^k$	[27]
$(\mathbf{AD})^k = \mathbf{A}^k \mathbf{D}^k$	[27]
$\begin{aligned} \text{vec}(\mathbf{AD}) &= (\mathbf{I}_s \otimes \mathbf{A})\text{vec}(\mathbf{D}) \\ &= (\mathbf{D}^T \otimes \mathbf{I}_p)\text{vec}(\mathbf{A}) \\ &= (\mathbf{D}^T \otimes \mathbf{A})\text{vec}(\mathbf{I}_q) \end{aligned}$	[27]
$\text{trace}(\mathbf{ADW}) = (\text{vec}(\mathbf{A}^T))^T (\mathbf{I}_p \otimes \mathbf{D})\text{vec}(\mathbf{W})$	[77]
$\text{trace}(\mathbf{A}^T\mathbf{H}) = (\text{vec}(\mathbf{A}^T))^T \text{vec}(\mathbf{H})$	[77]
$\text{vec}(\mathbf{AD}) = \sum_k^q (\mathbf{D}^T)_{.k} \otimes \mathbf{A}_{.k}$	[77]

APPENDIX B: STEADY-STATE CONSIDERATIONS

Steady-state response is the behavior of the system outputs as time approaches infinity. The steady-state solution of dynamic systems with constant inputs is also often of interest.

As discussed in Chapter 3, when the decomposition based physical model reduction procedure is used, there might be a steady-state error (DC gain difference), if some components are eliminated without adding their effects to elsewhere (or combining them with other parameters/components appropriately). In this appendix, bond graphs are employed to obtain information about steady-state [65].

B.1. Calculating Steady-State Error from Bond Graphs

It is well known that, one way of calculating the steady-state values is the use of algebra. Namely, at steady-state, $\dot{\mathbf{x}} = 0$, then

$$\dot{\mathbf{x}} = \mathbf{A}\mathbf{x} + \mathbf{B}\mathbf{u} \tag{B.1}$$

$$\Rightarrow \quad \mathbf{x}_{ss} = -\mathbf{A}^{-1}\mathbf{B}\mathbf{u}_{ss} \tag{B.2}$$

and[11]

$$\mathbf{y} = \mathbf{C}\mathbf{x} \quad \Rightarrow \quad \mathbf{y}_{ss} = \mathbf{C}\mathbf{x}_{ss} \tag{B.3}$$

When $\mathbf{A}$ is singular, $\mathbf{x}_{ss}$ cannot be calculated by Equation (B.2). As a result, parameters that are responsible for the steady-state solution cannot be detected.

[11] Here, $\mathbf{u}_{ss}$ is the constant value of the input at steady-state, i.e. if the input is a step, then this step value will be $\mathbf{u}_{ss}$.

In order to eliminate such problems and to get more information from the system structure, one can use a procedure on bond graphs to get the steady-state solution, just by solving a set of algebraic equations [78]. In this appendix, a slightly different algorithm than [78] will be presented to obtain the steady-state solution [65]:

i. Complete causality assignment on the bond graph,
ii. Remove energy storage elements with derivative causality,
iii. Replace remaining energy storage elements by sources with the same causality (i.e. $C \rightarrow S_e$ and $I \rightarrow S_f$),
iv. Write down new junction equations,
v. Set output of newly added sources to zero and solve for their inputs. These values will be the steady-state values of their corresponding states[12] .

Now we will briefly go over the 5th order physical system of Chapter 4, while keeping in mind the discussion above.

B.2. A 5th Order Physical System

In Chapter 4 of this thesis, it is indicated that, for the 5th order physical system we have a very small steady-state error (DC gain difference). Basically, this error can be compensated by one of the three approaches:

1. By adding a gain to the reduced order model with a numerical value of $\frac{y_{ss}}{y_{\text{red}_{ss}}}$,
2. By increasing the order of the reduced order system (with increasing the number of subsystems retained),
3. By computing the steady-state error, and then modifying the reduced order model accordingly [79].

Note that, in the first approach, adding a gain may lead to incorrect results in the transient region of the simulation.

[12] This algorithm is similar to setting the derivatives of the states to zero, in order to calculate the steady-state values.

Here, for this 5th order system, the first approach will be presented. The compensated simulation results with the modified DC gain and the same parameters as before can be seen in Figure B.1.

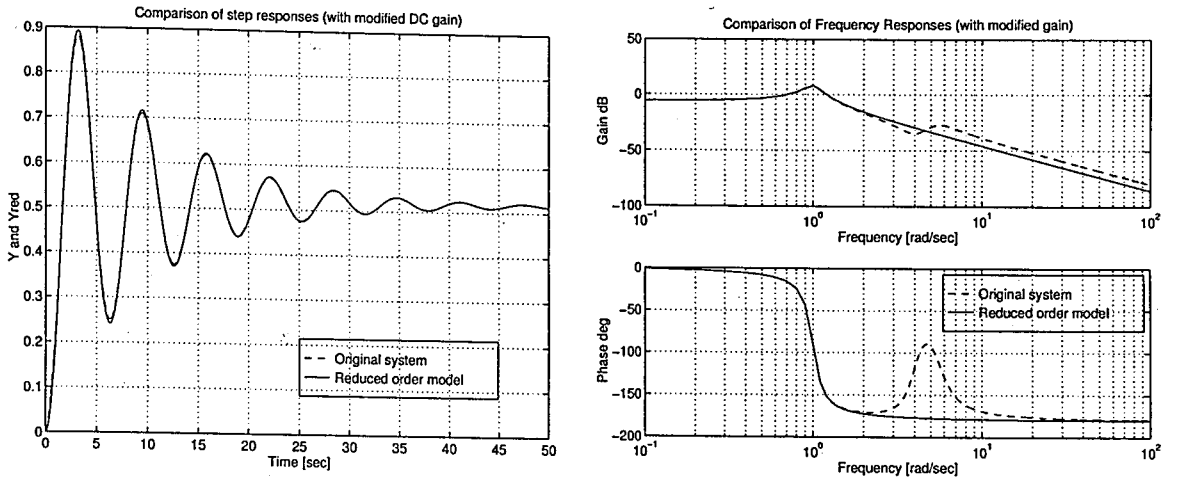

(a) Comparison of step responses (b) Comparison of Bode plots

Figure B.1. Comparison of full order and reduced order model of the 5th order physical system with modified DC gain

Now, let's calculate the steady-state values from the bond graph. The modified bond graph representation of this physical system with the discussion on steady-state can be seen in Figure B.2.

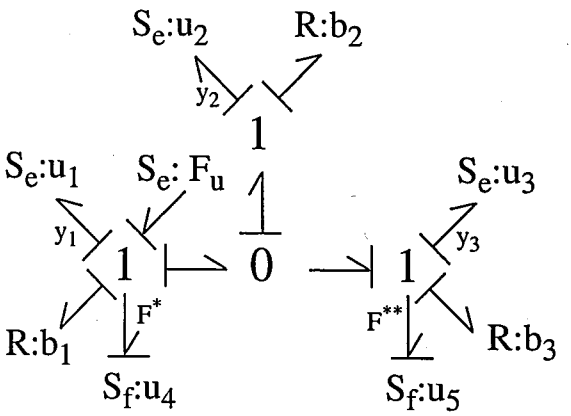

Figure B.2. Modified bond graph representation of the 5th order system

In this figure, u_1, u_2, u_3, u_4 and u_5 are the extra inputs[13] . Then the steady-state calculations are:

$$\begin{aligned} F^* &= F_u - u_1 - b_1 u_4 - u_2 - b_2(u_4 - u_5) \\ F^{**} &= u_2 + b_2(u_4 - u_5) - u_3 - b_3 u_5 \\ y_1 &= u_4 \\ y_2 &= u_4 - u_5 \\ y_3 &= u_5 \end{aligned} \tag{B.4}$$

By setting $F^* = F^{**} = y_1 = y_2 = y_3 = 0$ and solving for u_i's one gets:

$$\begin{aligned} &u_1 = F_u - u_2 \Rightarrow F_{k_{1_{ss}}} = F_u - F_{k_{2_{ss}}} \\ &u_2 = u_3 \Rightarrow F_{k_{2_{ss}}} = F_{k_{3_{ss}}} \\ &u_4 = u_5 = 0 \Rightarrow \dot{x}_{1_{ss}} = \dot{x}_{2_{ss}} = 0 \end{aligned} \tag{B.5}$$

Furthermore, if desired, one can calculate the steady-state values of the positions by replacing forces on springs by their equations (force = spring constant $\times$ position):

$$\begin{aligned} F_u &= k_1 x_{1_{ss}} + k_2(x_{1_{ss}} - x_{2_{ss}}) \\ k_2(x_{1_{ss}} - x_{2_{ss}}) &= k_3 x_{2_{ss}} \end{aligned} \tag{B.6}$$

$$\Rightarrow x_{1_{ss}} = \frac{k_2+k_3}{k_2} x_{2_{ss}} \quad \text{and} \quad x_{2_{ss}} = \frac{k_2 F_u}{(k_1+k_2)(k_2+k_3)-k_2^2}$$

Notice that, this solution reveals important information about the system structure. For example, it is observed that $F_{k_{2_{ss}}} = F_{k_{3_{ss}}}$ no matter what values one picks for k_2 and k_3. This kind of information can easily be used in future designs and analyzes of this physical system.

[13] Keep in mind that u_1, u_2, u_3, u_4 and u_5 will give the steady-state values of $F_{k_1}, F_{k_2}, F_{k_3}, \dot{x}_1$ and $\dot{x}_2$, respectively.

APPENDIX C: MIMO RESIDUE METHOD FOR MODEL REDUCTION

The model approximation idea is to preserve all of the important modes of the 'truth' model in the low-frequency region. The neglected dynamics will be taken care of in the description of the modeling uncertainty. The stability robustness of the reduced-order design will be guaranteed by singular value inequalities.

The MIMO residue method offers a straightforward and powerful method for model simplification [80]. The idea behind the MIMO residual method for model reduction is simple and is outlined here:

Consider the state-space description of a 'square' linear time-invariant system with the same number of inputs and outputs,

$$\begin{aligned} \dot{\mathbf{x}}(t) &= \mathbf{A}\mathbf{x}(t) + \mathbf{B}\mathbf{u}(t) \\ \mathbf{y}(t) &= \mathbf{C}\mathbf{x}(t) \end{aligned} \tag{C.1}$$

with $\mathbf{x}(t) \in \mathcal{R}^n$, $\mathbf{u}(t) \in \mathcal{R}^p$ and $\mathbf{y}(t) \in \mathcal{R}^p$.

Let λ_i $(i = 1, 2, \ldots, n)$ be the distinct eigenvalues of $\mathbf{A}$, $\mathbf{u}_i$ the corresponding right eigenvector (column vector), and $\mathbf{v}_i^T$ the corresponding left eigenvector (row vector). Thus, for $i = 1, 2, \ldots, n$,

$$\begin{aligned} \mathbf{A}\mathbf{u}_i &= \lambda_i \mathbf{u}_i \\ \mathbf{v}_i^T \mathbf{A} &= \lambda_i \mathbf{v}_i^T \end{aligned} \tag{C.2}$$

In the frequency domain, the system of Equation (C.1) is represented by the $p \times p$ transfer function matrix $\mathbf{G}(s)$ so that

$$\mathbf{y}(s) = \mathbf{G}(s)\mathbf{u}(s) \tag{C.3}$$

where

$$\mathbf{G}(s) = \mathbf{C}\,(s\mathbf{I} - \mathbf{A})^{-1}\,\mathbf{B} \tag{C.4}$$

Under the assumption of distinct eigenvalues (poles of $\mathbf{G}(s)$), the MIMO partial fraction expansion is

$$\mathbf{G}(s) = \sum_{i=1}^{n} \frac{\mathbf{R}_i}{s - \lambda_i} = \sum_{i=1}^{n} \frac{\mathbf{R}_i/\lambda_i}{(s/\lambda_i) - 1} \tag{C.5}$$

The $p \times p$ (complex-valued) matrix $\mathbf{R}_i$ is called the residue matrix at pole $s = \lambda_i$, $i = 1, 2, \ldots, n$. The residue matrices can be readily calculated from the time-domain description (Equation (C.1)) and the left and right eigenvectors defined in Equation (C.2) as follows:

$$\mathbf{R}_i = \mathbf{C}\mathbf{u}_i\mathbf{v}_i^T\mathbf{B} \tag{C.6}$$

For $s = j\omega$, Equation (C.5) reduces to

$$\mathbf{G}(j\omega) = \sum_{i=1}^{n} \frac{\mathbf{R}_i/\lambda_i}{(j\omega/\lambda_i) - 1} \tag{C.7}$$

The magnitude of each residue matrix provides a measure of the importance of the contribution of the corresponding pole in the MIMO input/output system description [80].

Using the MIMO residues a straightforward model simplification method can be performed as follows [80]:

The choice of the poles to be retained and the poles to be neglected should be made in accordance of the magnitude of the residue matrix and of the pole location (frequency) relative to the bandwidth specifications. For example, a pole that has a 'large' residue matrix may be neglected if its frequency is much higher than the desired crossover frequency. A pole within the desired bandwidth may also be neglected provided that its residue matrix is 'small', a characteristic of approximate MIMO pole-zero cancellation. A step-by-step model reduction method explained in [80] will be presented here:

Assume that the reduced model $\mathbf{G}_r(s)$ of order r is of the form

$$\dot{\mathbf{z}}(t) = \mathbf{F}\mathbf{z}(t) + \mathbf{G}\mathbf{u}(t) \tag{C.8}$$

$$\mathbf{y}(t) = \mathbf{H}\mathbf{z}(t) + \mathbf{D}\mathbf{u}(t) \tag{C.9}$$

with $\mathbf{z}(t) \in \mathcal{R}^r$, $\mathbf{u}(t) \in \mathcal{R}^p$ and $\mathbf{y}(t) \in \mathcal{R}^p$, $r > n$, and

$$\mathbf{z}(t) = \mathbf{K}\mathbf{x}(t) \tag{C.10}$$

where $\mathbf{K}$ is an $r \times n$ constant matrix. Note that the physical significance and dimensions of the control $\mathbf{u}(t)$ and output $\mathbf{y}(t)$ have been retained. The five step model reduction method is as follows [80]:

1. Write the system transfer function matrix in the residue matrix sum as in Equation (C.7) and find the magnitude of the residue matrices (any norm can be used). According to the crossover specifications and the magnitude of the residues, *decide which poles will be eliminated.* Suppose that the reduced model has as eigenvalues the subset of the $\mathbf{A}$ matrix eigenvalues $[\lambda_1(\mathbf{A}), \ldots, \lambda_r(\mathbf{A})]$, suitably arranged.
2. Define the matrix

$$\mathbf{T} = \begin{bmatrix} T_1 & & 0 \\ & \ddots & \\ 0 & & T_j \end{bmatrix} \tag{C.11}$$

where

$$T_k = \begin{cases} 1 & \text{for each distinct real eigenvalue that is retained,} \\ \begin{bmatrix} 1/2 & -j/2 \\ 1/2 & j/2 \end{bmatrix} & \text{for each complex pair of eigenvalues retained.} \end{cases}$$

and $\sum_{k=1}^{j} = \dim(T_k) = r$.

3. Calculate the matrix $\mathbf{K}$ in Equation (C.10) by

$$\mathbf{K} = (\mathbf{T})^{-1} \begin{bmatrix} \mathbf{v}_1^T \\ \vdots \\ \mathbf{v}_r^T \end{bmatrix} \tag{C.12}$$

and the matrix $\mathbf{M}$ by

$$\mathbf{M} = (\mathbf{u}_1, \ldots, \mathbf{u}_r)\, \mathbf{T} \tag{C.13}$$

with the $\mathbf{u}_i$ and $\mathbf{v}_j$ defined in Equation (C.2).

4. The matrices in the reduced-state space model (Equations (C.8) and (C.9)) are computed by

$$\mathbf{F} = \mathbf{KAM} \tag{C.14}$$

$$\mathbf{G} = \mathbf{KB} \tag{C.15}$$

$$\mathbf{H} = \mathbf{CM} \tag{C.16}$$

$$\mathbf{D} = \sum_{i=r+1}^{n} \frac{\mathbf{R}_i}{(-\lambda_i)} \tag{C.17}$$

where $(\lambda_{r+1}, \ldots, \lambda_n)$ are the neglected eigenvalues. Note that the transfer function of the reduced model $\mathbf{G}_r(s)$, given by (Equations (C.8) and (C.9)) is

$$\mathbf{G}_r(s) = \mathbf{H}\,(s\mathbf{I} - \mathbf{F})^{-1}\,\mathbf{G} + \mathbf{D} \tag{C.18}$$

and that

$$\mathbf{G}_r(s) = \sum_{i=1}^{r} \frac{\mathbf{R}_i/\lambda_i}{(s/\lambda_i) - 1} + \sum_{i=r+1}^{n} \frac{\mathbf{R}_i}{(-\lambda_i)} \tag{C.19}$$

Thus, the original model and the reduced model agree at DC ($s = 0$).

5. Plot the singular values versus frequency of both the original and reduced systems. If the differences are significant go to Step 1 and redefine the eigenvalue set to be retained.

C.1. An Example

The results of this model reduction procedure will be illustrated by an example. A Jordan form system is selected to give a concise argument.

Consider the MIMO system,

$$\dot{\mathbf{x}} = \begin{bmatrix} -1 & 0 & 0 \\ 0 & -2 & 0 \\ 0 & 0 & -10 \end{bmatrix} \mathbf{x} + \begin{bmatrix} 1 & 0 \\ 0 & 1 \\ 2 & 0 \end{bmatrix} u = \mathbf{A}\mathbf{x} + \mathbf{B}u \tag{C.20}$$

$$\mathbf{z} = \begin{bmatrix} 1 & 0 & 0 \\ 0 & 1 & 1 \end{bmatrix} \mathbf{x} = \mathbf{C}\mathbf{x} \tag{C.21}$$

The eigenvectors are given by $\mathbf{u}_i = \mathbf{e}_i$, $\mathbf{v}_i = \mathbf{e}_i$, $i = 1, 2, 3$, with $\mathbf{e}_i$ the ith column of the 3×3 identity matrix. Thus, the transfer function is given by the partial fraction expansion

$$\mathbf{G}(s) = \frac{\mathbf{R}_1}{s+1} + \frac{\mathbf{R}_2}{s+2} + \frac{\mathbf{R}_3}{s+10} \tag{C.22}$$

with

$$\mathbf{R}_1 = \begin{bmatrix} 1 & 0 \\ 0 & 0 \end{bmatrix}, \qquad \mathbf{R}_2 = \begin{bmatrix} 0 & 0 \\ 0 & 1 \end{bmatrix}, \qquad \mathbf{R}_3 = \begin{bmatrix} 0 & 0 \\ 2 & 0 \end{bmatrix} \tag{C.23}$$

To find the reduced order system that retains the poles at $\lambda = -1$ and $\lambda = -2$, define

$$\mathbf{T} = \begin{bmatrix} 1 & 0 \\ 0 & 1 \end{bmatrix}, \qquad \mathbf{K} = \begin{bmatrix} 1 & 0 & 0 \\ 0 & 1 & 0 \end{bmatrix}, \qquad \mathbf{M} = \begin{bmatrix} 1 & 0 \\ 0 & 1 \\ 0 & 0 \end{bmatrix} \tag{C.24}$$

and compute the approximate system

$$\dot{\mathbf{z}} = \begin{bmatrix} -1 & 0 \\ 0 & -2 \end{bmatrix} \mathbf{z} + \begin{bmatrix} 1 & 0 \\ 0 & 1 \end{bmatrix} u = \mathbf{F}\mathbf{z} + \mathbf{G}u \tag{C.25}$$

$$\mathbf{y} = \begin{bmatrix} 1 & 0 \\ 0 & 1 \end{bmatrix} \mathbf{z} + \begin{bmatrix} 0 & 0 \\ 0.2 & 0 \end{bmatrix} u = \mathbf{H}\mathbf{z} + \mathbf{D}u \tag{C.26}$$

This has a transfer function of

$$\mathbf{G}_r(s) = \frac{\mathbf{R}_1}{s+1} + \frac{\mathbf{R}_2}{s+2} + \mathbf{D} \tag{C.27}$$

Singular value plots of the original plant (Equations (C.20) and (C.21)) and the reduced order approximation (Equations (C.25) and (C.26)) are shown in Figure C.1.

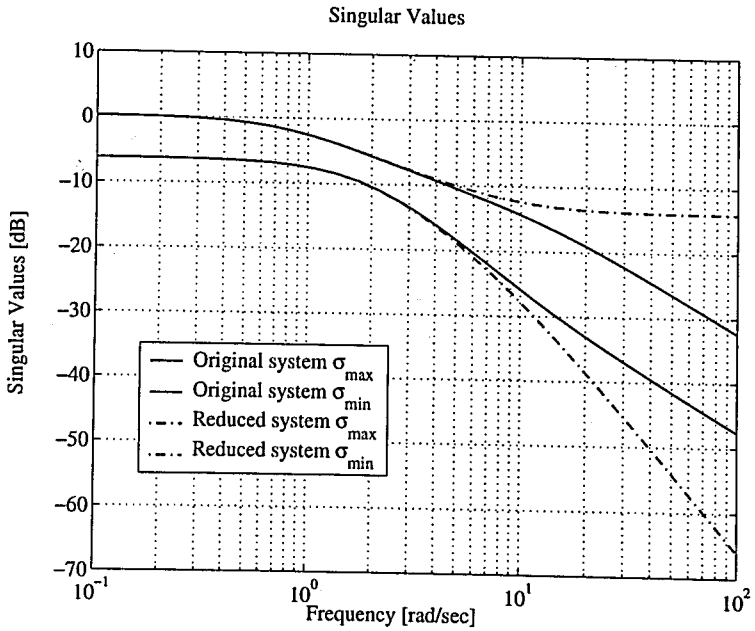

Figure C.1. Singular value plots of the original and reduced order systems

REFERENCES

1. Rosenberg, R. C., *A Users Guide to ENPORT-4*, Wiley, New York, 1974.

2. Lorenz, F., *Modelling System 1, User's Manual*, Lorenz Simulation, Liege, Belgium, 1997.

3. Granda, J. J., "Computer Generation of Physical System Differential Equations Using Bond Graphs", *Journal of the Franklin Institute*, Vol. 319, No. 1/2, pp. 243–256, 1985.

4. Broenink, J. F., *Computer-Aided Physical-Systems Modeling and Simulation: A Bond-Graph Approach*, Ph.D. Thesis, University of Twente, Enschede, Netherlands, 1990.

5. Broenink, J. F., "Modelling, Simulation and Analysis with 20-SIM", *Journal A, Special issue on CACSD*, Vol. 38, No. 3, pp. 22–25, 1997.

6. Zhou, K., J. C. Doyle, and K. Glover, *Robust and Optimal Control*, Prentice Hall, Inc., Englewood Cliffs, New Jersey, 1996.

7. Glover, K., "All Optimal Hankel-Norm Approximations of Linear Multivariable Systems and Their L^∞-Error Bounds", *International Journal of Control*, Vol. 39, No. 6, pp. 1115–1193, 1984.

8. Rivera, D. E. and M. Morari, "Control Relevant Model Reduction Problems for SISO, H_2, H_∞, and μ Control Synthesis", *International Journal of Control*, Vol. 46, p. 505, 1987.

9. Yae, K. H. and D. J. Inman, "Techniques in Control-Oriented Reduction of Finite Element Modeling in Structural Dynamic Systems", in C. T. Leonedes (Ed.), *Structural Dynamic Systems Computational Techniques and Optimization: Dy-*

namic Analysis and Control Techniques, pp. 1–54, Gordon and Breach Science Publishers, Amsterdam, 1999.

10. Moore, B. C., "Principal Component Analysis in Linear Systems: Controllability, Observability, and Model Reduction", *IEEE Transactions on Automatic Control*, Vol. AC-26, No. 1, pp. 17–32, 1981.

11. Davidson, A. M. and I. R. Walters, "Linear System Reduction Using Approximate Moment Matching", *IEE Proceedings, Part D*, Vol. 135, No. 2, pp. 73–78, 1988.

12. Lalonde, R. J., T. T. Hartley, and J. A. De Abreu-Garcia, "Least Squares Model Reduction", *Journal of the Franklin Institute*, Vol. 329, No. 2, pp. 215–240, 1992.

13. Skelton, R. E. and A. Yousuff, "Component Cost Analysis of Large Scale Systems", *International Journal of Control*, Vol. 37, No. 2, pp. 285–304, 1983.

14. Xihang, H., "FF-Padé Method of Model Reduction in Frequency Domain", *IEEE Transactions on Automatic Control*, Vol. 32, pp. 243–246, March 1987.

15. Shieh, L. S. and F. F. Gaudiano, "Matrix Continued Fraction Expansion and Inversion by the Generalized Matrix Routh Algorithm", *International Journal of Control*, Vol. 20, No. 5, pp. 727–737, 1974.

16. Safonov, M. G. and R. Y. Chiang, "A Schur Method for Balanced-Truncation Model Reduction", *IEEE Transactions on Automatic Control*, Vol. 34, pp. 729–733, July 1989.

17. Louca, L. S., J. L. Stein, G. M. Hulbert, and J. Sprague, "Proper Model Generation: An Energy-Based Methodology", in *Proceedings of ICBGM'97, 3rd International Conference on Bond Graph Modeling and Simulation*, January 1997.

18. Rosenberg, R. C. and T. Zhou, "Power Based Model Insight", in *Proceedings of the 1988 ASME Winter Annual Meeting on Automated Modeling for Design*, ASME, The Dynamic Systems and Controls Division, November 1988.

19. Sueur, C. and G. Dauphin-Tanguy, "Bond Graph Approach for Multi-Time Scale System Analysis", *Journal of the Franklin Institute*, Vol. 328, No. 5, pp. 1005–1026, 1991.

20. Dauphin-Tanguy, G. and P. Borne, "Multi-Time Scale Systems: Dynamical Location", in M. G. Singh (Ed.), *Systems and Control Encyclopedia. Theory, Technology, Applications*, first ed., pp. 3176–3180, Pergamon Press, New York, 1987.

21. Anderson, B. D. O. and J. B. Moore, *Optimal Control: Linear Quadratic Methods*, Prentice Hall, Inc., Englewood Cliffs, New Jersey, 1990.

22. Shokoohi, S., L. M. Silverman, and P. M. Van Dooren, "Linear Time-Variable Systems: Balancing and Model Reduction", *IEEE Transactions on Automatic Control*, Vol. AC-28, pp. 810–822, August 1983.

23. Walker, D. G., J. L. Stein, and A. G. Ulsoy, "An Input-Output Criterion for Linear Model Deduction", in *Proceedings of the Dynamic Systems and Controls Division*, ASME, IMECE, 1996.

24. Glover, K., "Model Reduction: A Tutorial on Hankel-Norm Methods and Lower Bounds on L^2 Errors", in *IFAC 10th Triennial World Congress, Munich, FRG*, pp. 293–298, 1987.

25. Rivera, D. E. and M. Morari, "Control-Relevant Model Reduction Problems for SISO, H_2, H_∞, and μ-Controller Synthesis", *International Journal of Control*, Vol. 46, No. 2, pp. 505–527, 1987.

26. Leyva-Ramos, J., "A New Look at Partial Fraction Expansion of Transfer Function Matrices from a Computational Viewpoint", *Computers and Mathematical Applications*, Vol. 26, No. 3, pp. 27–35, 1993.

27. Bellman, R., *Introduction to Matrix Analysis*, McGraw-Hill, New York, 1960.

28. DeCarlo, R. A., *Linear Systems: A State Variable Approach with Numerical Im-*

plementation, Prentice-Hall, Englewood Cliffs, NJ, 1989.

29. Kailath, T., *Linear Systems*, Prentice-Hall, Englewood Cliffs, NJ, 1980.

30. Zadeh, L. A. and C. A. Desoer, *Linear System Theory*, McGraw-Hill, New York, 1963.

31. Chen, C. F. and G. Freeman, "A New Formula for Partial Fraction Expansion of a Transfer Matrix", *Proceedings of the American Control Conference, ACC86*, 1986.

32. Chen, C. F., "A New Approach to Matrix Heaviside Expansion", *International Journal of Control*, Vol. 3, pp. 431–448, 1970.

33. Gantmacher, F. R., *The Theory of Matrices*, Chelsea, New York, 1959.

34. Rosenbrock, H., "Partial Fraction Expansion of a Transfer Matrix", *Electronics Letters*, Vol. 1, 1966.

35. Leyva-Ramos, J., "Partial Fraction Expansion in System Analysis", *International Journal of Control*, Vol. 3, pp. 619–639, 1991.

36. Brewer, J. W., "Kronecker Products and Matrix Calculus in System Theory", *IEEE Transactions on Circuits and Systems*, Vol. 9, pp. 772–781, 1981.

37. Leyva-Ramos, J. and E. D. Denman, "Matrix Partial Fraction Expansion Method", *Electronics Letters*, Vol. 3, pp. 99–100, 1983.

38. Leyva-Ramos, J., "A Method for Partial Fraction Expansion of Transfer Matrices", *Transactions on Automatic Control*, Vol. 12, pp. 1472–1475, 1991.

39. Fernando, K. V. and H. Nicholson, "On the Structure of Balanced and Other Principal Representations of SISO Systems", *IEEE Transactions on Automatic Control*, Vol. AC-28, pp. 228–231, February 1983.

40. Paynter, H. M., *Analysis and Design of Engineering Systems*, MIT Press, Cambridge, MA, 1961.

41. Karnopp D. C. and R. C. Rosenberg, *Analysis and Simulation of Multiport Systems - The Bond Graph Approach to Physical System Dynamics*, MIT Press, Cambridge, MA, 1968.

42. Karnopp D. C. and R. C. Rosenberg, *System Dynamics, A Unified Approach*, John Wiley, New York, NY, 1975.

43. Karnopp D. C., D. L. Margolis, and R. C. Rosenberg, *System Dynamics, A Unified Approach*, John Wiley, New York, NY, 2nd ed., 1990.

44. Rosenberg, R. C. and D. C. Karnopp, *Introduction to Physical System Dynamics*, McGraw Hill, New York, NY, 1983.

45. Thoma, J. U., *Introduction to Bond Graphs and Their Applications*, Pergamon Press, Oxford, 1975.

46. Van Dixhoorn, J. J., "Bond Graphs and the Challenge of a Unified Modelling Theory of Physical Systems", in F. E. Cellier (Ed.), *Progress in Modelling and Simulation*, pp. 207–245, Academic Press, New York, 1982.

47. Breedveld, P. C., *Physical Systems Theory in Terms of Bond Graphs*, Ph.D. Thesis, University of Twente, Enschede, Netherlands, 1984.

48. Breedveld, P. C., "Multi-Bond Graph Elements in Physical Systems Theory", *Journal of the Franklin Institute*, Vol. 319, No. 1/2, pp. 1–36, 1985.

49. Chiu, T.-Y., "Model Reduction by the Low-Frequency Approximation Balancing Method for Unstable Systems", *IEEE Transactions on Automatic Control*, Vol. 41, No. 7, pp. 995–997, 1996.

50. Prakash, R., "Properties of a Low-Frequency Approximation Balancing Method

of Model Reduction", *IEEE Transactions on Automatic Control*, Vol. 39, No. 5, pp. 1135–1141, 1994.

51. Tombs, M. S. and I. Postlethwaite, "Truncated Balanced Realization of a Stable Non-Minimal State-Space System", *International Journal of Control*, Vol. 46, No. 4, pp. 1319–1330, 1987.

52. Watanabe, T., K. Yasuda, and R. Yokoyama, "Balanced Truncation Preserving Poles in a Specified Disk", *SICE'95*, pp. 1387–1390, July 1995.

53. Davidson, A. M., "Balanced Systems and Model Reduction", *Electronics Letters*, Vol. 22, No. 10, pp. 531–532, 1986.

54. Davison, E. J., "A Method for Simplifying Linear Dynamic Systems", *IEEE Transactions on Automatic Control*, Vol. AC-11, pp. 93–101, January 1966.

55. Varga, A., "Enhanced Modal Approach for Model Reduction", *Mathematical Modelling of Systems*, Vol. 1, pp. 91–105, 1995.

56. Rosenberg, R. E. and G. Ermer, "A Bond Graph Visualization Tool to Improve Engineering System Design", *Systems Analysis, Modeling, Simulation*, Vol. 18 - 19, p. 173, 1995.

57. Wilson, B. H. and J. L. Stein, "An Algorithm for Obtaining Proper Models of Distributed and Discrete Systems", *Transactions of the ASME*, Vol. 117, pp. 534–540, 1995.

58. Louca, L. S. and J. L. Stein, "Energy Based Model Reduction of Linear Systems", in *International Conference on Bond Graph Modeling, San Francisco, CA*, 1999.

59. Bjork, A., R. J. Plemmons, and H. Schneider, *Large Scale Matrix Problems*, Elsevier North Holland Inc., New York, 1981.

60. Horn, R. A. and C. R. Johnson, *Matrix Analysis*, Cambridge University Press,

New York, 1985.

61. Zeid, A. and R. Rosenberg, "Estimating Eigenvalues for a Class of Dynamic Systems", *Journal of the Franklin Institute*, pp. 21–40, July 1985.

62. Huang, S.-Y., *Structural Analysis from System Configurations for Modeling and Design of Multi-Energy Domain Dynamic Systems*, Ph.D. Thesis, Mechanical Engineering Department, Massachusetts Institute of Technology, June 1997.

63. Evans, D. J., *Sparsity and its Applications*, Cambridge University Press, New York, 1985.

64. Kokotovic, P., H. K. Khalil, and J. O'Reilly, *Singular Perturbation Methods in Control, Analysis and Design*, Academic Press, London, 1986.

65. Orbak, Â. Y., *Physical Domain Model Reduction for Design and Control of Engineering Systems*, Mech.E. Thesis, Mechanical Engineering Department, Massachusetts Institute of Technology, June 1998.

66. Abdul-Haj, C. and N. Hogan, "An Emulator System for Developing Improved Elbow-Prosthesis Designs", *IEEE Transactions on Biomedical Engineering*, Vol. BME-34, pp. 724–737, September 1987.

67. Burrows, C. R. and O. S. Türkay, "A Sensitivity Analysis of Squeeze-film Bearings", *Transactions of ASME Journal of Lubrication Technology*, Vol. 104, pp. 516–522, 1982.

68. El-Kady, M. A. and A. A. Al-Ohaly, "Fast Eigenvalue Sensitivity Calculations for Special Structures of System Matrix Derivatives", *Journal of Sound and Vibration*, Vol. 199, No. 3, pp. 463–471, 1997.

69. Brooks, P. C. and R. S. Sharp, "A Computational Procedure Based on Eigenvalue Sensitivity Theory Applicable to Linear System Design", *Journal of Sound and Vibration*, Vol. 114, pp. 13–18, 1987.

70. Van Ness, J. E., J. M. Boyle, and F. P. Imad, "Sensitivities of Large Multiple-Loop Control Systems", *IEEE Transactions on Automatic Control*, Vol. AC-10, No. 7, pp. 308–315, 1965.

71. Pérez-Arriaga, J. I., G. C. Verghese, and F. C. Schweppe, "Selective Modal Analysis with Applications to Electric Power Systems. Part I: Heuristic Introduction. Part II: The Dynamic Stability Problem", *IEEE Transactions on Power Apparatus and Systems*, Vol. PAS-101, pp. 3117–3134, September 1982.

72. Pagola, F. L., J. I. Pérez-Arriaga, and G. C. Verghese, "On Sensitivities, Residues and Participations", *IEEE Transactions on Power Systems*, Vol. PWRS-5, pp. 278–285, February 1989.

73. Ye, Y. and K. Youcef-Toumi, "Subsystem's Influence on a System Eigenvalue", in *Proceedings of the IEEE Southeastcon 2000*, pp. 261–267, IEEE, April 2000.

74. Rosenberg, R., "State-Space Formulation for Bond Graph Models of Multiport Systems.", *Journal of Dynamic Systems, Measurement and Control*, March 1971.

75. Orbak, Â. Y., O. S. Türkay, and E. Eşkinat, "Model Reduction in the Physical Domain", in *Proceedings of the 6th Biennial Conference on Engineering Sytems Design and Analysis (ESDA 2002)*, pp. 261–267, ASME, July 2002.

76. Neudecker, H., "A Note on Kronecker Matrix Products and Matrix Equation Systems", *SIAM Journal of Applied Mathematics*, Vol. 17, May 1969.

77. Neudecker, H., "Some Theorems on Matrix Differentiation with Special Reference to Kronecker Matrix Products", *Journal of American Statistics Association*, Vol. 64, pp. 953–963, 1969.

78. Gawthrop, P. J. and L. Smith, "Causal Augmentation of Bond Graphs with Algebraic Loops", *Journal of the Franklin Institute*, Vol. 329, No. 2, pp. 291–303, 1992.

79. Orbak, Â. Y., K. Youcef-Toumi, and Masaaki Senga, "Model Reduction and Design of a Power Steering System", in *Proceedings of the American Control Conference, ACC99*, pp. 4476–4481, June 1999.

80. Athans, M., P. Kapasouris, E. Kappos, and H. A. Spang III, "Linear-Quadratic Gaussian with Loop-Transfer Recovery Methodology for the F-100 Engine", *Journal of Guidance and Control*, Vol. 9, pp. 45–52, January-February 1986.

81. Al-Saggaf, U. M., "Model Reduction for Discrete Unstable Systems Based on Generalized Normal Representations", *International Journal of Control*, Vol. 55, No. 2, pp. 431–443, 1992.

82. Anderson, B. D. O. and Y. Liu, "Controller Reduction: Concepts and Approaches", *IEEE Transactions on Automatic Control*, Vol. 34, No. 8, pp. 802–812, 1989.

83. Antoulas, A. C., "A Behavioral Approach to Model Reduction", in *Proceedings of the 34th Conference on Decision and Control*, pp. 490–491, 1995.

84. Bavely, C. A. and G. W. Stewart, "An Algorithm for Computing Reducing Subspaces by Block Diagonalization", *SIAM Journal on Numerical Analysis*, Vol. 16, pp. 359–367, April 1979.

85. Beck, C. and J. Doyle, "Model Reduction of Behavioral Systems", in *Proceedings of the 32nd Conference on Decision and Control*, pp. 3652–3657, 1993.

86. Bruinsma, N. A. and M. Steinbuch, "A Fast Algorithm to Compute the H_∞-Norm of a Transfer Function Matrix", *Systems & Control Letters*, Vol. 14, pp. 287–293, 1990.

87. Chen, C.-F and L.-S. Shieh, "Continued Fraction Inversion by Routh's Algorithm", *IEEE Transactions on Circuit Theory*, Vol. CT-16, pp. 197–202, May 1969.

88. Lamba, S. S., "Model Simplification: Frequency-Domain Approach", in M. G. Singh (Ed.), *Systems and Control Encyclopedia. Theory, Technology, Applications*, first ed., pp. 3071–3077, Pergamon Press, New York, 1987.

89. Lamba, S. S. and S. V. Rao, "Aggregation Matrix for the Reduced-Order Continued Fraction Expansion Model of Chen and Shieh", *IEEE Transactions on Automatic Control*, Vol. AC-23, No. 1, pp. 81–83, 1978.

90. Maskarinec, G. J. and P. R. Chitrapu, "Linear Algebraic Properties of the Realization Matrix with Applications to Principal Axis Realizations", *IEEE Transactions on Circuits and Systems-1: Fundamental Theory and Applications*, Vol. 39, pp. 628–640, August 1992.

91. Mitchell, J. R., R. D. Irwin, and G. A. Huston, "Practical Model Reduction for Flexible Structures", *The Journal of the Astronautical Sciences*, Vol. 41, No. 2, pp. 227–247, 1993.

92. Shoji, F. F., K. Abe, and H. Takeda, "Model Reduction for a Class of Linear Dynamic Systems", *Journal of the Franklin Institute*, Vol. 319, No. 6, pp. 549–558, 1985.

93. Mahmoud, M. S. and M. G. Singh, *Large Scale Systems Modelling*, Vol. 3 of *International Series on Systems and Control*, Ch. 5, pp. 189–264, Pergamon Press, Oxford, New York, Toronto, Sydney, Paris, Frankfurt, 1981.

94. Wang, W. and M. G. Safonov, "Comparison Between Continuous and Discrete-Time Model Truncation", in *Proceedings of the 29th Conference on Decision and Control*, pp. 494–499, 1990.

95. Van Loan, C., "Using the Hessenberg Decomposition in Control Theory", *Mathematical Programming Study*, Vol. 18, pp. 102–111, 1982.

96. Yousuff, A. and M. Breida, "Model Reduction of Mechanical Systems", *Journal*

of Guidance, Vol. 16, No. 2, pp. 408–410, 1992.

97. Enright, W. H. and M. S. Kamel, "On Selecting a Low-Order Model Using the Dominant Mode Concept", *IEEE Transactions on Automatic Control*, Vol. AC-25, pp. 976–978, October 1980.

98. Orbak, Â. Y., *Identification and Self-Tuning Control of Dynamic Systems*, M.S. Thesis, Mechanical Engineering Department, Massachusetts Institute of Technology, June 1995.

99. Çoban, S. and A. Uraz, "Recursive Algorithm for Computing the Matrix Partial Fraction Expansion of Transfer Matrices Having Multiple Quadratic Poles", *International Journal of Control*, Vol. 60, No. 6, pp. 1393–1400, 1994.

100. Margolis, D. L. and M. Tabrizi, "Reduction of Models of Interacting Lumped and Distributed Systems Using Bond Graphs and Repeated Modal Decomposition", *Journal of the Franklin Institute*, Vol. 317, pp. 309–322, May 1984.

101. Margolis, D. L., "An Algorithm for Incorporating Subsystem Modes into Overall Dynamic System Models", *Journal of the Franklin Institute*, Vol. 310, pp. 107–117, August 1980.

102. Kwakernaak, H., "Polynomial Computation of Hankel Singular Values", in *Proceedings of the 31st Conference on Decision and Control*, pp. 3595–3599, IEEE Control System Society, IEE Conference Publication, December 1992.

103. Senga, M., *Modeling and Analysis of Power Steering Systems*, Mech.E. Thesis, Mechanical Engineering Department, Massachusetts Institute of Technology, January 1995.

104. Botti, J., G. Venizelos, and N. Benkaza, "Simulation of Vibration on Power Steering Systems for Passenger Cars", *28th International Symposium on Automotive Technology and Automation*, pp. 769–776, 1995.

105. Masson, C. and A. Yazman, "Usability of Component Models in Automotive Industry: Application to Power Steering Systems", *Simulation Series*, Vol. 27, No. 1, pp. 103–108, 1995.

106. Ajumobi, S. O., "Model of an Automotive Power Steering System via the Linear Graph Technique", *Mathematical Computation and Modelling*, Vol. 12, No. 9, pp. 1113–1116, 1989.

107. Yang, W. C. and W. E. Tobler, "Dynamic Modeling and Analysis of Electronically Controlled Power Steering System", *ASME Advanced Dynamics Technologies*, Vol. DSC-52, pp. 267–278, 1993.

108. Fukumura, K., K. Haga, M. Suzuki, and K. Mori, "Center-Closed Rotary Servo Valve for Power Steering", *Suspension and Steering Technology*, Vol. SP-1136, pp. 85–92, 1996.

109. Borutzky, W., "Tearing in Bond Graphs with Causal Cycles", *Simulation Series*, Vol. 29, No. 1, pp. 65–71, 1997.

110. Zeid, A., "Some Bond Graph Structural Properties: Eigen Spectra and Stability", in *Proceedings of ASME Winter Annual Meeting*, pp. 75–82, 1988.

111. Chen, C. T., *Linear System Theory and Design*, Holt, Rinehart and Winston, New York, 1984.

112. Elrazaz, Z. and N. K. Sinha, "On the Selection of the Dominant Poles of a System to be Retained in a Low-Order Model", *IEEE Transactions on Automatic Control*, Vol. AC-25, No. 5, pp. 792–793, 1979.

113. Mahapatra, G. B., "A Further Note on Selecting a Low-Order System Using the Dominant Eigenvalue Concept", *IEEE Transactions on Automatic Control*, Vol. AC-24, pp. 135–136, February 1979.

114. Gregory Jr., C. Z., "Reduction of Large Flexible Spacecraft Models Using Internal

Balancing Theory", *AIAA Journal of Guidance, Control, and Dynamics*, Vol. 7, No. 6, pp. 725–732, 1984.

115. Skelton, R. E. and P. C. Hughes, "Modal Cost Analysis for Linear Matrix Second Order Systems", *Journal of Dynamic Systems, Measurement, and Control*, Vol. 102, pp. 151–158, 1980.

116. Skelton, R. E., P. C. Hughes, and H. B. Hablani, "Order Reduction for Models of Space Structures Using Modal Cost Analysis", *AIAA Journal of Guidance, Control, and Dynamics*, Vol. 5, No. 4, pp. 351–357, 1982.

117. Orbak, Â. Y., O. S. Türkay, E. Eşkinat, and K. Youcef-Toumi, "Model Reduction in the Physical Domain", *Journal of Systems and Control Engineering. Proceedings of the Institution of Mechanical Engineers, Part I*, 2003, (in review).